Parametric Inversion from Well Log Data: A Performance and Robustness Analysis

by

Gaurav Rewari

Submitted to the Department of Electrical Engineering and Computer Science
in partial fulfillment of the requirements for the degrees of

Bachelor of Science

and

Master of Science

at the

MASSACHUSETTS INSTITUTE OF TECHNOLOGY

September 1992

Author .....
Department of Electrical Engineering and Computer Science
July 30, 1992

Certified by .....
Professor Alan S. Willsky
Thesis Supervisor

Certified by .....
Orhan Arikan
Company Supervisor

Accepted by .....
Campbell Searle
Chairman, Departmental Committee on Graduate Students

Parametric Inversion from Well Log Data:

A Performance and Robustness Analysis

by

Gaurav Rewari

Submitted to the Department of Electrical Engineering and Computer Science
on July 30, 1992, in partial fulfillment of the
requirements for the degrees of
Bachelor of Science
and
Master of Science

Abstract

In this thesis we consider the processing of well log data, in which the measurements taken from instruments lowered into oil and gas boreholes depend on a set of parameters characterizing the state of the geological formation surrounding the boreholes. From a finite collection of noisy, well log measurements it is desired to estimate the unknown parameters characterizing the formation or some subset of these parameters, assuming the remaining to be known. In this thesis, we conduct a performance analysis to characterize the accuracy with which parameters may be estimated from finite, noisy log measurements as well as a robustness analysis to characterize the adverse effect of modelling error; i.e., imprecise knowledge of the parameters which are assumed to be known.

Thesis Supervisor: Professor Alan S. Willsky
Title: Professor of Electrical Engineering, MIT

Thesis Supervisor: Orhan Arikan
Title: Research Scientist, Schlumberger Doll Research

Parametric Inversion from Well Log Data:
A Performance and Robustness Analysis

by

Gaurav Rewari

Submitted to the Department of Electrical Engineering and Computer Science
on July 30, 1992, in partial fulfillment of the
requirements for the degrees of
Bachelor of Science
and
Master of Science

Abstract

In this thesis we consider the processing of well log data, in which the measurements taken from instruments lowered into oil and gas boreholes depend on a set of parameters characterizing the state of the geological formation surrounding the boreholes. From a finite collection of noisy, well log measurements it is desired to estimate the unknown parameters characterizing the formation or some subset of these parameters, assuming the remaining to be known. In this thesis, we conduct a performance analysis to characterize the accuracy with which parameters may be estimated from finite, noisy log measurements as well as a robustness analysis to characterize the adverse effect of modelling error; i.e., imprecise knowledge of the parameters which are assumed to be known.

Thesis Supervisor: Professor Alan S. Willsky
Title: Professor of Electrical Engineering, MIT

Thesis Supervisor: Orhan Arikan
Title: Research Scientist, Schlumberger Doll Research

Acknowledgments

I wish to thank Orhan Arikan and Professor Alan Willsky for their support during the course of this research project. Professor Willsky assisted in the initial formulation of the problem and was a constant source of ideas, constructive criticism and enthusiasm throughout this endeavour. To Orhan goes my heartfelt appreciation for the amount of time we spent discussing matters pertaining to, and completely unrelated to this thesis. His patience, clarity of analysis, and contagious love of his subject will stay etched in my memory always.

I would also like to acknowledge the support of Dave Rossi, T.S Ramakrishnan, Nihal, Suhail and Ram, whose assistance at Schlumberger was cheerfully given, and shamelessly taken. I would also like to thank Romeo and Cathy Petroni, my old friends from Ridgefield, for their wonderful hospitality.

My friends at MIT have made the past five years a greatly enrichening chapter of my life. To them, who have endured me in my every color of emotion, and who still care, all I can say is, keep up the good work, and that I care too.

Professor Illona Karmel, who claims to have known me from her infancy, I thank for fiercely guarding me from ever devaluing the liberating power of imagination. To Professors Neil Todreas, Robert Halfman and Amar Bose I owe a special thanks for their wisdom and advice, of which I have so often been a glad recepient. The persistent efforts of Deans Levak and Perkins found me a solution where once none looked possible. To the rest of my professors at MIT, and at Campion and Jai Hind, go my appreciation for assisting me in trying to carve an education out of my schooling.

I would like to thank Mummy and Daddy (Delhi Branch) for the generosity of their affection. Shravan has taught me what I know about grit. Aparna I thank for her friendship and warm concern. To Maussi, Raj uncle, Astra, Reitu and Anamika go my thanks for providing me with a home away from home. To the rest of my family, I sustain a debt of gratitude far beyond my means to ever repay. And thanks to Rinks too, wherever she is; may she always find a warm sun to snooze under.

Lastly, I wish to thank my parents, (providers and sustainers of life, scorners of too-much-love-spoils-the-kid theorists, owners of eternally young hearts), to whom every effort is dedicated. The sheer abundance and extravagance of their love makes competition from my end impossible, and acceptance the only option.

To my family,

and to the memory of Bauji, Alan Twigg and Joseph Sheth

Contents

List of Figures

List of Tables

Chapter 1

Introduction

With the development and availability, in recent years, of fast forward models to simulate the responses of geophysical well logging tools [3], there has been considerable interest and activity in trying to find explicit use of these models in petrophysical interpretation, i.e., the problem of evaluating a geological formation for hydrocarbon presence and recoverability. Frequently, some of the formation descriptors, such as the formation resistivity, neutron porosity and the depth of invasion [5] of the drilling fluid, enter the problem nonlinearly; therefore, the model-based approach to the inversion for these quantities is typically iterative, with fast forward models in the loop.

It is the ambition of this thesis to provide the methodology for enabling a quantitative characterization of the uncertainty associated with the final estimates obtained using such an inversion method. For this purpose, we have studied two specific ways of characterizing this uncertainty:

- When the source of the uncertainty is the measurement sensor noise, (e.g., nuclear counting statistics, electrical noise, cross-talk, etc).
- When the source of this uncertainty includes the case where some of the quantities involved in the tool/formation description (e.g., bed boundary locations, tool sample locations, invaded zone properties) are not precisely known during the estimation procedure.

In order to address these two problems systematically, and develop insight into the senstivities to various sources of uncertainty, we have focussed on the problem of the induction tool response [3] in a three layer, invaded medium, to be described at length in the following chapter. It must be stressed that, ultimately, this methodology of assessing uncertainty is applicable to much more complex formations and more sophisticated tool response models.

There exist explicit mathematical models and computer codes that describe how the induction tool responds to particular formation heterogeneities, principally due to layering and invasion [13]. We have chosen the three layer, invaded formation model to illustrate the developed methodology because it allows us, with the complexity of the formation model kept at a minimum, to capture the physical effects that also influence more complicated models of the formation. It is worth noting that inversion for the petrophysical quantities of the formation (in the case of the induction tool this is the true conductivity of the formation) is routinely carried out for multi-layered formations with more than one invaded zone, i.e., models with very large numbers of parameters. The large number of parameters does not make the estimation of the desired parameters impossible; what it curtails is an adequate error characterization of any such estimation process. With the three layer, invaded model, however, it is possible to incorporate the complicating physical effects, (e.g., presence of the borehole and the shoulder beds, invasion and tool depth imprecision), and to analyze the performance of the estimation process and its robustness to various sources of error.

The inherently stochastic nature of the observed logs demand that recourse be taken to statistical methods for the characterization of the errors in the estimated properties. As was mentioned previously, since the core of most of the forward models is nonlinear, the error characterization will require the use of tools new to petrophysical interpretation such as the Cramer-Rao lower bound [15] on the error variance of the estimate. The resulting framework provides a natural means for assessing the contribution of different measurements to the quality of the estimated parameters. This serves as a benchmark with which to compare other measurement concepts, current and of the future.

The rest of this thesis is organized as follows: Chapter 2 attempts to bridge the terrains of geophysical well logging and classical estimation theory. Well logging is introduced as the process by which measurement devices are lowered into the well to obtain important petrophysical information about the formation. These formation measurables, however, are not always of direct interest to us. The procedure by which these measurables are used to obtain estimates of the porosity, ϕ, and water saturation, S_w - parameters that reflect the hydrocarbon presence and producibility - is termed formation evaluation or interpretation. The fundamental principles of formation hydrocarbon evaluation are presented.

Induction logging provides resistivity information that is important for locating hydrocarbon-bearing formations and estimating reserves. Since the methodology of error characterization is to be illustrated using the induction log response, the physics of the induction logging tool is presented. The geometric factor theory [14] is used to explain the induction tool response and is extended to account for the skin or propagation effect [11] observed in the induction logs.

Parametric or model-based inversion is discussed next. The central assumption here is that the formation geometry conforms to a model that can be described with a finite number of parameters. The assumption that such a formation model exists enables fast and reasonably precise forward (tool response) models to be developed that simulate the response of a given tool to the formation model. One such fast forward model, Hybres [2], is then discussed. The three layer, invaded model to be employed in this thesis is presented, with a discussion of its salient features and the factors governing its choice. Estimation theory is then reviewed with special attention given to the issues that emerge in the statistical estimation of parameters that arise nonlinearly into the measurement equation. The nonlinear estimation algorithm for the estimate of the true conductivity of the formation from a set of noisy induction logs is then reviewed. The various sources of error that could arise in such an estimation schme are then discussed. The chapter closes with an outline of how the characterization of the error in this estimation is to be examined in four different performance/robustness cases.

In the first part of Chapter 3 estimator performance is considered when the only

source of uncertainty is the measurement noise. In the second part of the chapter we assume that some of the parameters in the tool/formation description are not precisely known. The imprecision in some of these parmeters are a source of error in the estimate of the desired quantity, the deep conductivity of the formation. The goal of this part of the study is twofold: we first seek to establish whether measurement noise or parametric imprecision is the major source of error in the estimation, and secondly, we desire a means to rank the parameters according to the amount of error they individually contribute to the overall estimation error. This will enable us to identify those parameters to which the estimate of the deep conductivity is most sensitive.

In Chapter 4 we extend the performance analysis to two further situations. Firstly, in order to minimize the degradation of the deep conductivity estimate that results from the imprecise knowledge of the tool/formation descriptor values, these values are themselves refined via a joint estimation of the deep conductivity and the tool/formation descriptors. Since this additional refinement derives from the same log data that is used to determine the deep conductivity (i.e., estimating more parameters from the same log data), a corresponding degradation in the quality of the deep conductivity estimate is to be expected. The trade-off between the refinement in the tool/formation description which leads to less error in the deep conductivity estimate is examined on a quantitative basis.

Secondly, the methodology is expanded to determine the extent to which additional measurements of the formation descriptors (e.g., information about the bed thickness from the Formation MicroScanner [7]) translate to a reduction in the uncertainty in the final estimate of the deep conductivity.

In Chapter 5 some complementary issues relating to the analysis of Chapters 3 and 4 are addressed. These include extending the sensitivity analysis of Chapter 3 to include errors due to imprecision in the tool sample locations, and a consideration of how different choices of tool/formation descriptor values may influence some of the conclusions made in the previous chapters.

In Chapter 6, which concludes this thesis, the principal contributions of the study are summarized and possible directions for future work are suggested.

Chapter 2

Background

2.1 Introduction

In this chapter geophysical well logging is overviewed. The process of well logging is introduced and the well logging environment is discussed. The petrophysical characteristics of an undisturbed reservoir are described followed by an examination of the complications that drilling and tool related effects introduce into such a description. The central difficulty in evaluating a formation for the presence and recoverability of hydrocarbon is that few of the petrophysical parameters that are necessary for such an evaluation are amenable to direct measurement. They must be derived from formation measurables such as the resistivity, bulk density and the spontaneous potential of the formation for example. The means for going from such information to the actual petrophysical descriptors is provided by fundamental log interpretation relationships that are considered in a section on formation hydrocarbon evaluation.

Resistivity measurements lie at the core of these log interpretation relationships. The process of induction logging is introduced as a tool for obtaining resistivity information about the formation. The physics of the induction tool is presented and a mathematical expression for the tool response is developed under certain assumptions. The tool response is seen to be a nonlinear function of the formation parameters. The inversion problem involves going from noisy induction logs to estimates of the formation parameters. If, as in this thesis, this inversion is done under the assumption that the formation geometry conforms to a certain model that can be described with a

finite number of parameters then the inversion is termed model-based or parametric. A general model of the earth is discussed and it is shown how the assumption of such a model enables fast and reasonably precise forward response codes to be developed.

The model considered in this thesis is chosen to be a subset of the general model and consists of a borehole, a central, invaded bed and two uninvaded shoulder beds. The motivation for choosing such a model is explained. At this stage the parametric inversion problem for the three bed model is stated. It is observed that the formalization of a rule for obtaining the model parameters from noisy induction logs requires the techniques of statistical estimation.

Estimation theory is then reviewed. The notational conventions and some key results of probability theory are stated, then the various techniques of classical estimation theory are described. Bayesian and non-Bayesian estimators are considered; the means for constructing the estimates is reviewed as also the methods of error analysis of the estimation. The Cramer-Rao lower bound is introduced as a lower bound that can be placed on the error variance of the estimate. Bounds such as this are of importance in nonlinear problems in which no straightforward expression for the error variance exists. A separate section on nonlinear estimation is included to provide an appreciation for the practical difficulties inherent in obtaining estimates in such problems.

At this stage the parametric inversion problem for the three bed problem is restated in estimation terms. The sources of error in the estimation are then discussed. A four tiered approach to the analysis of inversion performance and inversion robustness is described.

2.2 An Overview of Geophysical Well Logging

The purpose of this section is to provide a brief overview of well logging. No exhaustive study of the logging process is intended, instead the emphasis is on providing an exposition of:

- what well logs are, and why they are important,
- the well logging environment, and

- the interpretation of well logs and how that enables the evaluation of a geophysical formation.

2.2.1 Well Logging

Definition of a Well Log

A *log*, or measurement by an instrument lowered into oil and gas boreholes, provides information about the potential hydrocarbon production from the well. These measurements are presented versus depth and provide a record of characteristics of rock formations traversed by a measuring apparatus in the well bore. The logs, sometimes referred to as 'wireline logs' or 'well logs', are obtained by means of instrument packages, or *logging tools*, lowered on cable (wireline) into the well. The part of the earth under investigation, including both the rock and fluid components, is termed the *formation.*

The Importance of Well Logs

Well logging, as the process of obtaining these logs is called, is usually performed after an interruption or upon cessation of drilling activity. Little knowledge about the producibility of a well can be gleaned as it is being drilled. Further, the process of *coring*, in which cuttings of subsurface rock are returned to the surface for examination by geologists, cannot by itself furnish the data necessary for a quantitative evaluation of the hydrocarbons in the formation. While it may indicate the general lithology under investigation and may reveal traces of hydrocarbon, it does not permit an estimate of the oil and gas in situ. Well logging, as will be seen, provides the information necessary for such decision making, and is therefore "the most important part of the drilling and completion process. Obtaining accurate and complete log data is imperative. Logging costs account for only about 5 percent of completed well costs, so it is false economy to cut corners in this phase."[5]

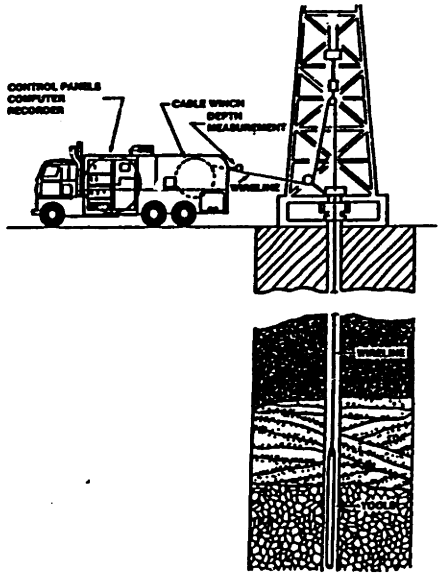

Figure 2-1: Wellsite setup for logging.[5]

2.2.2 The Well Logging Environment

In this section the actual technique of well logging, as it is carried out in the field, will be overviewed. A brief description of the characteristics of an undisturbed reservoir will then be presented, followed by an examination of the complicating factors that drilling and logging may introduce into such a description. An understanding of the petrophysical properties of rocks is essential to an appreciation of log interpretation.

The Logging Procedure

Figure 2-1 provides a schematic of the wireline logging operation.

Log measurements are made by lowering a measurement device, or *sonde*, into the well by means of a cable from a winch which is mounted on a logging truck or offshore unit. In addition to enabling the lowering and raising of the tools, the logging cable provides depth measurements, control over tool speed, and an electrical interface between the downhole tool and the recording and processing equipment on the surface.

This computer based control and data acquisition system is programmed so that a continuously recorded log is made of a physical parameter versus depth as the tool is raised back to the surface. Taking the logs during the tool's ascent from the well assures better depth control and a tauter cable. Though the stretch coefficient of the cable in its normal operating range is small, corrections may sometimes have to be

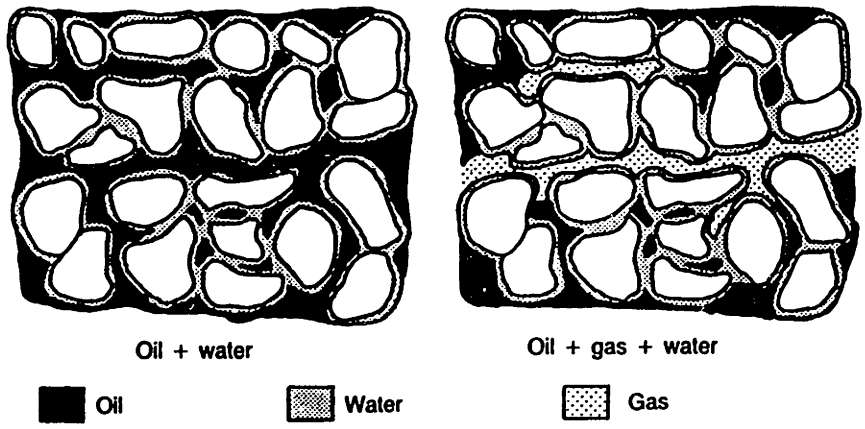

Figure 2-2: Section through a Hydrocarbon bearing rock.[5]

made for elastic stretch and this is done either automatically or by means of a hand-crank adjustment. The log data is recorded using digital recording techniques; this facilitates the transmission of the information over modern electronic channels. Signal processing can be carried out adaptively downhole, uphole in the logging truck, or, once the data is stored and transmitted, post-processing can be done at a computing center.

The Undisturbed Reservoir

Oil and gas producing formations, or *reservoirs*, occur in a wide variety of shapes and sizes. The rocks that constitute reservoirs are believed to have been laid down in layers or beds. As such, their physical characteristics tend to be different in different directions. This is known as anisotropy and is a consideration of great relevance in reservoir engineering.

The oil and gas recovered today comes predominantly from hydrocarbon accumulations in the pore spaces of reservoir rocks. Figure 2-2 illustrates a section through a hydrocarbon bearing rock. The rock consists of solid matrix and fluid components. The matrix consists of grains of sand, limestone, dolomite or mixtures of these. The fluid component comprises oil, water and, occasionally, gas. Fluid occupies the pore space of the rock. Typically, water occupies very fine pores and forms a continuous path through the rock space; oil and gas usually occupy, in that order, the larger pores.

The properties essential to determining formation producibility are porosity, wa-

ter saturation and permeability. The former two provide information regarding the amount of hydrocarbon present while the latter determines how recoverable or producable that amount is.

• Porosity, ϕ, is defined to be the pore volume per unit volume of formation. In other words it is the fraction of the total volume that is pore space. Porosity depends on the grain size distribution; it is higher if all the grains are of the same size than if the grain sizes varied widely so that small grains could fill the spaces between larger grains.

• Water Saturation, S_w, is the fraction of pore space containing water. Since the pore space contains water or hydrocarbon, the fraction of pore space containing oil or gas, the hydrocarbon saturation, S_h, equals $(1 - S_w)$. Therefore, the fraction of total formation volume that is hydrocarbon is ϕS_h or $\phi(1 - S_w)$.

• Permeability, k, is a measure of the rate at which fluid will flow through a given area of porous rock under a specified gradient. It measures the ease with which fluid can flow through the pore system of the rock, and depends on grain size and the tortuosity of the path that connects pores through the rock medium. Greater permeability usually corresponds to greater porosity but this does not always have to be the case.

Hydrocarbon bearing rocks include sands, limestones and dolomites. Formations containing just these are termed 'clean' and are relatively easy to interpret with logs. Interpretation, it should be remembered, must take into account all of the above three rock properties. Limestone, for instance, has low porosity which would indicate that there is less pore space for possible hydrocarbon accumulation. However, a limestone formation may consist of dense rock with deep fractures or fissures; this would translate to high permeability (despite low porosity). Therefore, if it is determined by some means that the water saturation of the formation is small (or equivalently, the hydrocarbon saturation is large), then the oil and gas that is present should be easy to recover[1].

The interpretation of formations that contain clays or shales (the 'dirty' forma-

[1] Actually, it would be more correct to say that the fraction of pore space that contains *immovable* water, the irreducible water saturation, S_{wi}, should be small

tions) is not as simple. These may have large porosity but very small permeability, so that a large part of the fluid may be bound and hence unable to flow. Accounting for the presence of clays and shale in the evaluation of hydrocarbon formations presents serious complications.

Complicating Factors

There are a host of problems specific to well log measurements. Although the logs should ideally be measurements of the formation, in reality the log responses of the tools are affected by the presence of the borehole, the phenomenon of *invasion*[14], and problems specific to the tool being used. In addition, operational problems may be encountered due to temperature and pressure in the well and hostile environmental conditions.

- **Tool Related Effects** The problems associated with the tools are much a function of which tool is being employed, but in general a few common issues can be identified. There are the obvious complications introduced by the hostility of the well environment; the tools must be able to withstand severe temperatures and pressures downhole. These adverse conditions are sources of mechanical and electrical error in the log measurements. The fact that measurements are made while the tool is in motion is another source of complications. Different tools have different logging speeds and the errors that enter due to incorrect depth recordings have to be removed by depth correction procedures[2].

- **Effects due to Drilling** Wells are usually drilled with a special rotary bit positioned at the end of a long drillstring or drillpipe that is rotated by powerful engines at the well surface. While drilling, a specially prepared liquid drilling mud is pumped down through the pipe and out through holes in the bit. This fluid provides necessary lubrication for the bit and also creates a hydrostatic pressure within the well that is substantial enough to prevent the pore fluids in the formation from seeping in and causing blowout.

[2]The issue of depth imprecision and 'tool yoyo' is examined more closely in Chapter 6

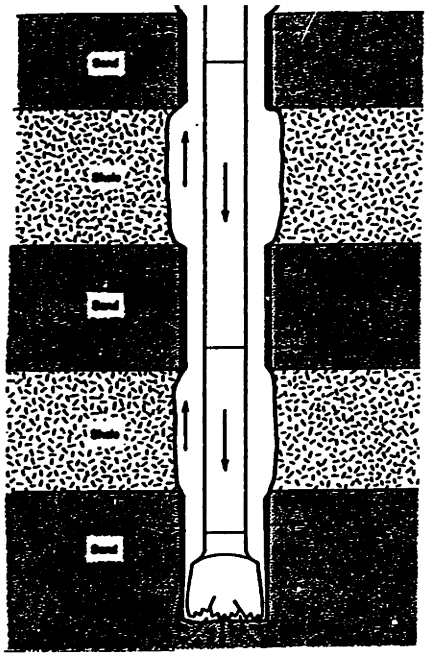

Figure 2-3: The Invasion Process.[5]

1) Borehole Mud

The presence of the borehole mud influences well log measurements. This influence depends on the radius, r, of the well (hence, also, the amount of mud present over a certain depth) and the type of drilling mud employed. The response of any logging tool will contain a contribution from the mud in the wellbore; this contribution clearly is a function of which mud is used and how large the well is.

2) Invasion

The process of invasion is illustrated in Figure 2-3 . Because of the high pressure of the mud within the borehole there is initially a flow of the fluid component of the drilling mud (the mud filtrate) into permeable formations. This creates an altered area around the borehole. As the process continues the particulate component of the mud is filtered out onto the borehole wall forming a mudcake. Once the mudcake forms an impermeable layer within the borehole, the outward flow of the mud filtrate ceases and the process of invasion is completed. Due to their low permeability shales do not invade or build up mud cakes. This is not the case for sands as can be seen from the same figure.

The altered area refered to above develops in the following way: in the immediate vicinity of the wellbore is the *flushed zone* followed by a *transition zone* and then the unperturbed or *uninvaded zone*. Proceeding outward from the well, the mud filtrate pushes the formation fluids away from the well. In the flushed zone it is assumed that

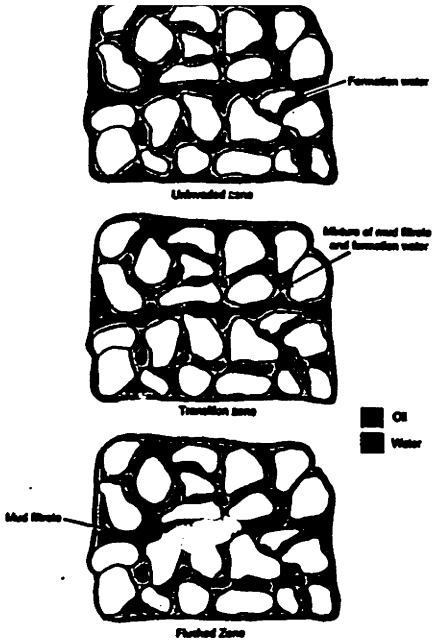

Figure 2-4: Section through invaded rock.[5]

all the formation water is replaced with mud filtrate. If the formation is hydrocarbon bearing then some but not all the oil will be pushed out. The presence of mud filtrate gradually tapers out further away from the wellbore; the displacement of formation fluids by the drilling mud is less noticable within the transition zone than in the flushed. This process is summarized by the three Figures 2-4. The invasion pattern usually takes a few days to reach its equilibrium condition.

2.2.3 Formation Hydrocarbon Evaluation

The central difficulty in evaluating a formation for the presence and recoverability of hydrocarbon is that few of the petrophysical parameters discussed above are amenable to direct measurement. Instead, they must be derived from logs of other physical parameters of the formation such as the resistivity, the bulk density, the interval transit time, the spontaneous potential, the natural radioactivity, and the hydrogen content of the rock[13]. The process by which the desired petrophysical parameters are obtained from these measurable parameters is termed log interpretation. It is the means by which a formation is evaluated for its hydrocarbon content and producibility.

The presence of hydrocarbons in the pore spaces is primarily sensed by measuring the electrical resistance (or its inverse, the electrical conductivity) of the formation. Electrical logging techniques exploit the fact that the saline water found in the pore spaces is several times more conductive (or less resistive) than the hydrocarbon. This

simple fact provides a basis for determining oil and water saturations via resistivity measurements. The actual resistivity of the formation is measured and is compared with the resistivity that would have been obtained had all the pores contained water. If the measured resistivity is much higher than the calculated resistivity, the presence of hydrocarbons can be concluded. The means for going from this resistivity information to the petrophysical parameters is provided by fundamental interpretation relations usually referred to as the petro-physical mixing laws.

Petro-physical mixing laws Obtaining values for ϕ and S_w from measurable formation quantities involve a transformation described by the empirical petro-physical mixing laws.

$$\sigma_t = \phi^m S_w^n (\frac{\sigma_w}{a}) \tag{2.1}$$

where:

σ_t = The (measured) formation conductivity

σ_w = The (known) conductivity of the formation water

m, n, a are constants.

The above relationship is more commonly known as Archie's law and is the basic Equation of log interpretation.

The second relationship identifies the measured density of the rock as the sum of the densities of solid matrix and fluid weighted by their relative volumes as given by the porosity of the rock.

$$\rho_b = \rho_f \phi + \rho_m (1 - \phi) \tag{2.2}$$

where:

ρ_b = The density, measured by the Litho-density tool[8].

ρ_f = The density of fluid in the rock, (1 gm/cc if water, oil)

ρ_m = Density of solid matrix. (Assumes lithology is known, eg, if the rock type is quartz, ρ_m = 2.75 gm/cc)

These two relationships provide the means for obtaining the desired petro-physical parameters from logs of resistivity and density. The density logs are obtained from

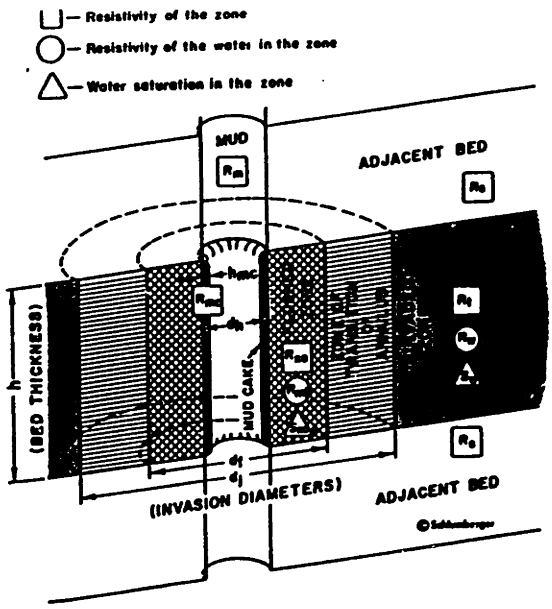

Figure 2-5: Zones created by invasion.[13]

density, neutron and sonic tools while the resistivity information is provided by electrode and induction tools. This thesis shall concern itself primarily with a resistivity (or conductivity) tool. The impact of invasion on resistivity measurements is discussed next.

Effect of invasion on resistivity measurements

In the above discussion the conductivity σ_t (and the corresponding resistivity, R_t) was that of the undisturbed formation. In reality, however, invasion makes the measurement of R_t a more difficult task. This can be appreciated by looking at Figure 2-5. Invasion produces a succession of zones of different resistivity: proceeding outwards from the center of the well there is the well itself, the mudcake, the flushed zone, the transition zone and, lastly, the uninvaded zone whose resistivity, R_t, is actually desired.

Clearly, then, any measurements of R_t must come from deep reading instruments. However, there is a fundamental trade-off that occurs in the vertical resolution of any tool when it is made to measure more deeply into the formation. As such, what is done in practice is to run three resistivity curves simultaneously -a shallow, medium and deep curve- and use the first two to correct the latter curve for invasion.

In performing the correction mentioned above it is assumed that the invasion or resistivity profile has a step-like nature as shown in Figure 2-6 (a). The actual

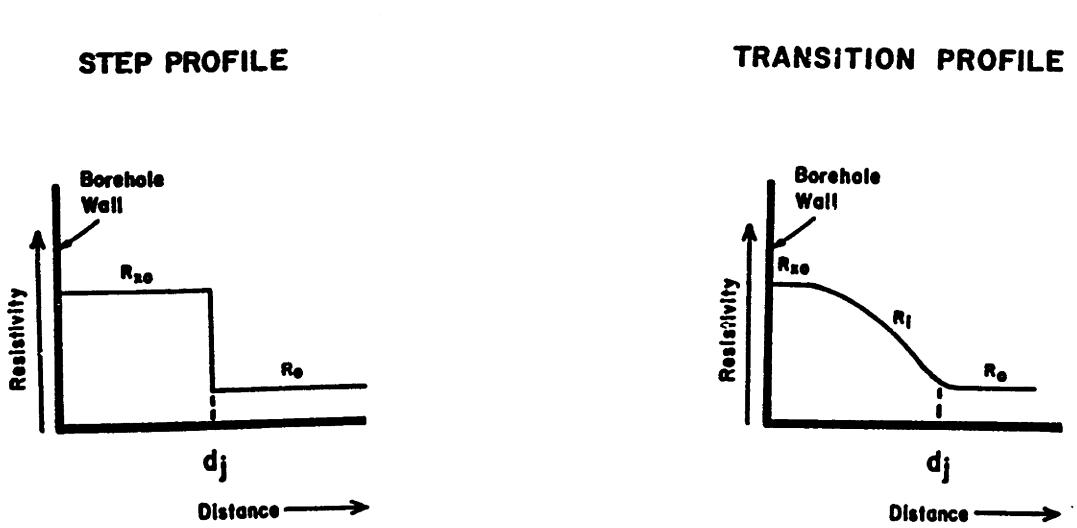

Figure 2-6: Invasion profiles. (a) Step and (b) Transition.[12]

profile is usually something like that shown in Figure 2-6 (b), and the effect of this assumption is to ignore the transition zone. Field and laboratory tests have indicated that such an approximation is not unsatisfactory [5]. Further, the contribution of the mudcake restivity to the overall resistivity measurement is usually small enough to be ignored. In that case, the resistivities of the mud, the flushed zone and the uninvaded zone are taken to be the contributors to the measured resistivity signal.

The foregoing discussion served to emphasize the utility of knowing the formation resistivity and brought to light the complicating factors that invasion introduced into its measurement. There are two basic kinds of tools that are used to obtain resistivity information: electrode and induction tools. In this thesis we shall consider exclusively a type of induction tool, the Dual Induction Tool, (DIT)[13], that comprises a deep-reading induction, a medium-reading induction and a shallow focussed-electrode array.

2.3 Induction logging

As indicated earlier, induction logging provides resistivity information that is important for locating hydrocarbon-bearing formations and estimating reserves. By measuring the electrical conductivity of down-hole formations and fluid, the induction tool can distinguish between nonconductive hydrocarbon-bearing formations and

conductive water-bearing formations.

The basic induction logging tool, shown in Figure 2-7, comprises a receiver and a transmitter coil both of which are mounted some distance apart on an insulating mandrel. A constant amplitude, sinusoidal current fed into the transmitter coil creates a magnetic field around the tool which causes eddy currents to flow in circular paths around the borehole axis. These eddy currents are 90 degrees out of phase with the transmitter current; their magnitude depends on the surrounding formation's conductivity. The eddy currents create their own magnetic field and induce in the receiver coil an alternating voltage a further 90 degrees out of phase, i.e., 180 degrees out of phase with the transmitter current. The measurement of this signal is called the induction log.

The induction response is usually explained by the geometrical factor theory. This theory assumes that the receiver voltage is the sum of contributions from an infinitely large number of eddy current loops. This is an approximate theory because it ignores the interaction between such loops.

Biot-Savart's law is used to determine the contribution of a single, infinitesimal loop of current having unit cross-sectional area, radius r, and situated distance z from the midpoint of the two coils[11]:

$$v_R = \overbrace{\left(\frac{4\pi\omega^2 A^2 N_T N_R I_T}{L}\right)}^{K}\overbrace{\left(\frac{L}{2}\frac{r^3}{[r^2+(L/2-z)^2]^{3/2}[r^2+(L/2+z)^2]^{3/2}}\right)}^{g_{GF}(r,z)}\sigma(r,z) \quad (2.3)$$

where:

ω = the frequency of the transmitter current

A = cross-sectional area of the coils

N_T = number of turns in the transmitter coil

N_R = number of turns in the receiver coil

I_T = transmitted current amplitude

L = the transmitter-receiver spacing

$\sigma(r,z)$ = The conductivity of the formation within the loop (assumed to be con-

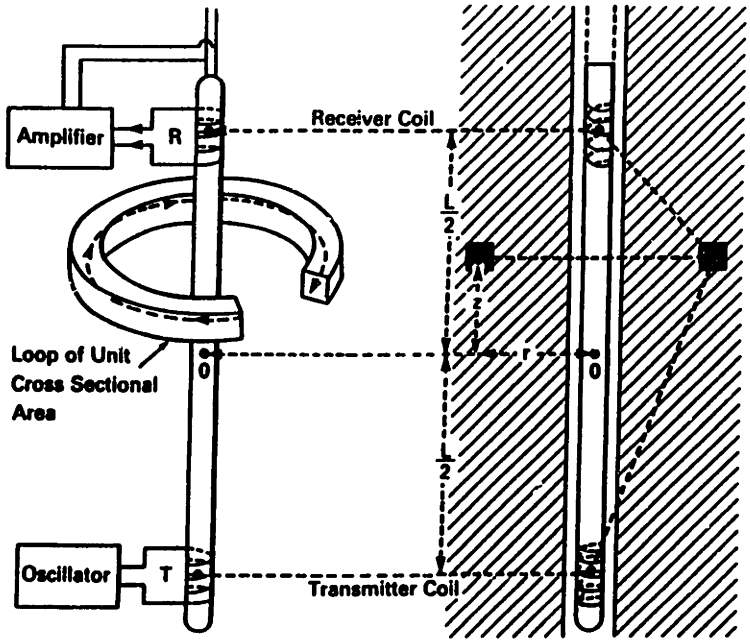

Figure 2-7: The basic two-coil induction tool. Transmitter T and Receiver R, separated by a distance L, are wound on an insulating mandrel. T produces an eddy current in a loop of unit cross-sectional area in the formation. This in turn induces in R an emf which is proportional to the conductivity of the material in the loop.[14]

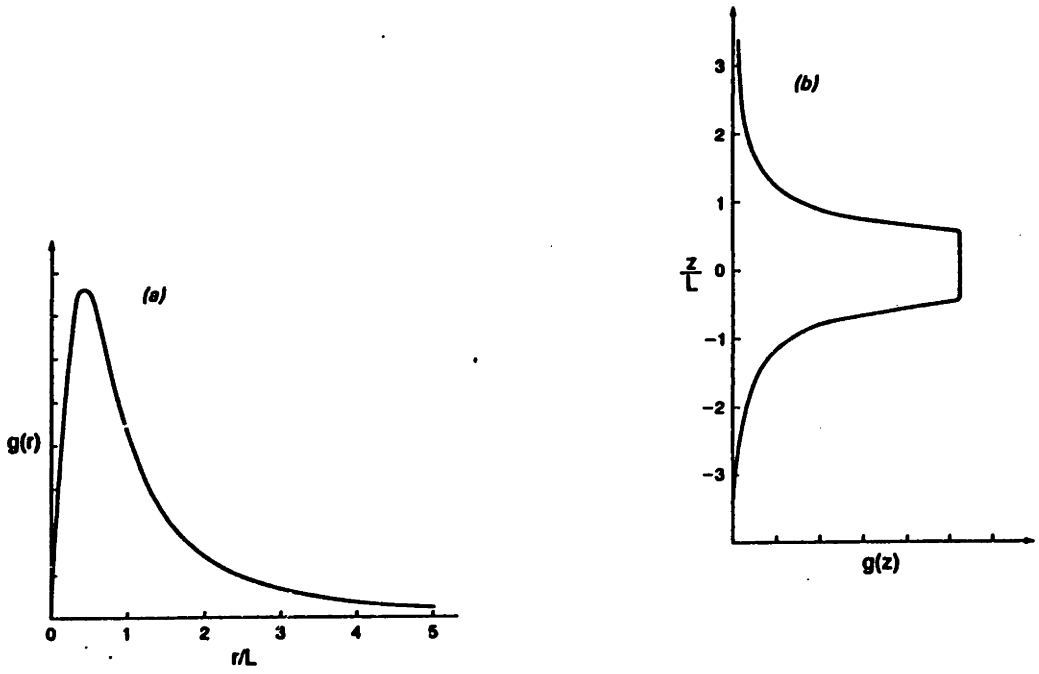

Figure 2-8: Radial and Vertical differential geometric factors for the two coil induction tool calculated using the geometric factor theory. (a) Radial and (b) Vertical.[14]

stant).

The first term in parentheses consists of quantities associated with the tool, and is therefore called the sonde constant, K. The second term in parentheses contains mostly positional information; this is the differential geometric factor, $g_{GF}(r,z)$[14].

The single loop expression can therefore be written as:

$$v_R = K g_{GF}(r,z)\sigma(r,z) \tag{2.4}$$

Extending the above result to an infinite number of such loops we obtain as the expression for the tool response the following *linear* convolution:

$$V_R(z) = K \int_{-\infty}^{+\infty} \int_0^{\infty} g_{GF}(r, z'-z)\sigma(r,z')drdz' \tag{2.5}$$

As before the absence of azimuthal variation is made explicit by the notation $\sigma(r,z)$. In order to examine the radial and vertical investigation characteristics of the two coil sonde it is convenient to define two other geometric factors:

1) The differential radial geometric factor, which is defined to be:

$$g_{GF}(r) = \int_{-\infty}^{+\infty} g_{GF}(r,z)dz \tag{2.6}$$

This provides the relative importance of each of the cylindrical shells of radius, r, to the overall response. Figure 2-8(a) shows the radial dependence of this differential radial geometric factor. It can be seen that cylindrical formation layers with radius somewhat less than the coil separation, L, assume most importance.

2)The differential vertical geometric factor,

$$g_{GF}(z) = \int_0^{+\infty} g_{GF}(r,z)dr \tag{2.7}$$

This gives the contribution of a slice of unit thickness located at position z to the overall response. Figure 2-8(b) shows the response curve as a function of z. For slices of the formation contained between the two coils a fairly flat response is observed.

For simple formation geometries such as the one in Figure 2-11 (to be discussed in detail later), the total signal, σ_i, can be expressed as

$$\sigma_i = G_m\sigma_m + G_{xo}\sigma_{xo} + G_t\sigma_t + G_s\sigma_s \tag{2.8}$$

where the $G_i s$ are the integrated geometric factors[14] of the respective zones and represent the relative contribution of each zone to the overall signal. Their sum, therefore, must obey:

$$G_m + G_{xo} + G_t + G_s = 1 \tag{2.9}$$

When formation geometries such as the one in Figure 2-11 apply, such a visualization of the overall signal is of great value because it enables the development of mathematically sound correction charts for the effects of borehole mud, invasion and adjacent beds on the measurement of the true zone conductivity, σ_t.

Since the primary aim of induction tools is to obtain resistivity information of the true zone, it is important to minimize the contributions of the adjacent beds, the invaded zone and the borehole mud to the overall signal; this is achieved by minimizing the corresponding integrated geometric factors with a *focussed* signal. The focussed signal is obtained by using multicoil or focussed sondes which typically consist of several auxiliary transmitter and/or receiver coils in addition to the basic two coils. The response of each coil pair is weighted by the number of turns on the two coils and their cross-sectional area. The responses of all such coil pairs are then added in some optimum way in order to achieve better vertical resolution and radial depth of investigation. The former is achieved by suppressing the response from the adjacent beds and the latter by suppressing the response from the mud and the invaded zone. The induction tool considered in this thesis is of the focussed type.

Although the geometric factor theory described above is conceptually very useful, it does not take into consideration the electromagnetic interaction between eddy currents flowing in nearby loops. The attenuation and finite velocity of electromagnetic fields propogating in the conductive media surrounding the sonde affect the magnitudes, phases, and spatial distribution of the eddy currents. These are manifestations

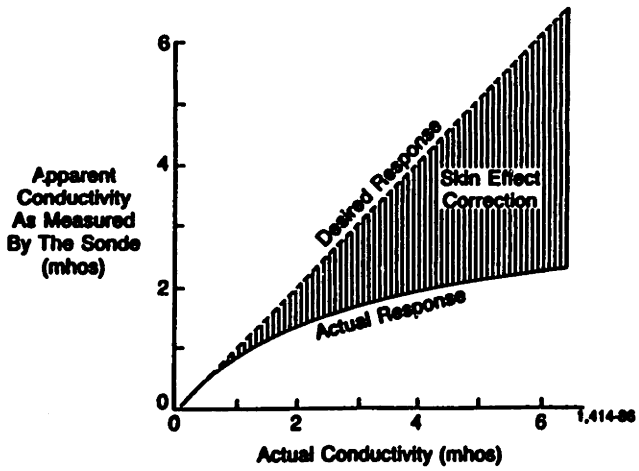

Figure 2-9: Presence of skin effect in induction logs.[13]

of the *skin* or *propagation effects.*

Figure 2-9 shows the discrepancy between the actual response of an induction log and its response modeled without skin effect for various values of the actual conductivity. It can be seen that skin effect becomes more pronounced for surrounding formations that are more conductive. Skin effect corrections are usually carried out on the received signals.

The observed alteration of the tool response with formation conductivity implies that the geometric factor theory cannot describe this skin effect unless the geometric factor is itself a function of conductivity[11]. By adopting such an approach we obtain for the real component of the output signal the following *nonlinear* convolution[11]:

$$V_R(z) = K \int_{-\infty}^{+\infty} \int_0^{\infty} g_{GF}(r, z' - z, \sigma)\sigma(r, z')drdz' \tag{2.10}$$

where:

$g_{GF}(r, z, \sigma)$ = the generalized or propagated differential geometric factor.

It can be shown[14] that

$$g_{GF}(r, z, \sigma) \approx g_{GF}(r, z)\mathrm{Re}[(1 - ikr)e^{ikr}] \tag{2.11}$$

where $k^2 = i\omega\mu\sigma$ with μ denoting the magnetic permeability of the formation.

2.4 Parametric Inversion

In the previous section the physics of the induction tool response was developed. Equation 2-10 yielded the tool response as a function of the conductivity distribution, $\sigma(r, z)$, of the formation. The induction logs themselves will be the tool response corrupted with measurement error or *noise*. The objective of the inversion procedure is to obtain from these induction logs the conductivity distribution of the formation. Similar inversion procedures are carried out for other measurable petro-physical parameters. The different estimates so obtained can be used in turn to obtain estimates of the desired petro-physical quantities, ϕ and S_w, by a transformation governed by the petro-physical mixing laws.

In this thesis the procedure of inversion from induction log data shall be considered. Two possible approaches to this inversion are possible. In the first, $\sigma(r, z)$ varies continuously over r and z, and in the second it is assumed that $\sigma(r, z)$ obeys a layered model. Additional complexity can be folded into such a model-based description of the formation by incorporating invasion, the dipping of layers, rugosity of the borehole wall for example. Whatever be the appropriate model of the formation under consideration, the effect of adopting a model is to reduce the description of $\sigma(r, z)$ to one that can be completely represented with a finite number of parameters. For this reason, the method of inversion that assumes a model shall henceforth be refered to as model-based or parametric inversion. This thesis will concern itself with this approach.

The central assumption in the parametric approach is that the information needed to develop a realistic model for the formation is available through some means. The necessary mathematical description of the formation derives from geological sources; it is the sum total of knowledge derived from past geological modeling, bedding patterns, laboratory studies of cores, rock fracture characterizations and data from various other logs such as that of the Formation MicroScanner tool (FMS)[7]. The availability of such information enables the development of a model that can then be used as the basis both for the parametric inversion of data from different logs, and the subsequent inversion of the petrophysical mixing laws.

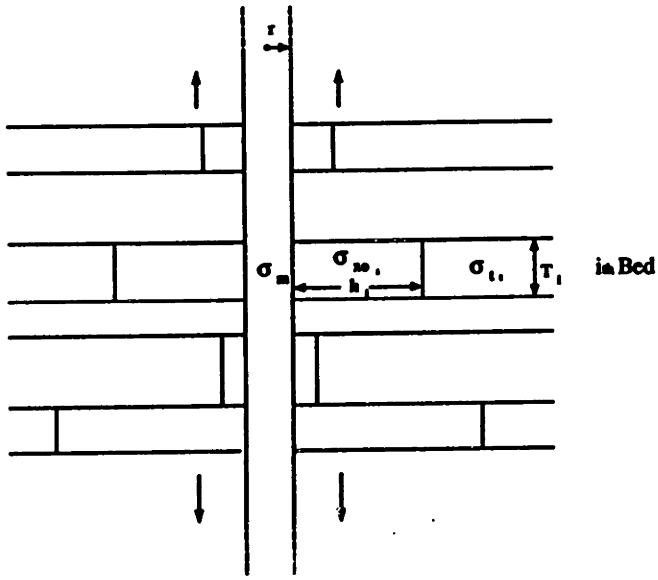

Figure 2-10: General model of the formation

Consider a general model of the earth formation as shown in Figure 2-10. This model assumes the following:

- The earth consists of several layers or beds that are assumed to be perfectly horizontal.
- A borehole of fixed radius, i.e., no mudcake is present and there are no caves in the formation.
- The beds may be invaded. The invasion profiles are piston-like, i.e., the resistivity varies in a step-like fashion such as that shown earlier in Figure 2-6 (a). In other words, no transition layer is assumed to be present.
- The formation is symmetric about the borehole axis. The conductivity distribution is said to be 2-D axisymmetric.

The following set of parameters now provide a complete description of the conductivity distribution of the formation. The parameters of primary interest in the inversion are the $\sigma_{ti}'s$, the uninvaded zone conductivities.

As shall be made more clear later, the availability of codes that model the tool responses is essential to the inversion process and to the characterization of errors in the estimated properties. A principal motivation for adopting a model-based approach is that we can obtain fast, approximate forward tool responses given the model parameters. The forward responses for the cases where the conductivity continuously varies over r and z involve finite element method codes which, while precise, are computationally intensive. Furthermore, for simple models such as the one that will be

employed in this thesis the approximate code yields very satisfactory results[2]

There exists a hybrid code, Hybres[2], that is used to model the response of a variety of induction tools for any formation geometry that is accommodated by the above model within a certain allowable range of conductivity contrasts.

2.4.1 Induction Tool Modelling: The Hybres Code

The principle behind the hybrid approach is shown in Figures 2-11 (a) - (c). It is desired to obtain the induction log for the geometry shown in Figure 2-11 (a). This geometry is partitioned into two sub-geometries shown in Figures 2-11 (b) and (c). The first sub-geometry consists of a purely layered medium. This corresponds to the undisturbed formation developed in Section 2.2.2 .The apparent conductivity for this component can be expressed in closed form and therefore a rigorous solution is possible.

The second sub-geometry essentially serves to correct for the borehole effect and invasion. The contribution of this sub-geometry is obtained by making use of the Born approximation[10] which assumes that field in the formation is the incident field, i.e., no multiple scattering effect of the field is considered.

The hybrid signal is the superposition of these two signals, i.e.,:

$$\text{Hybrid Signal} = \underbrace{\text{Layered medium signal}}_{\text{Rigorous}} + \underbrace{\text{Born Approximation}}_{\text{Approximation}} \tag{2.12}$$

The drawbacks of this type of modeling are that multiple scattering is not accounted for, and that only low conductivity contrasts can reasonably be modelled because of the Born approximation. However, as mentioned earlier, for simple models such as the one considered in this thesis, the Hybres code yields satisfactory results.

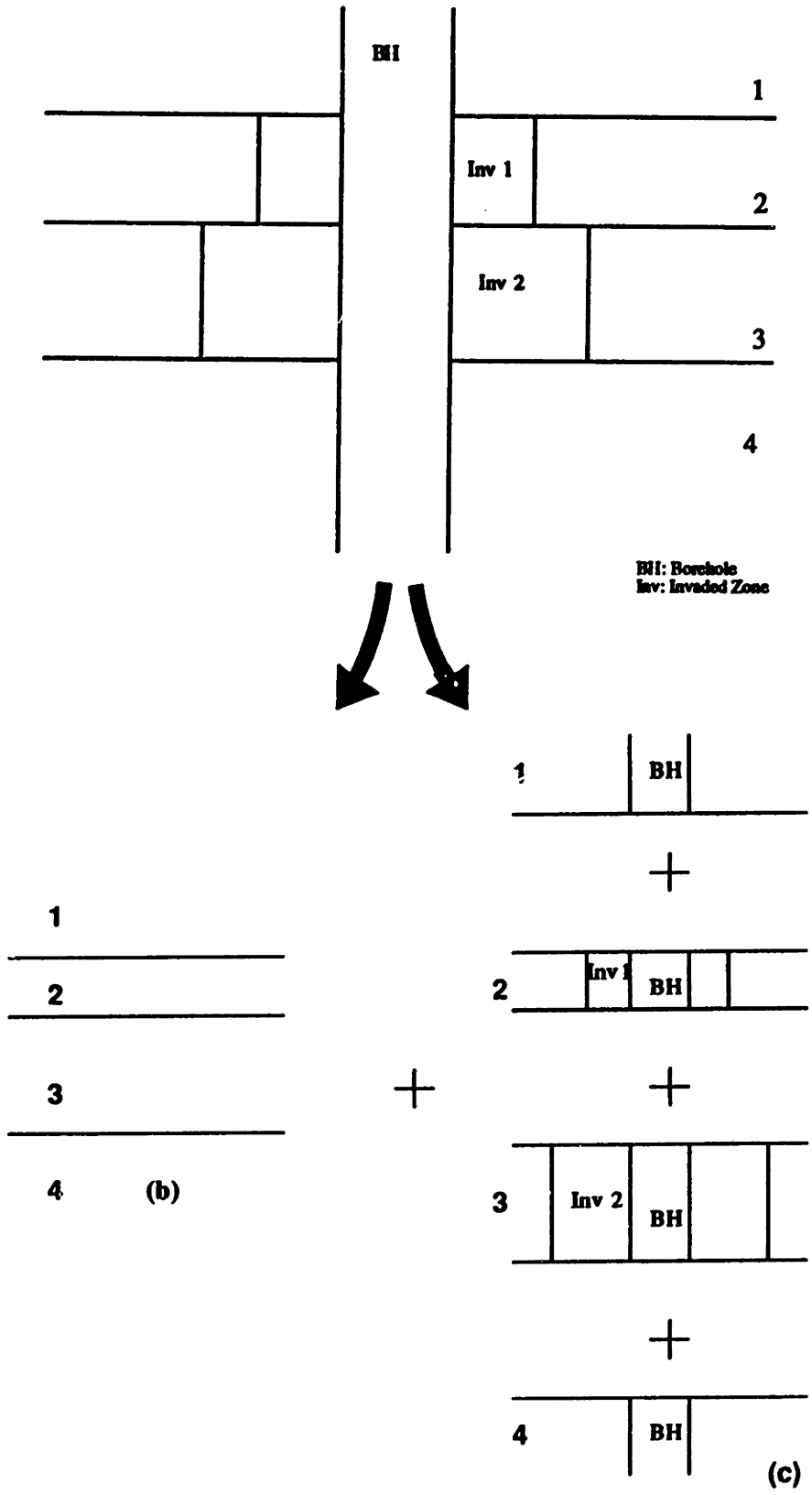

Figure 2-11: Principle behind the hybrid approach. (a) complete geometry, (b) and (c) are the two sub-geometries

2.4.2 A 3-bed model

For the purposes of this investigation we shall consider the model shown in Figure 2-12. This is a simple subset of the general model of Figure 2-10 that assumes:

1) three beds, those at the two extremes, also known as the shoulder beds, are assumed to be semi-infinite in extent and equal in conductivity,

2) the center bed is invaded,

3) there is a borehole of fixed radius.

This model consists of the following parameters:

- σ_m, the conductivity of the mud present in the borehole, (in mhos)
- r, the radius of the borehole, (in inches)

The above two parameters characterize the borehole effect.

- σ_{xo}, the conductivity of the invaded or flushed zone, (in mhos)
- h, the invasion depth, (in inches)

The latter two quantities represent the process of invasion.

- T, the center bed thickness, (in inches)
- σ_t, the true conductivity, (in mhos)
- σ_s, the shoulder bed conductivities, (in mhos)
- $\mathbf{z} = \{z_k, k = 1, ...K\}$, the tool positions at which measurements are available.

For the simulations performed in this study, the number of measurement depth points will be $K = 21$ with a sample spacing denoted as $delz$ inches along the borehole axis.

The symmetry of the model is made clear in Figure 2-13 which shows a cross-section of this model with resistivities indicated instead of the conductivities. The centered tool, referred to as the mandrel, is also shown in the borehole.

A set of values for the above parameters constitutes an *operating point.* For a given operating point the simulated tool response can be obtained at every depth position specified in $\mathbf{z}$ using the Hybres code. The tool response is a nonlinear function of the above parameters.

Setting the tool specific parameter, $\mathbf{z}$, aside, the rest of the parameters can be conceptually divided into those that provide a description of the formation geometry (T, h and r) and those that provide a description of the conductivity distribution,

($\sigma_m, \sigma_{xo}, \sigma_t$ and σ_s). Then, letting h and T, two of the parameters that define the formation geometries allowable under this model, vary over a prescribed range, and keeping all other parameters at a fixed value, we say that we have a family of operating points. This terminology shall be used throughout this thesis.

Motivation for choosing this model: The above model incorporates the following complicating effects:

1) The borehole effect. The borehole mud has a conductivity that could vary between 0 and 100 mhos. If the mud conductivity is much larger than the true conductivity, ($\sigma_m >> \sigma_t$), and if the wellbore is large (i.e., r is large), then the presence of the borehole may have a dominant effect on the signal energy sensed by the tool.

2) Invasion. If the invasion is severe, (h large), and the invaded zone conductivity is much greater than that of the uninvaded zone, ($\sigma_{xo} >> \sigma_t$), then the contribution of the invaded zone to the overall signal received by the tool may be dominant.

3) The shoulder effect. If the center bed is very thin, (T small), and if the shoulder beds are much more conductive than the uninvaded zone, ($\sigma_s >> \sigma_t$), then the effect of the shoulders on the tool response may be pronounced.

This is the simplest layered model that can be used to understand the above effects. Before expanding the treatment to include more beds it is worthwile to understand performance limits (i.e., how well can we obtain the requisite formation resistivity information) in this simple 3 bed case. In doing so we keep the number of parameters as small as possible while still capturing physical effects that would be present even in a more complicated model.

It must be stressed at this point that inversion for the true conductivities of the layers is routinely carried out for multi-layered formations with invasion, i.e., models with very large number of parameters. The large number of model parameters does not make the estimation of the desired parameters impossible; what it curtails is an adequate analysis of the performance of any such estimation process and its robustness to various sources of error. This, fortunately, is not the case for the simpler model just discussed. Such an analysis for the simpler model is of relevance because with a smaller set of parameters one can still capture effects that will also influence a larger

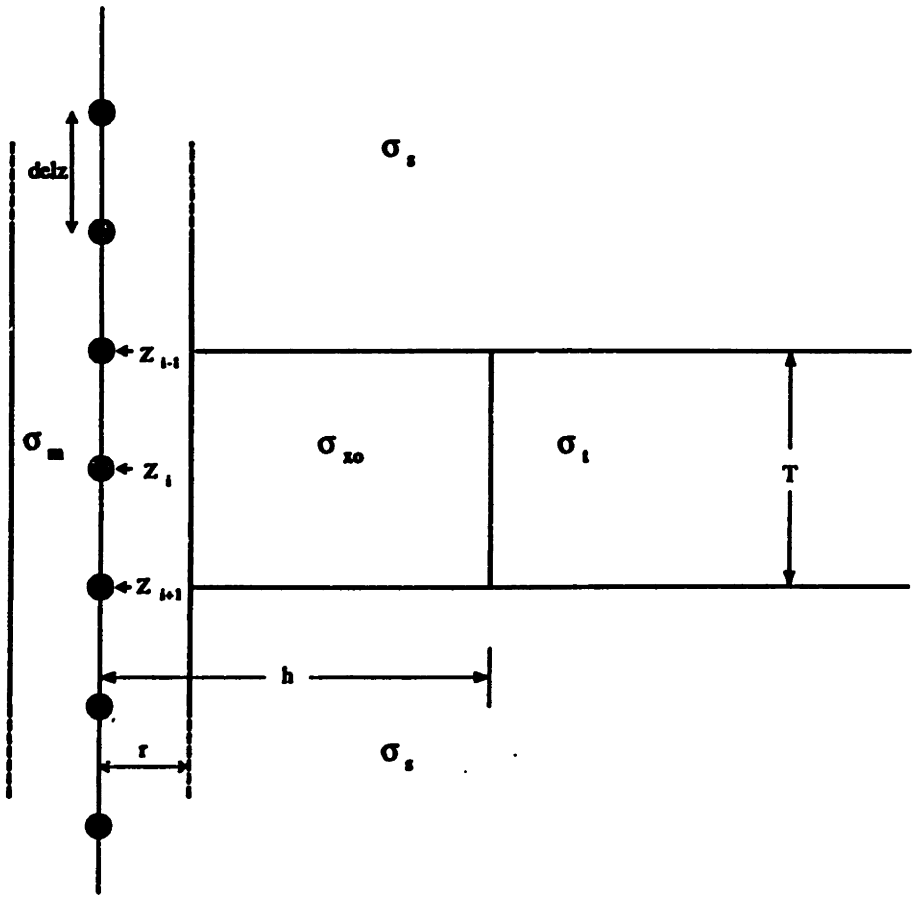

Figure 2-12: Three Bed model for thesis

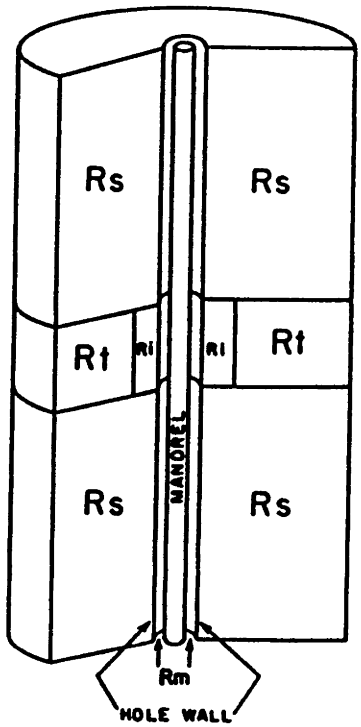

Figure 2-13: Thesis model showing mandrel and assumed symmetry of formation.[8]

model, and because the results of such an analysis provide an upper bound on the performance one can expect when a more complex model is used which has more parameters and more possible sources of modeling and measurement error.

A statement of the parametric inversion problem

For this chosen model, the model parameters may be collected into a parameter set $\mathbf{p} = (T, \sigma_{xo}, \sigma_t, \sigma_s, \sigma_m, h, \mathbf{z})$, and the logging tool measurement set may be represented by the following nonlinear forward model:

$$\mathbf{y} = \mathbf{h}(\mathbf{p}) + \mathbf{e} \tag{2.13}$$

where:

$\mathbf{y}$ = the vector of observations, or the logs

$\mathbf{p}$ = the vector of formation parameters

$\mathbf{e}$ = the measurement error

In the absence of measurement error, we would obtain values for the observation that would identically be that predicted by the forward model $\mathbf{h}(\mathbf{p})$. Such observations will be refered to as the noise-free measurements. Notice that as indicated by Equation 2-10, the tool response and hence the logs themselves are a nonlinear function of the formation parameters. The error in the measurement, $\mathbf{e}$, which may be electronic or mechanical, is assumed to be additive in nature.

The inversion problem is the following: given a finite number of noisy measurements $\mathbf{y}$, estimate the formation parameters $\mathbf{p}$.

The formalization of a rule for inverting for the desired formation parameters and an error characterization of such an inversion require the techniques of statistical estimation that are reviewed next.

2.5 Estimation Theory

2.5.1 Introduction

In the previous sections we touched upon the range of issues associated with parametric or model based inversion of induction logs to obtain estimates of the true

uninvaded conductivity. In particular, we have chosen to consider the model shown in Figure 2-12 because of the fact that using this model we can capture the physical effects that would generally influence any chosen layered model while still keeping the size of the parameter set at a minimum.

Along with the model comes a host of complicating factors. This thesis addresses the need to understand the effect of all these parameters on the chosen model. In this chapter we advance the theoretical tools that will be used to enable the analysis and understanding of the effects of these complicating factors on the quality of our estimated quantities.

We shall introduce some methods of statistical estimation in this chapter. Our observed values of the logs are stochastic quantities because of the presence of random noise in the measurement process. This noise has a certain probabilistic description that is determined experimentally. Knowing this enables us to arrive at a probabilistic relationship between the measured output and the input geological parameters -desired and undesired. The random nature of this relationship allows for the techniques of Bayesian, Maximum a posteriori, maximum likelihood and linear weighted and unweighted least squares type estimation to be used to determine the unknown parameters of the model. The above methods of estimation are discussed with emphasis on the underlying motivation behind their use and their relative merits.

We then consider means of establishing estimator performance. A seperate section is devoted to the problem of nonlinear estimation with special attention given to the fundamental problems inherent in performance analysis in a nonlinear setting. To this end we introduce the Gauss-Newton method that combines the elements of linearized analysis with those of classical estimation theory discussed above into a framework for analyzing nonlinear problems about some operating point.

Given the above generalized approach, some issues specific to the estimation problem of our model are addressed.

We begin with a brief overview of probability theory.

2.5.2 Probability Theory

In situations where the physical system being modeled is inherently random or too complex to allow a deterministic characterization, recourse is taken to probability theory. Probability theory consitutes the mathematical description of statistical phenomena.

It is assumed here that basic probabilistic concepts are known to the reader; this section serves to establish the notational conventions for random vectors that will subsequently be employed and to present certain properties of Gaussian random vectors that will be used freely from here on.

The probability density function (PDF) for a continuous random vector is defined as [6]

$$\mathrm{p}_x(\mathbf{X})d\mathbf{x} = Pr[X_1 \leq x_1 < X_1 + dX_1, X_2 \leq x_2 < X_2 + dX_2, ..., X_n \leq x_n < X_n + dX_n] \tag{2.14}$$

The notation $Pr[X_i \leq x_i < X_i + dX_i]$ is the probability that the ith component of $\mathbf{x}$ takes on a value between X_i and $X_i + dX_i$.

The mean of a random vector is defined as

$$\mathrm{E}[\mathbf{x}] = m_{\mathbf{x}} \tag{2.15}$$

and the Covariance matrix as

$$\mathrm{Cov}(\mathbf{x}, \mathbf{x}) = \Lambda_{xx} = \Lambda_x = \mathrm{E}[(\mathbf{x} - m_{\mathbf{x}})(\mathbf{x} - m_{\mathbf{x}})^H] = \mathrm{E}[\mathbf{x}\mathbf{x}^H] - m_{\mathbf{x}} m_{\mathbf{x}}^H \tag{2.16}$$

Since we shall restrict our attention to real valued matrices, the transpose operator, T, will be used instead of H, the Hermitian operator.

Bayes' rule for random vectors yields

$$\mathrm{p}_{x|y}(\mathbf{X}|\mathbf{Y}) = \frac{\mathrm{p}_{y|x}(\mathbf{Y}|\mathbf{X})\mathrm{p}_x(\mathbf{X})}{\mathrm{p}_y(\mathbf{Y})} \tag{2.17}$$

Certain properties of Gaussian random variables and vectors will be of imporantance to us throughout this thesis.

The notation $N(m, \sigma^2)$ will be used in this thesis to denote a random variable, say y, that is Gaussian with mean m and variance σ^2. The PDF of y is

$$\mathrm{p}_y(Y) = \frac{1}{\sqrt{2\pi\sigma^2}} e^{-\frac{(Y-m)^2}{2\sigma^2}} \tag{2.18}$$

The PDF of a Gaussian random variable is completely specified by its first two moments.

A Gaussian random vector is similarly defined by $\mathbf{x} = N(m_{\mathbf{x}}, \Lambda_x)$. Each component of $\mathbf{x}$ is a Gaussian random variable and the Gaussian random vector represents the joint PDF of these random variables.

Further, Gaussianity is preserved under linear operations so that if $\mathbf{x}$ and $\mathbf{y}$ are Gaussian random vectors and

$$\mathbf{z} = A\mathbf{x} + B\mathbf{y} + \mathbf{b} \tag{2.19}$$

then $\mathbf{z}$ is Gaussian with mean

$$m_{\mathbf{z}} = Am_{\mathbf{x}} + Bm_{\mathbf{y}} + \mathbf{b} \tag{2.20}$$

and Covariance matrix

$$\Lambda_z = A\Lambda_x A^T + B\Lambda_y B^T + A\Lambda_{xy} B^T + B\Lambda_{yx} A^T \tag{2.21}$$

where

$$\Lambda_{xy} = \Lambda_{yx}{}^T = \mathrm{E}[(\mathbf{x} - m_{\mathbf{x}})^T(\mathbf{y} - m_{\mathbf{y}})^T] \tag{2.22}$$

Further, if $\mathbf{x}$ and $\mathbf{y}$ are independent Gaussian random vectors then

$$m_{\mathbf{z}} = Am_{\mathbf{x}} + Bm_{\mathbf{y}} + \mathbf{b} \tag{2.23}$$

but the cross Covariance matrix, Λ_{xy}, is zero so that

$$\Lambda_z = A\Lambda_x A^T + B\Lambda_y B^T \tag{2.24}$$

2.5.3 Estimation Techniques

In the earlier section a model-based code that simulated the physics of the induction tool was introduced. In the absence of any measurement noise, we would expect this code to simulate the actual tool response precisely. In reality, however, there is bound to be measurement noise and the actual log data will differ from that yielded by a simulation. The process by which values for the parameters of the model are chosen so as to fit the related simulated response to the observed data is termed estimation. We shall review here the methods of basic or classical estimation theory which basically amounts to estimation of parameters from a vector of observations.

The following are common elements of a classical estimation problem:

1) a vector of parameters, $\mathbf{x}$

2) an observation vector, $\mathbf{y}$, that has a probabilistic mapping from $\mathbf{x}$

3) it is desired to estimate $\mathbf{x}$ based on $\mathbf{y}$.

Depending on whether $\mathbf{x}$ is treated as random or non-random, the estimate of $\mathbf{x}$ is said to be of the Bayesian or non-Bayesian type respectively. In either case the estimate $\hat{\mathbf{x}}$ is a function of the stochastic observation vector, $\mathbf{y}$, and is hence a random vector.

Bayesian Estimation

Bayesian estimates arise from the minimization of the Bayes' risk which is the expected value of a cost function $C(\mathbf{x}, \hat{\mathbf{x}})$. The minimization will yield an estimate that is optimal for that cost assignment.

1) Bayesian Least Squares Estimation (BLSE)[16] assumes the following cost function:

$$C(\mathbf{x}, \hat{\mathbf{x}}) = ||\mathbf{x} - \hat{\mathbf{x}}||^2 \tag{2.25}$$

also referred to as the minimum mean square error criterion. The possibly nonlinear estimate $\hat{\mathbf{x}}_B$ obtained by minimizing the expected value of this cost function is the mean of the a posteriori density $\mathrm{p}_{x|y}(\mathbf{X}|\mathbf{Y})$, i.e., $\hat{\mathbf{x}}_B = \mathrm{E}[\mathbf{x}|\mathbf{y}]$.

2) Bayesian Linear Least Squares Estimation (LLSE)[16] assumes the same cost function as above but has the additional constraint that the estimate must be a linear function of the observation, i.e.,

$$\hat{\mathbf{x}}_L = A\mathbf{y} + \mathbf{c} \tag{2.26}$$

where A and $\mathbf{c}$ are to be obtained from the minimum mean square error criterion.

The advantage of the LLSE is that the estimate requires knowledge of only the second moments of $\mathbf{x}$ and $\mathbf{y}$ instead of their joint probability distribution as the BLSE would require. This simplification may come at the cost of possibly reduced performance. In the Gaussian case, i.e., when $\mathbf{x}$ and $\mathbf{y}$ are jointly Gaussian, $\hat{\mathbf{x}}_L = \hat{\mathbf{x}}_B$.

3) Maximum a Posteriori Estimation (MAP)[16] arises from a Bayes' risk formulation in which all errors are equally bad. The associated cost function is

$$C(\mathbf{x}, \hat{\mathbf{x}}) = \begin{cases} K > 0, & \text{if } \hat{\mathbf{x}} \neq \mathbf{x}; \\ 0, & \text{if } \hat{\mathbf{x}} = \mathbf{x} \end{cases} \tag{2.27}$$

The estimate is obtained by solving the following equations

$$\frac{\partial}{\partial \mathbf{X}} \mathrm{p}_{x|y}(\mathbf{X}|\mathbf{Y}) = \mathbf{0} \tag{2.28}$$

Using Bayes' rule and the fact that the natural logarithm is a non-decreasing function over the set of real numbers, solving the above equation is equivalent to solving

$$\frac{\partial}{\partial \mathbf{X}} \ln \mathrm{p}_{y|x}(\mathbf{Y}|\mathbf{X}) + \frac{\partial}{\partial \mathbf{X}} \ln \mathrm{p}_x(\mathbf{X}) = \mathbf{0} \tag{2.29}$$

A solution of the above is a local maximum if

$$\frac{\partial^2}{\partial \mathbf{X}^2} \mathrm{p}_{x|y}(\mathbf{X}|\mathbf{Y}) < \mathbf{0} \tag{2.30}$$

If multiple maxima exist, the MAP estimate is taken to be the maximum among them.

Non-Bayesian Estimation

In this class of estimation techniques, $\mathbf{x}$ is assumed to be deterministic; i.e., the parameters in $\mathbf{x}$ have unknown constant values. It must be remembered that the estimates will still be non-deterministic because they are functions of random observations. The difference lies in the fact that either because its probability density function is not known or because it is truly so, $\mathbf{x}$ is treated as deterministic in the process of developing an estimation rule.

1) Maximum Likelihood Estimation (ML)[16]

The ML estimate, $\hat{\mathbf{x}}_{ML}$, is chosen to be that value of $\mathbf{x}$ which makes the observation $\mathbf{y}$ the most likely. Therefore

$$\hat{\mathbf{x}}_{ML} = \arg \max_{\mathbf{x}} \mathrm{p}_{y|x}(\mathbf{Y}|\mathbf{X}) \tag{2.31}$$

This is equivalent to solving the ML Equation

$$\frac{\partial}{\partial \mathbf{X}} \ln \mathrm{p}_{y|x}(\mathbf{Y}|\mathbf{X}) = \mathbf{0} \tag{2.32}$$

A solution of the above is a local maximum if

$$\frac{\partial^2}{\partial \mathbf{X}^2} \mathrm{p}_{y|x}(\mathbf{Y}|\mathbf{X}) < \mathbf{0} \tag{2.33}$$

In the event of multiple maxima, the ML estimate is taken to be the largest among them.

It can be seen from Equation 2.29 that the MAP estimate reduces to the ML estimates if $\mathrm{p}_x(\mathbf{X})$ is constant; i.e., the density is uniform, or no prior information of

$\mathbf{x}$ exists.

2) Non Bayesian Least Squares Estimation

In this approach no probabilistic or statistical description of the estimation problem is assumed. It is assumed, however, that the following model exists:

$$\mathbf{y} = \mathbf{h}(\mathbf{x}) + \mathbf{e} \tag{2.34}$$

where:

$\mathbf{y}$ = the observation vector

$\mathbf{x}$ = the vector of unknown parameters

$\mathbf{e}$ = the measurement error vector.

The Least squares estimate is obtained by minimizing $\mathbf{e}\mathbf{e}^T$ This amounts to a component-wise minimization of the square of the error. If in fact it is known that certain observations are more reliable than others then a weighted least squares estimate (WLS) can be constructed that minimizes the quadratic measure $J = \mathbf{e}R^{-1}\mathbf{e}^T$ where R is a weighting matrix that adequately reflects our confidence in the respective observations.

If, in fact, the model is linear, i.e.,

$$\mathbf{y} = H\mathbf{x} + \mathbf{e} \tag{2.35}$$

then the weighted least squares estimate is given by

$$\hat{\mathbf{x}}_{WLS} = (H^T R^{-1} H)^{-1} H^T R^{-1} \mathbf{y} \tag{2.36}$$

This is the non-Bayesian, weighted LLSE.

If the probabilistic description of $\mathbf{e}$ is known, then R^{-1} has the interpretation of being the covariance matrix of $\mathbf{e}$.

Having elaborated on the various types of estimation procedures, it is important to know how an evaluation of the performance of the estimators can be conducted. Three criteria for judging estimator performance are used:

1) bias

2) error covariance

3) mean square error

If we define the estimation error to be

$$\mathbf{e} = \mathbf{x} - \hat{\mathbf{x}}(\mathbf{y}) \tag{2.37}$$

then the bias is given by

$$\mathbf{b} = \mathrm{E}[\mathbf{e}] \tag{2.38}$$

The error covariance matrix is:

$$\Lambda_e(\mathbf{x}) = \mathrm{E}(\mathbf{e} - \mathbf{b})(\mathbf{e} - \mathbf{b})^T \tag{2.39}$$

The (i,i)th element of this matrix is the error variance of the the estimate of the ith parameter in $\mathbf{x}$.

The mean-square estimation error is given by

$$\mathrm{E}[\mathbf{e}\mathbf{e}^T] = \Lambda_e(\mathbf{x}) + \mathbf{b}\mathbf{b}^T \tag{2.40}$$

The following two definitions (from [4]) are made now to facilitate subsequent discussion.

Accuracy is a measure of how close the outcome of a measurement, or a sequence of observations, approaches the *true value* of a specified parameter.

Precision is a measure of how close the outcome of a measurement, or a sequence of measurements, clusters about some *estimated value* of a specified parameter.

Precision implies repeatability of the observations and does not imply accuracy.

If the estimate is known to be biased, then the error variance is a measure of how far from the bias value the estimate can be expected to fall, i.e., the spread of the estimate about a constant offset value. A larger variance would then imply that the chances of the estimate being far from the bias value is larger than if the variance were smaller. The error variance can be thought of therefore as a measure of estimator precision. If, on the other hand, the bias is large then the expected value of

our estimate will be far from the true value and the estimate is said to be inaccurate. Bias is therefore a measure of estimator accuracy. A precise estimator by itself is not necessarily satisfactory because if the bias is large, i.e., the estimator is inaccurate, then the estimates will be clustered about a value that is way off from the true value. Precision when coupled with accuracy makes for a good estimator; i.e., an unbiased estimator with small error variance.

For general nonlinear problems such as the one that will be considered in this thesis it is not usually possible to obtain explicit formulas for the error covariance. For these cases there exists another measure of estimator performance in the form of a matrix inequality that provides a lower bound on the estimation error variance. It is known as the Cramer-Rao lower bound (CRLB)[15] and for an unbiased estimate is given as follows:

$$\Lambda_e(\mathbf{x}) \geq I_y(X) \tag{2.41}$$

where $I_y(X)$ is the Fisher's Information matrix and is given by:

$$I_y(X) = \mathrm{E}[[\frac{\partial}{\partial \mathbf{X}} \ln \mathrm{p}_{y|x}(\mathbf{Y}|\mathbf{X})]^2 | \mathbf{x} = \mathbf{X}] \tag{2.42}$$

$$= \mathrm{E}[[\frac{\partial^2}{\partial \mathbf{X}^2} \ln \mathrm{p}_{y|x}(\mathbf{Y}|\mathbf{X})] | \mathbf{x} = \mathbf{X}] \tag{2.43}$$

If an unbiased estimator satisfies the above equation with equality it is termed efficient. In the linear Gaussian problem this is always the case. Notice that one of the nice features of an analysis of the error covariance using the Cramer-Rao lower bound is that it does not require actual computation of the estimate.

2.5.4 Nonlinear Estimation

Suppose that the measurement vector $\mathbf{y}$ and the vector of parameters $\mathbf{x}$ are related by

$$\mathbf{y} = \mathbf{h}(\mathbf{x}) + \mathbf{v} \tag{2.44}$$

where $\mathbf{h}(\mathbf{x})$ is differentiable and $\mathbf{v}$ is N(0,R) with $R > 0$. This is an example of a nonlinear estimation problem. If $\mathbf{x}$ is assumed to be non-random, the techniques of weighted least squares estimation can be applied to obtain an estimate of $\mathbf{x}$. The estimate is obtained by minimizing the following quadratic measure:

$$J = (\mathbf{y} - \mathbf{h}(\mathbf{x}))^T \mathrm{R}^{-1} (\mathbf{y} - \mathbf{h}(\mathbf{x})) \tag{2.45}$$

This is equivalent to maximizing

$$l(\mathbf{x}) = \mathbf{h}^T(\mathbf{x}) \mathrm{R}^{-1} \mathbf{y} - \frac{1}{2} \mathbf{h}^T(\mathbf{x}) \mathrm{R}^{-1} \mathbf{h}(\mathbf{x}) \tag{2.46}$$

The estimation problem is now a nonlinear optimization problem for the global maxima of $l(\mathbf{x})$.

No straightforward expression for the error covariance is possible in such a problem, and so one of many possible bounds on the error covariance can be considered. It can be shown [16] that for the assumptions of this model, the Cramer-Rao lower bound can be simplified to

$$\Lambda_e(\mathbf{x}) \geq \left(\frac{\partial\, \mathbf{h}^T(\mathbf{x})}{\partial \mathbf{x}} \mathrm{R}^{-1} \frac{\partial \mathbf{h}(\mathbf{x})}{\partial \mathbf{x}}\right)^{-1} \tag{2.47}$$

In principle the estimate of $\mathbf{x}$ is obtained by evaluating $l(\mathbf{x})$ for all values of $\mathbf{x}$ and choosing the maximum. This is hardly a viable approach and in practice what is done is to apply the Gauss-Newton method which assumes that the nonlinear prediction function can be replaced by the first two terms of a Taylor series expansion.

It is hypothesized that a *sufficiently* good estimate $\hat{\mathbf{x}}_0$ of $\mathbf{x}$ exists, so that $\mathbf{h}(\mathbf{x})$

can be expanded into a Taylor series with only the first two terms retained. Thus,

$$\mathbf{h}(\mathbf{x}) \approx \mathbf{h}(\hat{\mathbf{x}}_0) + \frac{\partial \mathbf{h}(\hat{\mathbf{x}}_0)}{\partial \mathbf{x}} \delta \mathbf{x} \tag{2.48}$$

$$\doteq \mathbf{h}(\hat{\mathbf{x}}_0) + \mathbf{H}_x \delta \mathbf{x} \tag{2.49}$$

where

$$\delta \mathbf{x} = \mathbf{x} - \hat{\mathbf{x}}_0 \tag{2.50}$$

Using the above relationships in Equation 2-44 yields

$$\delta \mathbf{y} = \mathbf{H}_x \delta \mathbf{x} + \mathbf{v} \tag{2.51}$$

where

$$\delta \mathbf{y} = \mathbf{y} - \mathbf{h}(\hat{\mathbf{x}}_0) \tag{2.52}$$

This is now a linear estimation problem which can readily be solved as in Equation 2-36 for the required estimate of $\delta \mathbf{x}$. This yields a second estimate, $\hat{\mathbf{x}}_0 + \delta \mathbf{x}$, and the above process of linearization is repeated. This method of solution by successive perturbations, if it converges, does so to a local maxima of $\mathrm{l}(\mathbf{x})$.

The process of finding the global maxima can be conceptually visualized as consisting of two stages. In the first, a coarse search is performed in which the parameter space of $\mathbf{x}$ is coarsely divided up into intervals, then local maximas are found within some of these intervals[3] and a global maxima picked from among them.

Having identified the interval over which the global maxima is to be found, the problem reduces to a local search starting from that point. In the local search the linearization steps are iterated until a reasonable convergence criterion is satisfied.

The success of the above procedure assumes that no error is made in the first, coarse estimation step[4] and that convergence in the local search is guaranteed. The

[3]In practice, the local maximas are computed over a limited set of grid points in the parameter space. The intervals of search are the ones that appear most promising. The trade-off in such an ad hoc procedure is the time saved by searching fewer intervals versus the risk of missing the global peak by choosing too large an interval spacing

[4]with increasing noise variance the probability of such a *global* error increases; this behavior is

fact that an error is global is no indication of its size. A *local* error, made in the final step, where the correct interval has been chosen, could theoretically be as severe.

2.6 Parametric Inversion for the 3 Bed Model

The logging tool measurement set for the model shown in Figure 2-12 was represented by the forward model given in Equation 2-13. The tool response is given exactly by Equation 2-10, but under the assumption of this formation model a fast, approximate forward response model for the DIT is available using Hybres.

The observation vector, $\mathbf{y}$, consists of measurements from three separate channels which penetrate to different radial distances into the formation. Measurements are assumed to be taken at 21 different depth locations. At each depth 3 readings are obtained from the different channels thus yielding 63 measurements over the entire formation. The general form of the observation vector is shown below:

$$\mathbf{y} = \begin{pmatrix} y_1 \\ \vdots \\ y_{21} \\ y_{22} \\ \vdots \\ y_{42} \\ y_{43} \\ \vdots \\ y_{63} \end{pmatrix} \begin{matrix} \left.\begin{matrix} \\ \\ \end{matrix}\right\} \text{Channel 1} \\ \left.\begin{matrix} \\ \\ \\ \end{matrix}\right\} \text{Channel 2} \\ \left.\begin{matrix} \\ \\ \\ \end{matrix}\right\} \text{Channel 3} \end{matrix} \tag{2.53}$$

The measurement noise for the DIT has experimentally been determined to be a Gaussian random vector with a covariance matrix, R. The noise terms are independent, identically distributed within each channel, but their variances are different from one channel to the next. The covariance matrix has therefore the following structure:

---

refered to as the threshold phenomenon in nonlinear estimation problems

$$\mathbf{R} = \begin{pmatrix} \sigma_1{}^2 & 0 & 0 & 0 & 0 \\ 0 & \ddots & 0 & \vdots & \vdots \\ \vdots & 0 & \sigma_2{}^2 & 0 & \vdots \\ \vdots & \vdots & 0 & \ddots & 0 \\ \vdots & \vdots & \vdots & 0 & \sigma_3{}^2 \end{pmatrix} \tag{2.54}$$

where $\sigma_1{}^2$, $\sigma_2{}^2$ and $\sigma_3{}^2$ are the respective error variances for the three channels.

Therefore, the forward response can be represented by

$$\mathbf{y} = \mathbf{h}(\mathbf{p}) + \mathbf{v} \tag{2.55}$$

where:

$\mathbf{y}$ = the vector of observations

$\mathbf{p}$ = the vector of formation parameters

$\mathbf{v}$ = zero mean measurement additive Gaussian noise with covariance matrix R.

In practice, some subset of the parameters in $\mathbf{p}$ may be known beforehand, or the number of available measurements may be insufficient to estimate all the parameters in $\mathbf{p}$. Consequently, $\mathbf{p}$ is often divided into two subsets $\mathbf{x}$ and $\boldsymbol{\theta}$, where $\mathbf{x}$ are the parameters to be estimated and $\boldsymbol{\theta}$ are parameters which are assumed to be known.

In this case, the model in (2.55) may be rewritten as

$$\mathbf{y} = \mathbf{h}(\mathbf{x},\boldsymbol{\theta}) + \mathbf{v} \tag{2.56}$$

where:

$\mathbf{x}$ = vector containing the unknown parameters

$\boldsymbol{\theta}$ = vector of parameters assumed to be known a priori

In this case, the inversion problem may be stated as: given a finite set of noisy measurements $\mathbf{y}$, and a priori knowledge of the parameters $\boldsymbol{\theta}$, estimate the unknown parameters $\mathbf{x}$.

Given the above stochastic model, a choice must be made from the available techniques of estimation. Since the desired formation parameters are assumed to be

MODEL-BASED INVERSION

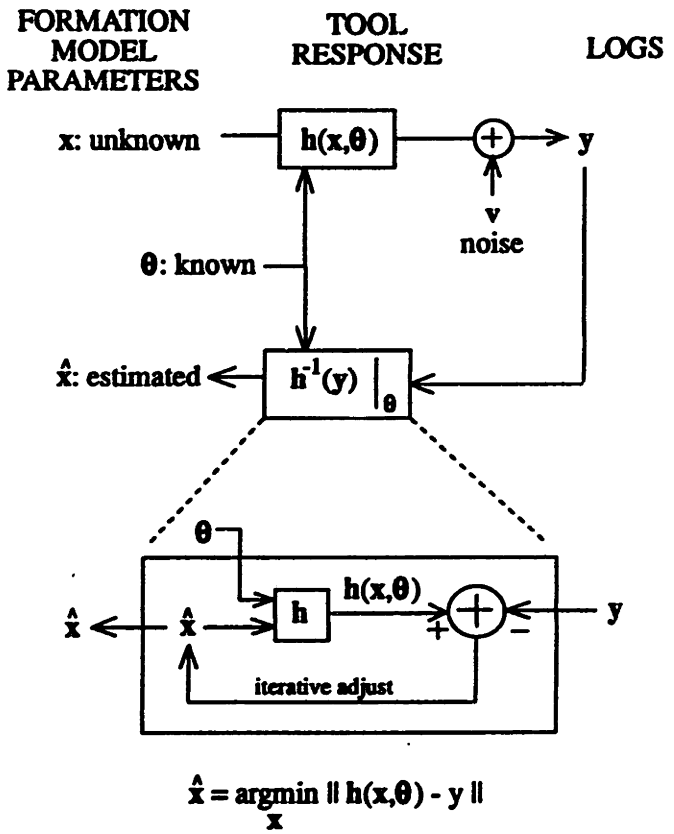

Figure 2-14: Iterative technique for obtaining the estimate of x

unknown constants, a non-Bayesian approach is to be followed. We shall employ the weighted least squares estimate with the weighting matrix being given by R. As indicated earlier this estimate is identical to the ML estimate under the Gaussian noise assumption.

The estimation of x is a nonlinear estimation problem. As was seen in the earlier section, this results in what is essentially a nonlinear optimization problem. A solution of this problem requires an iterative technique as shown in Figure 2-15 . It is assumed here that the parameters in θ are perfectly known. Each successive estimate is passed through the forward model and the predicted response is compared with the actual log. The minimization of this difference over the space of all possible estimates yields a new estimate. This process is continued until the estimation error falls within a tolerable threshold.

In this thesis we shall assume that no global error is made in the above inversion process. This being the case, the estimation process will iteratively seek out values for the estimate that converge to the neighborhood of the true value of the parameter; this is, therefore, a local search problem for a maxima that is known to be the global maxima. Further, it shall be assumed that this iterative procedure has reached a stage in which the estimate is at least so close enough to the true value of the parameter for it to be in the domain of the parameter space for which a linearization of the noise-free tool response about the true value of the parameter can be considered a valid enough representation of the nonlinear function. Mathematically, this is expressed as follows:

If we let $\mathbf{x_0}$ be the true value of the desired parameter, and $\boldsymbol{\theta}_0$ be the known, true value of the nuisance parameters then a Taylor series expansion about these values yields

$$\mathbf{h}(\mathbf{x},\boldsymbol{\theta}_0) = \frac{\partial \mathbf{h}(\mathbf{x_0},\boldsymbol{\theta}_0)}{\partial \mathbf{x}}(\mathbf{x}-\mathbf{x_0}) + \frac{\partial^2 \mathbf{h}(\mathbf{x_0},\boldsymbol{\theta}_0)}{\partial \mathbf{x}^2}(\mathbf{x}-\mathbf{x_0})^2 + \text{higher order terms} \quad (2.57)$$

For certain perturbations, $\delta\mathbf{x}$, where

$$\delta\mathbf{x} = \mathbf{x} - \mathbf{x_0} \quad (2.58)$$

it can be held that

$$\mathbf{h}(\mathbf{x},\boldsymbol{\theta}) \approx \frac{\partial \mathbf{h}(\mathbf{x_0},\boldsymbol{\theta}_0)}{\partial \mathbf{x}}\delta\mathbf{x} \quad (2.59)$$

Let $\delta\mathbf{x}_L$ be the largest perturbation so that the above linearized approximation remains valid. Now, if the i^{th} stage of the iterative adjustment process for the estimate of $\mathbf{x}$ yields the estimate $\hat{\mathbf{x}}_i$, then, defining

$$\delta\mathbf{x}_i = \hat{\mathbf{x}}_i - \mathbf{x_0} \quad (2.60)$$

it is required of the i^{th} and any subsequent stage of the estimation process that

$$|\delta \mathbf{x}_i| \leq |\delta \mathbf{x}_L| \tag{2.61}$$

for it to be a candidate for the analysis performed in this thesis.

Sources of Error:

The parameter whose value is of primary interest is σ_t. In addition, a few parameters like h and T may be of value in other aspects of the interpretation procedure. This subset of parameters are the desired parameters, $\mathbf{x}$; these are the quantities that we would like to estimate. The rest of the parameters are of no direct interest to us, however, knowing them is essential to the estimation of the desired parameters. These parameters are termed the nuisance parameters, $\boldsymbol{\theta}$. In the simple example in which σ_t is the sole parameter of interest, all the remaining parameters are the nuisance parameters and their values need to be obtained (either from the same or different set of log measurements) for an estimation of σ_t to be possible.

- Imprecise knowledge of these nuisance parameters is one of the important corrupting influences on the estimate of σ_t.
- There is in addition the obvious presence of noise in the measurement which will lead to errors in our estimation. This noise may derive from sources having to do with the tool itself; e.g., electronic noise or mechanical noise.
- Furthermore there may be errors due to the choice of model itself. In other words, while it may be true that the formation being considered is bedded and invaded, the beds may in fact be tilted, the invasion profile may not be vertical or symmetric about the borehole axis, the shoulder beds will not be infinite in extent or equal in conductivity, and the borehole wall may be rugose. All these are possible sources of error. It would be of great importance to know how robust the estimation is to these sources of error. Some of these issues are addressed in Chapter 5.

Error Analysis: The shape of things to come

In the procedure of inversion described above two issues arise, including the analysis of **inversion performance** (how well can $\mathbf{x}$ be estimated assuming $\boldsymbol{\theta}$ is perfectly known), and **inversion robustness** (how do errors in knowledge of $\boldsymbol{\theta}$ affect the es-

timate of $\mathbf{x}$). In this thesis we will consider four separate performance/robustness cases which address these two issues.

• Performance Analysis

It shall initially be assumed that $\boldsymbol{\theta}$ is perfectly known. In this case the only source of error is the measurement noise, $\mathbf{v}$. The question to be answered here is: how well can $\mathbf{x}$ be estimated from a finite number of noisy measurements, $\mathbf{y}$?

• Robustness Analysis

It is now assumed that $\boldsymbol{\theta}$ is not perfectly known. The obvious question is: what is the effect of uncertainty in $\boldsymbol{\theta}$ on the estimate of $\mathbf{x}$? It shall be shown that, to first order, the result of imprecision in $\boldsymbol{\theta}$ is an additive bias term in the estimate. We would then be interested in knowing which modelling errors (i.e., layer position errors or invasion depth errors or layer conductivity errors, etc) cause the largest bias?

• Multiparameter Estimation: (performance analysis)

If it is established from the robustness analysis that the bias produced by imprecise knowledge of the parameters in $\boldsymbol{\theta}$ is the dominant source of error in the estimation, then the estimation of some or all of the parameters in $\boldsymbol{\theta}$ may become necessary. If this multiparameter estimation is carried out then our estimates of the nuisance parameters ought to be more precise than before; as such, the bias introduced into the estimate of $\mathbf{x}$, on average, ought to be less. This enhanced accuracy in $\boldsymbol{\theta}$, however, comes at the cost of less precision in the estimate of $\mathbf{x}$. We would like to have a means of mathematically evaluating this trade-off.

• Auxiliary measurements

It is possible that somewhere in the overall interpretation procedure auxiliary information on some of the parameters within $\boldsymbol{\theta}$ may become available. First of all, it would be of importance to know how such additional sources of information would be folded into the existing estimation framework. Then, an analysis of estimator performance, in the light of this auxiliary information, should be conducted. A comparison of the performance analyses with and without the auxiliary information would then provide a means for determining the requisite worthiness of any further source of information to be of any value in improving estimator performance.

Each of the above mentioned issues shall be addressed in the forthcoming chapters.

The above study was conducted for 5 different choices of operating points (cases A-E) corresponding to commonly encountered geophysical formations. Chapters 3 and 4 focus on the results of one such choice of operating point, Case E, which will be described in detail in the next chapter. A few of the results of the other cases will be discussed in Chapter 5 with a view to displaying how these results complement the conclusions made about the results obtained under a different assumption of operating point.

Chapter 3

Sensitivity Analysis

3.1 Introduction

The preceding sections have served to explain the equation

$$\mathbf{y} = \mathbf{h}(\mathbf{x},\boldsymbol{\theta}) + \mathbf{n} \tag{3.1}$$

in the context of the induction logging tool. In addition, the process of inversion, i.e, obtaining an estimate of $\mathbf{x}$ from noisy measurements, $\mathbf{y}$ was discussed. It was seen that the process of estimating $\mathbf{x}$ became, in essence, a nonlinear optimization problem which required as its solution the unique maxima of a nonlinear likelihood function. The solution involved a three step procedure in which the parameter space of $\mathbf{x}$ is coarsely divided up into regions. The local maximas of the function are obtained in some promising intervals and the global maxima is picked from among these. This corresponds to an M-ary Hypothesis testing problem for the global peak of the function. What we obtain for the maxima, however, is assumed to be a coarse approximation to the true value. The problem then becomes a local search for the true value. From this point on in the thesis, the attention will be on a performance and robustness analysis of this stage of the estimation process.

In this chapter it shall first be assumed that the parameters in $\boldsymbol{\theta}$ are perfectly known. An estimator for $\mathbf{x}$ will be developed and a performance analysis will be undertaken. In this case measurement noise is the only source of error in the estimation,

and this performance analysis will provide an upper bound on achievable performance when noise is not the only complicating factor. In the second part of the analysis it shall be assumed that the parameters in θ are imprecisely known. This is a more realistic assumption. Now it is desired to determine the error that such imprecision in the knowledge of the parameters introduces into the estimation. This is done by employing the imprecise parameters in θ in the estimator rule developed under the assumption of precisely known θ. If the estimate so obtained is close enough to the one obtained by using precise values of θ, it can then be concluded that the estimate is robust to imprecisions or perturbations in the parameters of θ. An analysis along these lines constitutes a robustness analysis.

Together these analyses constitute a sensitivity analysis. The common thread between the two components is that the performance and robustness analysis are both conducted on an estimator that assumes for its development that θ is perfectly known. The overall result is to determine the sensitivity of an estimator engineered under such an assumption to the effects of measurement noise and imprecisions in the parameters assumed known.

The initial sensitivity analysis conducted in this chapter will set the stage for a multiparameter estimation approach to the problem in which the performance of a multiparameter estimator will be analyzed under the assumption that θ is imperfectly known.

3.2 Performance Analysis

It will initially be assumed that the parameters in θ are perfectly known, and a performance analysis of the estimate $\mathbf{x}$ will be undertaken. While such an idealized situation will never exist in practice, the purpose of such an investigation will be to determine what the estimator performance will be in the best of all scenarios. Therefore, it will provide an upper bound on optimistic estimator performance. Also, it characterizes performance with noise being the sole degrading factor. As such, it serves as a useful benchmark to be compared with future results obtained for cases where measurement noise is not the only complicating factor.

3.2.1 Mathematical Development

Performance Analysis: Error variance of the estimate of $\mathbf{x}$ assuming $\boldsymbol{\theta}$ is perfectly known.

To begin, denote the true values of $\mathbf{x}$ and $\boldsymbol{\theta}$ as $\mathbf{x_0}$, $\boldsymbol{\theta_0}$ and let $\mathbf{y_0}$ be the noise-free response to $\mathbf{x_0}$,$\boldsymbol{\theta_0}$, i.e.,

$$\mathbf{y_0} = \mathbf{h}(\mathbf{x_0},\boldsymbol{\theta_0}) \tag{3.2}$$

We consider $\mathbf{x}$ and $\mathbf{y}$ to be perturbations about $\mathbf{x_0}$ and $\mathbf{y_0}$

$$\mathbf{x} = \mathbf{x_0} + \delta\mathbf{x} \tag{3.3}$$

$$\mathbf{y} = \mathbf{y_0} + \delta\mathbf{y} \tag{3.4}$$

Linearizing about the operating point $\mathbf{x_0}$,$\boldsymbol{\theta_0}$, and ignoring second and all higher order terms yields

$$\delta\mathbf{y} \approx \frac{\partial \mathbf{h}(\mathbf{x_0},\boldsymbol{\theta_0})}{\partial \mathbf{x}}\delta\mathbf{x} + \mathbf{v} \tag{3.5}$$

$$\doteq H_x\delta\mathbf{x} + \mathbf{v} \tag{3.6}$$

It is assumed that the perturbations in (3.3) and (3.4) are small enough to ensure that the approximation in (5) remains valid.

The weighted least-squares estimate for $\delta\mathbf{x}$ with respect to the weighting matrix R, (also the maximum likelihood estimate under the assumption that $\mathbf{v}$ is zero-mean Gaussian noise of variance R), given noisy measurements of $\delta\mathbf{y}$[16] is

$$\delta\hat{\mathbf{x}}_{WLS} = {F_1}^{-1}{H_x}^T R^{-1}\delta\mathbf{y} \tag{3.7}$$

where F_1 is the Fisher's information matrix[15],

$$F_1 = (H_x{}^T R^{-1} H_x) \tag{3.8}$$

Substituting (3.6) into (3.7),

$$\delta\hat{\mathbf{x}}_{WLS} = \delta\mathbf{x} + F_1{}^{-1} H_x{}^T R^{-1}\mathbf{v} \tag{3.9}$$

The weighted least squares estimate of $\delta\mathbf{x}$ is seen to be the true $\delta\mathbf{x}$ plus a zero mean Gaussian variable whose variance is the same as the variance of $\delta\hat{\mathbf{x}}_{WLS}$, and is given by the Cramer-Rao lower bound [15],

$$CRB_1 = F_1{}^{-1} \tag{3.10}$$

The Cramer-Rao lower bound will enable us to evaluate the effect of electronic measurement noise, $\mathbf{v}$, on the estimate of the true conductivity in the electrical borehole logging problem.

As indicated earlier, σ_t is assumed to be the only desired parameter of interest at this stage of the analysis, so that:

$$\mathbf{x} = \{\sigma_t\}, \text{ and } \boldsymbol{\theta} = \{\sigma_s, \sigma_{xo}, \sigma_m, h, T, r, \mathbf{z}\}$$

In this case the Fisher's information matrix is a scalar:

$$F_1 = \Big(\frac{\partial \mathbf{h}(\mathbf{x_0}, \boldsymbol{\theta_0})}{\partial \sigma_t}\Big)^T R^{-1} \Big(\frac{\partial \mathbf{h}(\mathbf{x_0}, \boldsymbol{\theta_0})}{\partial \sigma_t}\Big) \tag{3.11}$$

The weighted least squares estimate of $\delta\sigma_t$ is given by:

$$\delta\hat{\sigma}_{tWLS} = \delta\sigma_t + \Big(\Big(\frac{\partial \mathbf{h}(\mathbf{x_0}, \boldsymbol{\theta_0})}{\partial \sigma_t}\Big)^T R^{-1} \Big(\frac{\partial \mathbf{h}(\mathbf{x_0}, \boldsymbol{\theta_0})}{\partial \sigma_t}\Big)\Big)^{-1} \Big(\frac{\partial \mathbf{h}(\mathbf{x_0}, \boldsymbol{\theta_0})}{\partial \sigma_t}\Big)^T R^{-1}\mathbf{v} \tag{3.12}$$

The Cramer-Rao bound for this single parameter estimation case reduces to:

$$\text{Error Variance}\,(\hat{\sigma}_{tWLS}) = CRB_1 = \frac{1}{F_1} \tag{3.13}$$

3.2.2 Results and Analysis

The CRLB on the error variance of the estimate of σ_t is computed as a function of T and h with all other parameters fixed. Such an approach makes it possible to compare the performance of the estimator for different formation geometries of interest that the chosen model supports. For example, the error variance of the estimate of σ_t for a thin bed with shallow invasion (i.e., T and h both small) can be compared with that obtained for a thicker bed with deeper invasion (i.e., T and h both large).

As indicated earlier, the operating point of the forward model is chosen to be that of Case E. The operating point is:

- $\sigma_t = 0.05$mho
- $\sigma_s = 0.2$mho
- $\sigma_{xo} = 0.5$mho
- $\sigma_m = 1$mho

  (The above choice of conductivities corresponds to a commonly encountered physical situation in which a less conductive sand bed is surrounded by more conductive shoulder beds of shale. Since sand is permeable and shale is not, the central sand bed suffers invasion. The invading fluid is more conductive than the virgin sand bed and creates an invaded zone which is ten times more conductive than the uninvaded zone. The wellbore itself contains conductive mud.)

- $r = 5$ inches
- $\mathbf{z} = 21$ samples every 6 inches (i.e., $delz = 6$ inches)
- h and T vary over the following ranges:

- h = 0 to 50 inches (in 5 inch increments)
- T = 1 to 10 feet (in 1 foot increments)

Each value of h and T corresponds to a single operating point. Therefore, Case E corresponds to the family of operating points in which the conductivities in the different zones of the model take on the fixed values specified above, while the geometry of the model itself varies over the range specified by h and T above.

Figure 3-1(a) shows that the error variance of σ_t decreases as T increases. This seems reasonable, because as T increases, the contribution of σ_t to the signal energy detected by the tool increases. On the other hand when T is small and h is large, i.e., the center bed is thin and has suffered deep invasion during drilling, it can be seen that the estimator performance is at its worst. The second Figure 3-1(b) shows the same surface, but with the standard deviation (St.Dev) of the error on σ_t expressed as a percentage of the true value of σ_t. In other words:

$$\%\text{St.Dev of error} = \frac{\sqrt{\text{Error Variance}}}{\sigma_{t0}} \times 100 \tag{3.14}$$

where σ_{t0} is the true value of σ_t.

Figure 3-2 shows the CRLB as a function of T for a set of four different invasion depths. It is evident that the effect of invasion is to reduce estimator performance; this deterioration is more evident in thinner beds. This is because for thin beds with deep invasion, the relative proportion of the uninvaded zone that falls within the range of investigation of the induction tool is at a minimum.

Certainly, then, in this scenario where the tool 'sees' σ_s as its major contributor, followed by σ_{xo} (σ_t contributes least of all), if the values of σ_s and σ_{xo} are very different from σ_t, (i.e., the associated conductivity contrasts are *high*), we would be in the very worst of all performance scenarios, while if the values of σ_s and σ_{xo} are reasonably close to σ_t, (i.e., the conductivity contrasts are *low*), we should hope to see better performance.

It can be seen that at worst the estimator has an error variance of 0.6 percent of the true value of σ_t. This tells us that under the assumption of perfect knowledge of

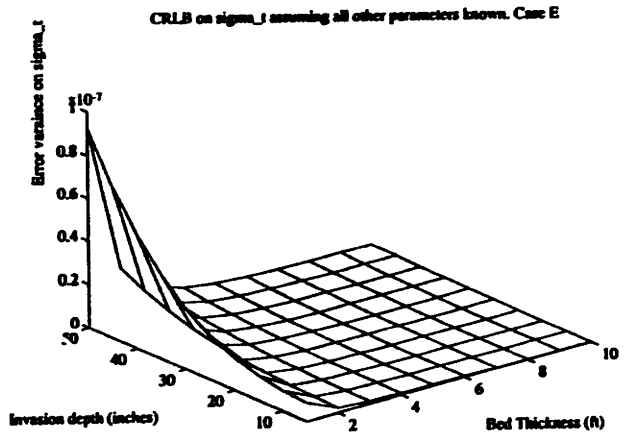

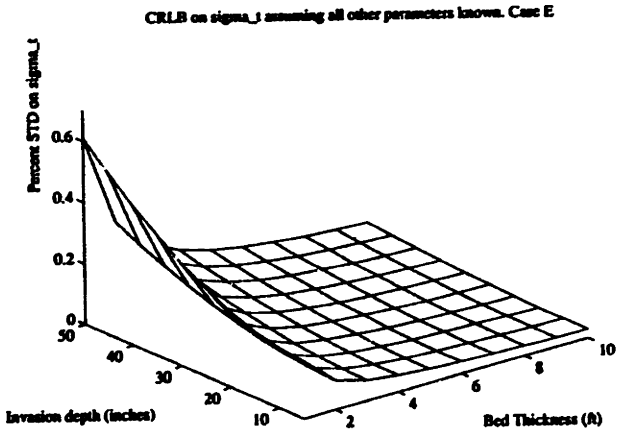

Figure 3-1: Cramer-Rao Lower Bound on σ_t assuming all other parameters are known

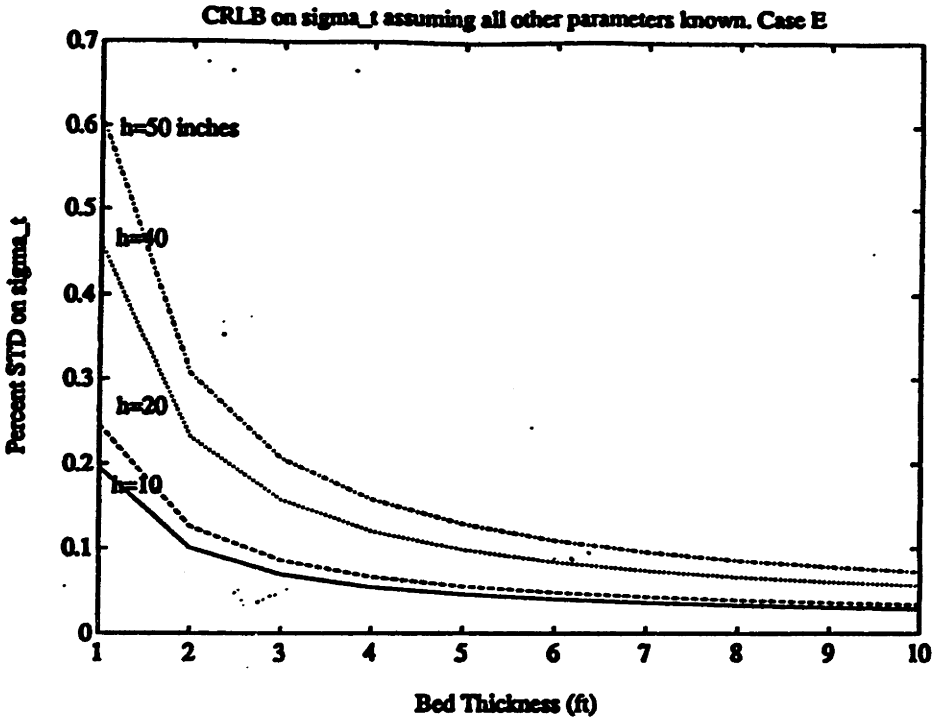

Figure 3-2: Cramer-Rao Lower Bound on σ_t for various invasion depths, assuming all other parameters are known

the nuisance parameters, and for this particular choice of operating point family, the estimate of σ_t can never be more than 0.6 percent of the true value of σ_t off from the true value. Further, in actuality, the bed thicknesses that are usually encountered in logging are more than 2 feet thick and therefore the estimate will be even less than 0.6 percent off from its true value. The results obtained for Cases A through D[1] reveal that not too dissimilar a performance can be expected on the whole even for the cases where the contrast of conductivities is considerably different from that considered in Case E.

Such performance indicates that for reasonably thick beds with modest invasion, we can expect to obtain estimates of σ_t that are almost pinpoint in their accuracy and precision, as long as the nuisance parameters are exactly known. The presence of electronic measurement noise, by itself, is not the major factor that leads to error in the estimation.

[1] A survey of the key results for the other cases will be presented in Chapter 5

3.3 Robustness Analysis

It will now be assumed that $\boldsymbol{\theta}$ is known to within some degree of precision. This is a more realisitic assumption because, in practice, some of the parameters in $\boldsymbol{\theta}$ are obtained from other measurements and the rest from a successive estimation procedure like the one used to obtain $\mathbf{x_0}$. As such, there is bound to be an error in the estimation of $\boldsymbol{\theta}$.

What the following analysis aims to do is to analyse the effect of imprecise knowledge of $\boldsymbol{\theta}$ on the estimate of $\mathbf{x}$ and to compare the error produced in the estimate of $\mathbf{x}$ by such imprecision in $\boldsymbol{\theta}$ with that produced by the noise alone. The entire procedure will enable us to establish whether or not the estimation error is noise driven or bias driven, i.e., whether the error variance due to noise or the bias produced due to parameter imprecision is the dominant source of estimation error. Further, it will allow us to determine to which of the parameters within $\boldsymbol{\theta}$ the estimate of $\mathbf{x}$ is most sensitive, or conversely, to the imprecisions in which parameters within $\boldsymbol{\theta}$ the estimation is fairly robust.

3.3.1 Mathematical Development

Robustness Analysis: Effect of imprecise knowledge of $\boldsymbol{\theta}$ on the estimate of $\mathbf{x}$.

Suppose $\boldsymbol{\theta}$ is not precisely known a priori. Let $\boldsymbol{\theta}$ correspond to a perturbation about $\boldsymbol{\theta_0}$,

$$\boldsymbol{\theta} = \boldsymbol{\theta_0} + \delta\boldsymbol{\theta} \tag{3.15}$$

Assuming the second and higher order terms are negligible, the following linearized measurement model is obtained

$$\delta\mathbf{y} \approx \frac{\partial \mathbf{h}(\mathbf{x_0}, \boldsymbol{\theta_0})}{\partial \mathbf{x}} \delta\mathbf{x} + \frac{\partial \mathbf{h}(\mathbf{x_0}, \boldsymbol{\theta_0})}{\partial \boldsymbol{\theta}} \delta\boldsymbol{\theta} + \mathbf{v} \tag{3.16}$$

$$\doteq H_x \delta\mathbf{x} + H_\theta \delta\boldsymbol{\theta} + \mathbf{v} \tag{3.17}$$

It shall be assumed that the perturbations are small enough to ensure that the approximation in (3.16) is valid. Substituting (3.17) into (3.7):

$$\delta\hat{\mathbf{x}}_{WLS} = \delta\mathbf{x} + F_1^{-1} H_x^T R^{-1} H_\theta \delta\boldsymbol{\theta} + F_1^{-1} H_x^T R^{-1} \mathbf{v} \tag{3.18}$$

$$= \delta\mathbf{x} + F_1^{-1} M_2 \delta\boldsymbol{\theta} + F_1^{-1} H_x^T R^{-1} \mathbf{v} \tag{3.19}$$

where

$$M_2 = H_x^T R^{-1} H_\theta \tag{3.20}$$

The weighted least squares estimate $\delta\hat{\mathbf{x}}_{WLS}$ is in this case equal to the true value $\delta\mathbf{x}$ plus two terms: a bias term, $\mathbf{b} = F_1^{-1} M_2 \delta\boldsymbol{\theta}$, and a zero mean Gaussian random variable.

The formulation provided in (3.15)-(3.20) is used to evaluate the size of the overall bias, $\mathbf{b}$, due to imprecise knowledge of any or all of the model parameters in $\boldsymbol{\theta}$. Since the bias term can be expressed as the sum of the individual biases it is possible to consider the individual contribution to the overall bias produced by imprecise knowledge of the bed thickness, T, invasion depth, h, tool positions, $\mathbf{z}$, shoulder conductivity, σ_s, mud conductivity, σ_m, and the conductivity of the invaded zone, σ_{xo}.

This makes it possible to identify those parameters within $\boldsymbol{\theta}$ to which the estimate of $\mathbf{x}$ is extremely sensitive, i.e., those parameters which produce a large bias in the estimate of σ_t for a small perturbation in their magnitude. These will play an important role as additional parameters to be estimated in the next chapter.

As in the preceding analysis, we have:

$$\delta\mathbf{x} = \{\delta\sigma_t\}, \text{ and } \delta\boldsymbol{\theta} = \{\delta\sigma_s, \delta\sigma_{xo}, \delta\sigma_m, \delta h, \delta T, \delta r, \delta\mathbf{z}\} \tag{3.21}$$

Two approaches are considered. In the first $\delta\boldsymbol{\theta}$ is assumed to be non-random, i.e., a vector of unknown constants, and in the second it is assumed to be random with a specified probabilistic description.

3.3.2 Results and Analysis

Non-random Perturbations

The formulation developed above is used to arrive at the total bias, b, due to imprecise knowledge of any or all of the model parameters in $\boldsymbol{\theta}$.

From Equation (3.19), the bias term is

$$\mathbf{b} = F_1^{-1} M_2 \delta\boldsymbol{\theta} \tag{3.22}$$

$$= F_1^{-1}(M_{2T}|M_{2h}|\ldots|M_{2\theta_i}|\ldots|M_{2r}) \begin{pmatrix} \delta T \\ \delta h \\ \vdots \\ \delta\theta_i \\ \vdots \\ \delta r \end{pmatrix} \tag{3.23}$$

$$= \sum_{i=1}^{n} F_1^{-1} M_{2\theta_i} \delta\theta_i \tag{3.24}$$

where N is the number of parameters within $\boldsymbol{\theta}$ that are imprecisely known.

Since the bias term can be expressed as the sum of the individual biases, it is possible to consider the individual contribution to the overall bias introduced by imprecise knowledge of any one parameter θ_i.

The first part of the following robustness analysis concerns itself with the actual bias introduced in the estimate due to imprecisions in each parameter. The second component of the analysis is directed at determining whether noise or bias is the major degrading factor in estimator performance.

Bias Factor due to unit fractional perturbation in T

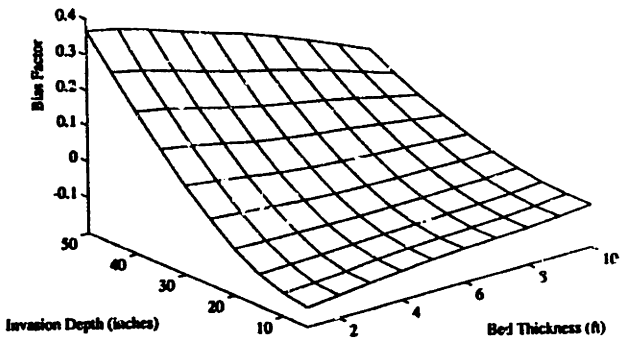

Bias Factor (absolute) due to unit fractional perturbation in T

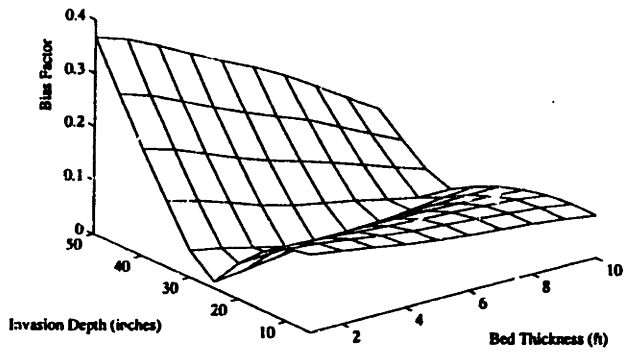

Bias Factor due to unit fractional perturbation in sigma_xo

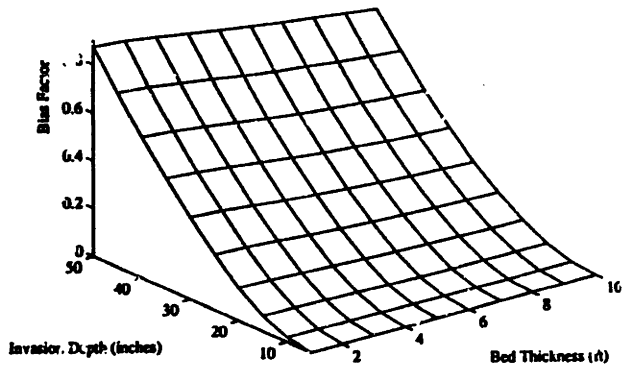

Bias Factor due to unit fractional perturbation in h

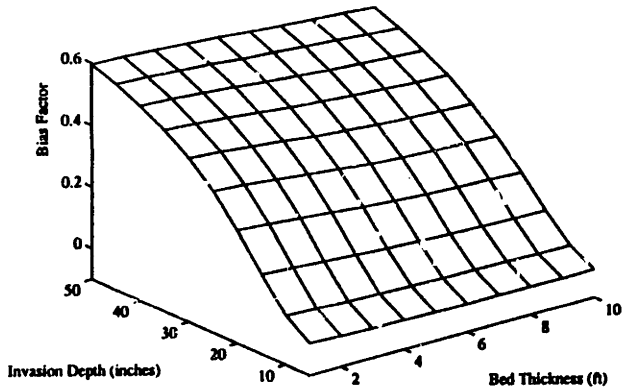

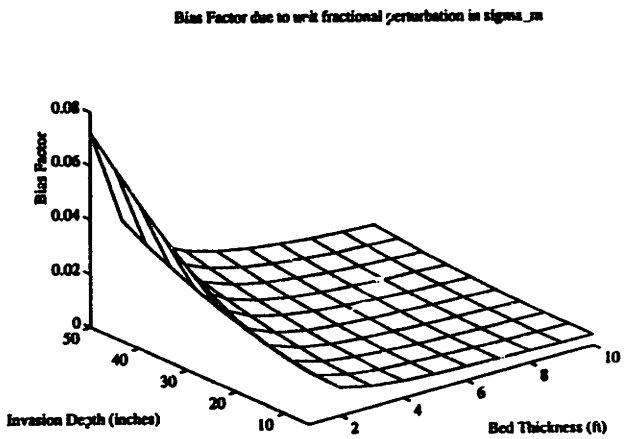

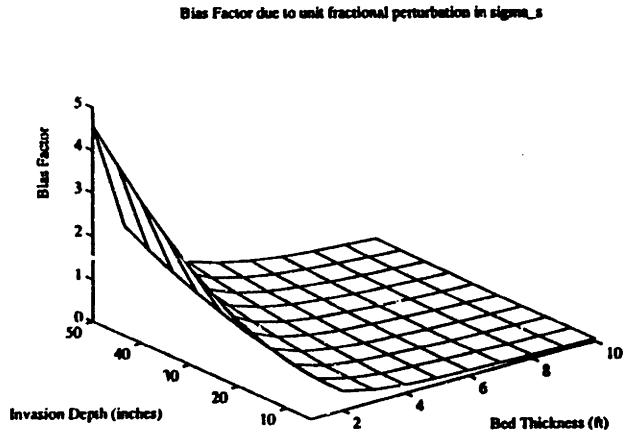

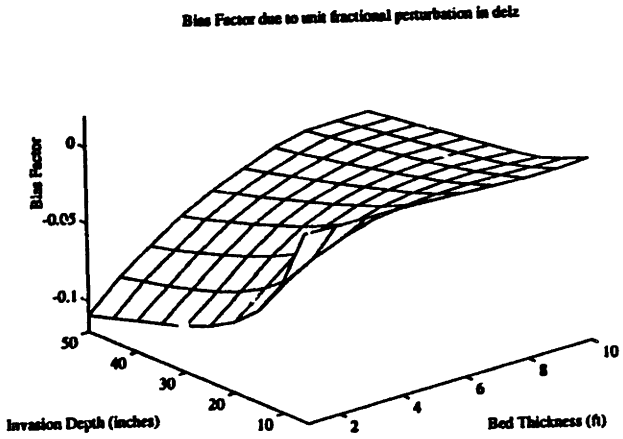

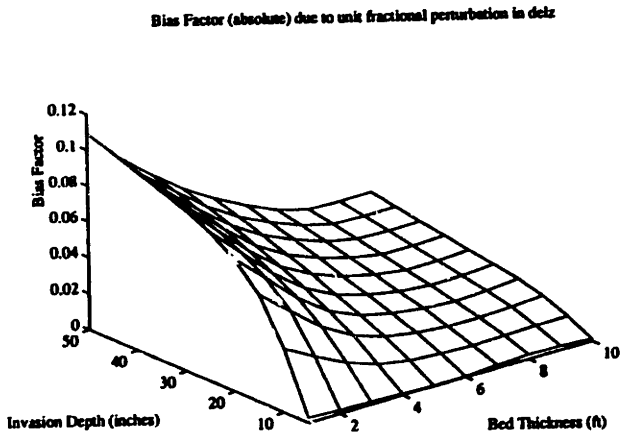

Figure 3-3: Bias Factors for the various parameters

• **Part 1**

From Equation (3.24)

$$\mathbf{b} = \sum_{i=1}^{n} F_1^{-1} M_{2\theta_i} \delta\theta_i \tag{3.25}$$

can be expressed as

$$\mathbf{b} = \sum_{i=1}^{n} \underbrace{F_1^{-1} M_{2\theta_i} \theta_i}_{\mathrm{G}_{\theta_i}=\text{Bias Factor}} \left(\frac{\delta\theta_i}{\theta_i}\right) \tag{3.26}$$

$$= \sum_{i=1}^{n} \mathrm{G}_{\theta_i} \left(\frac{\delta\theta_i}{\theta_i}\right) \tag{3.27}$$

where $\mathrm{G}'_{\theta_i}s$ are defined to be Bias Factors. They are termed bias factors because the bias produced by a perturbation in any given parameter can be derived from a simple linear operation on the associated bias factor of the parameter. Hence, an x% perturbation in θ_i will result in a bias in the estimate of magnitude $|\frac{x}{100} \times \mathrm{G}_{\theta_i}|$.

Figure 3-3 (a)-(h) shows the bias factors obtained for the parameters in $\boldsymbol{\ell}$ assuming the operating points in Case E. For T and $delz$, negative values are observed for a certain subspace of the parameter space, and for these two cases, the absolute bias factors are also displayed.

For the purposes of illustration, assume that the imprecision in each parameter is 1 percent of its true value[2] . The resulting bias introduced is examined for the cases of shallow (h = 10 inches), medium (h = 20 inches) and deep (h = 50 inches) invasion, in Figures 3.4(a)-(c). It must be remembered that the overall bias introduced in the estimate is the sum of all these individual bias terms.

[2]This will obviously not be the case in general. Different parameters will be known to different degrees of precision depending on the quality of the a priori knowledge of their values or the worthiness of the estimation procedure by which they are obtained. A more realistic scenario, in which the degree of precision of their a priori known values varies, will be considered in Chapter 5

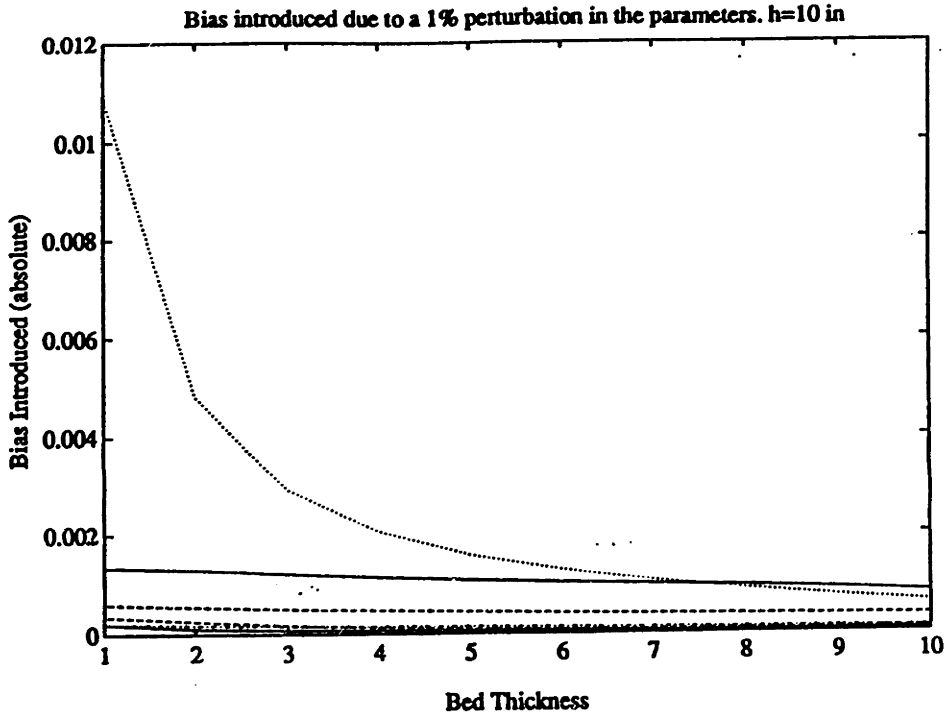
Bias introduced due to a 1% perturbation in the parameters. h=10 in
0.012
0.01
0.008
0.006
0.004
0.002
0
Bias Introduced (absolute)
1
2
3
4
5
6
7
8
9
10
Bed Thickness

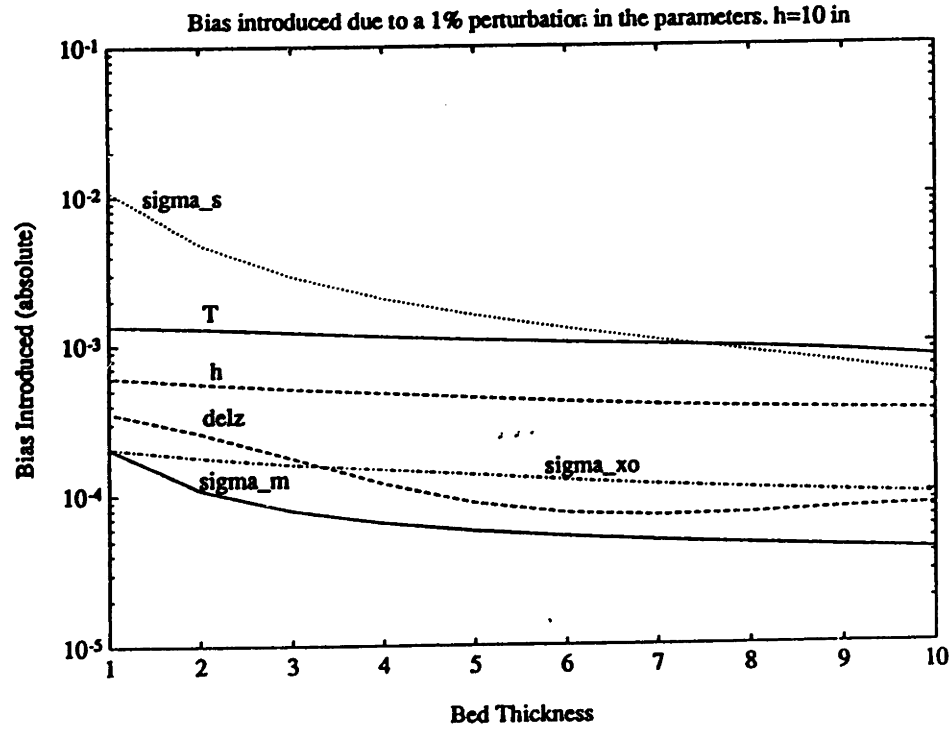
Bias introduced due to a 1% perturbation in the parameters. h=10 in
10-1
10-2
10-3
10-4
10-5
Bias Introduced (absolute)
sigma_s
T
h
delz
sigma_xo
sigma_m
1
2
3
4
5
6
7
8
9
10
Bed Thickness

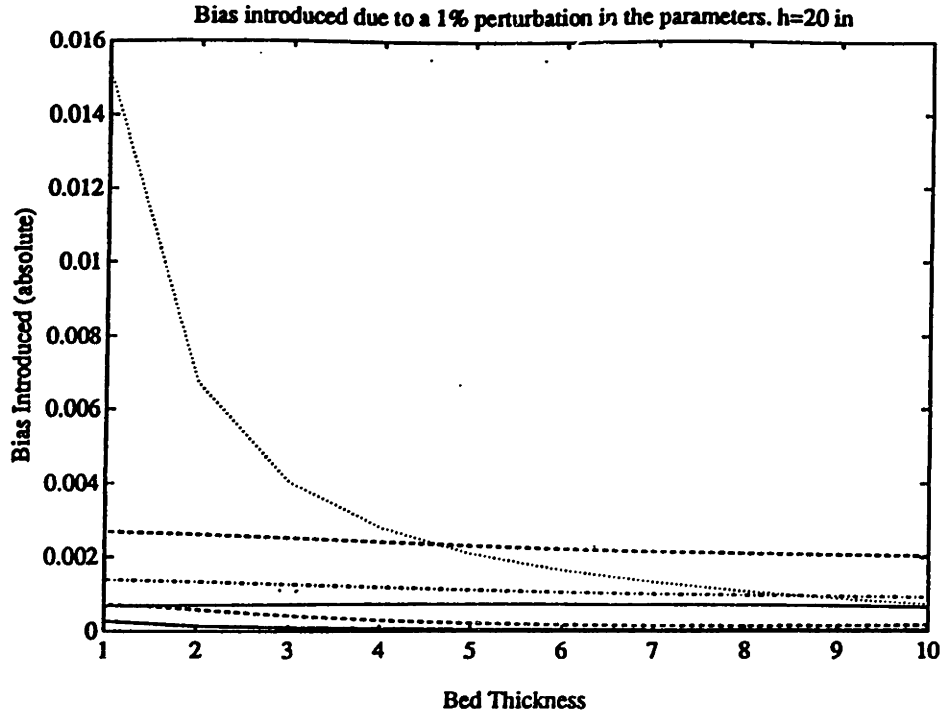
Bias introduced due to a 1% perturbation in the parameters. h=20 in
Bias Introduced (absolute)
0.016
0.014
0.012
0.01
0.008
0.006
0.004
0.002
0
1
2
3
4
5
6
7
8
9
10
Bed Thickness

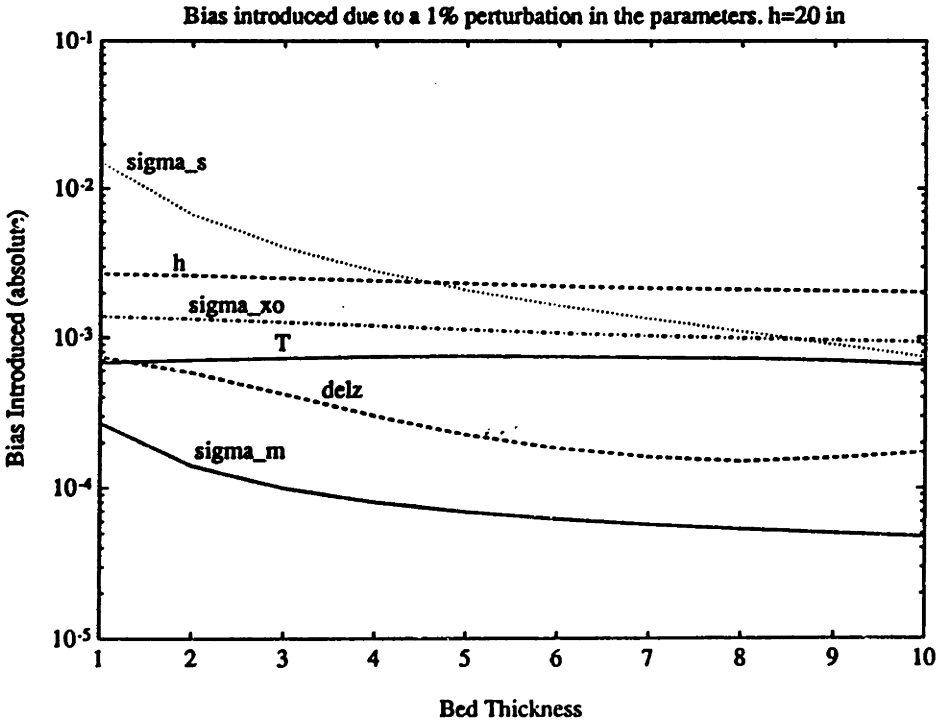
Bias introduced due to a 1% perturbation in the parameters. h=20 in
Bias Introduced (absolute)
10-1
10-2
10-3
10-4
10-5
sigma_s
h
sigma_xo
T
delz
sigma_m
1
2
3
4
5
6
7
8
9
10
Bed Thickness

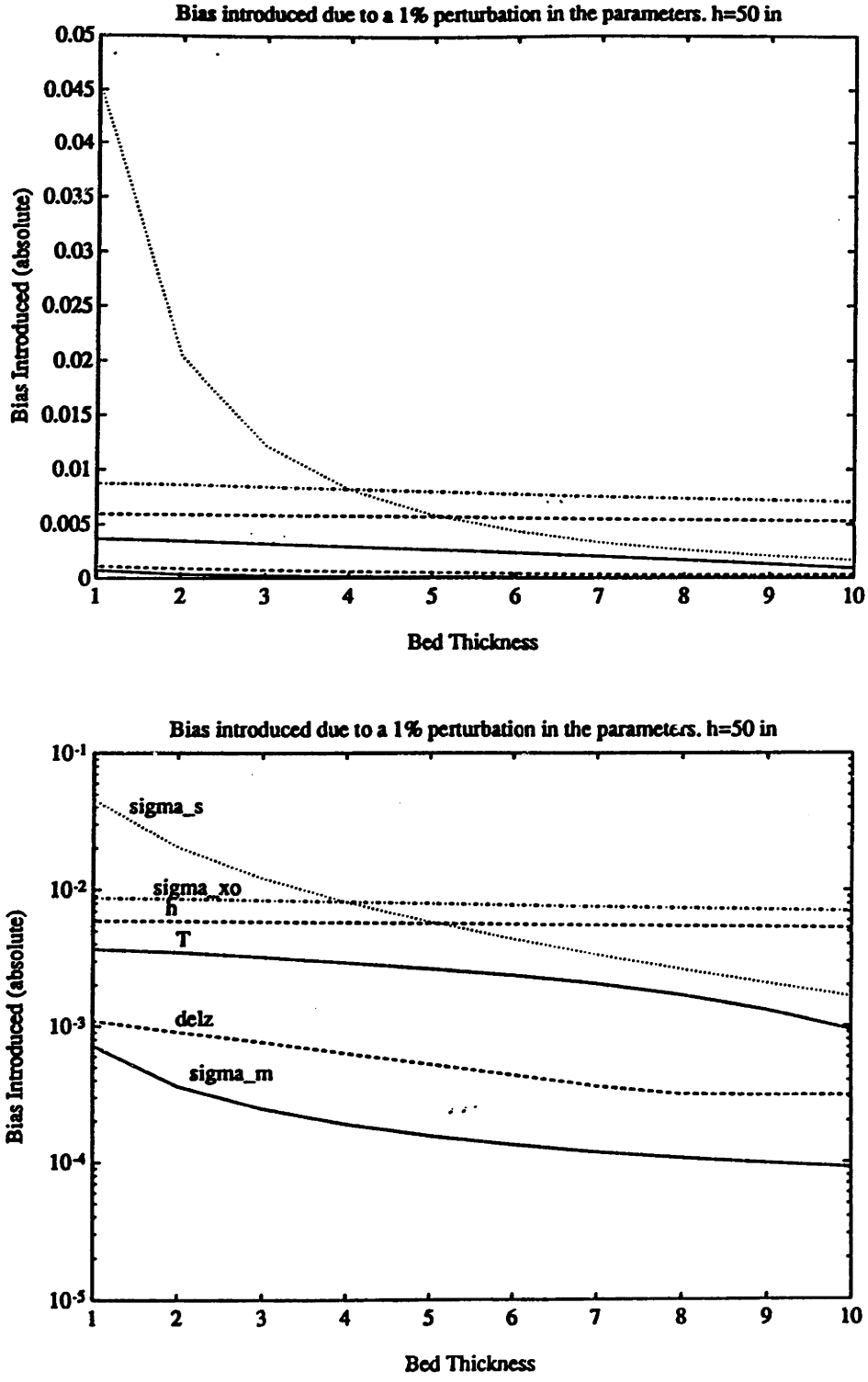

Figure 3-4: Bias introduced into the estimate of σ_t due to a 1% perturbation in the parameters, examined for 3 different invasion depths

It can be seen that as the depth of invasion increases, the relative contribution to the overall bias by h and σ_{xo}, the parameters associated with invasion, increases. In fact, as is exemplified in Figure 3-4(c), for thick enough beds ($T > 5$feet), the bias introduced by these two factors is larger in magnitude than that due to σ_s. This is because, for large T, the contribution of σ_s to the signal received by the tool is less. Further, for larger h, the contribution of σ_{xo} to the total signal increases, and the corresponding bias introduced due to imprecision in it is that much larger.

In all of the above, it must be remembered that the relative importance of the parameters from the point of view of 'sensitivity' (as measured by the bias introduced per unit perturbation), is very much a function of the family of operating points being considered. For a different choice of operating points we may obtain different sensitivity results. The above analysis provides a rule for determining a ranking of the parameters by their sensitivity given reasonable knowledge of the operating point. As we shall see, this is critical in determining the future course of action in estimating $\delta\mathbf{x}$.

As a final observation, it can be seen that the bias introduced by imprecision in σ_m and $delz$, the tool position, is much less than that due to the other parameters, and is fairly independent of the depth of invasion, h.

• **Part 2**

The objective of this part of the robustness analysis is to determine whether the estimation is bias or noise driven.

This is done as follows:

1) The bias introduced in the estimate by each parameter is set equal to the standard deviation of the estimate in (3.9). (This estimator assumes no bias, because the nuisance parameters are assumed to be known exactly. The estimation error in this case is solely due to the noise.)

i.e.,

$$b_{\theta_i} = \mathrm{G}_{\theta_i}\left(\frac{\delta\theta_i}{\theta_i}\right) = \sqrt{F_1^{-1}} \tag{3.28}$$

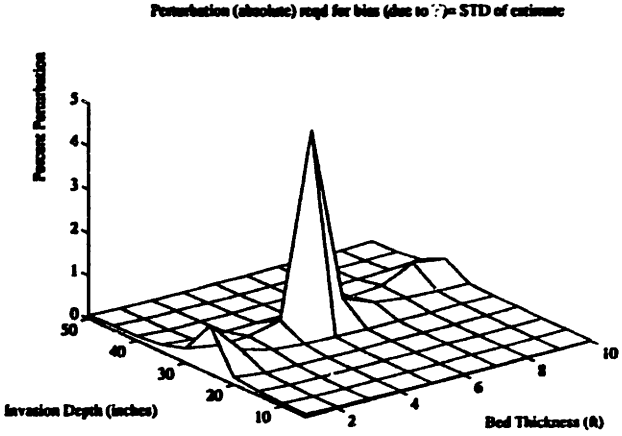
Perturbation (absolute) reqd for bias (due to ?)= STD of estimate
Percent Perturbation
5
4
3
2
1
0
50
40
30
20
10
Invasion Depth (inches)
2
4
6
8
10
Bed Thickness (ft)

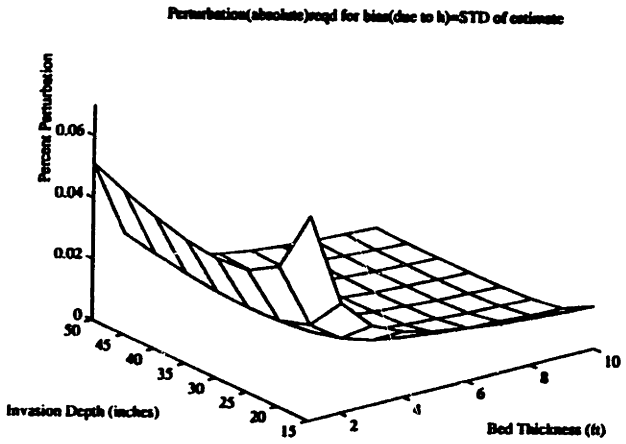
Perturbation(absolute)reqd for bias(due to h)=STD of estimate
Percent Perturbation
0.06
0.04
0.02
0
50
45
40
35
30
25
20
15
Invasion Depth (inches)
2
6
8
10
Bed Thickness (ft)

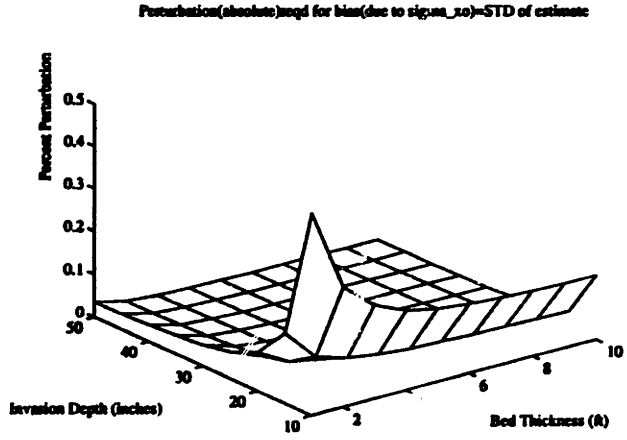
Perturbation(absolute)reqd for bias(due to sigma_xo)=STD of estimate
Percent Perturbation
0.5
0.4
0.3
0.2
0.1
0
50
40
30
20
10
Invasion Depth (inches)
2
6
8
10
Bed Thickness (ft)

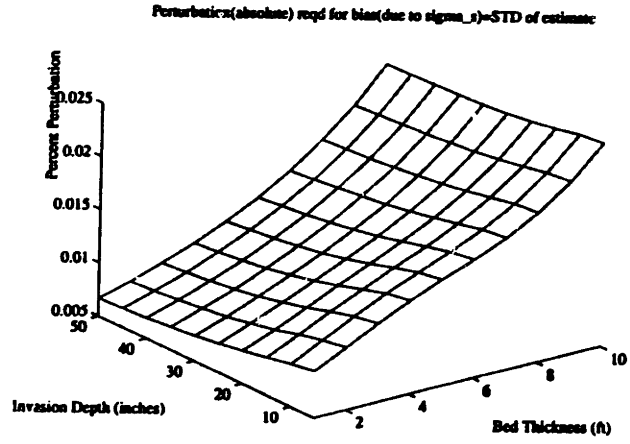
Perturbation(absolute) reqd for bias(due to sigma_s)=STD of estimate
Percent Perturbation
0.025
0.02
0.015
0.01
0.005
50
40
30
20
10
Invasion Depth (inches)
2
4
6
8
10
Bed Thickness (ft)

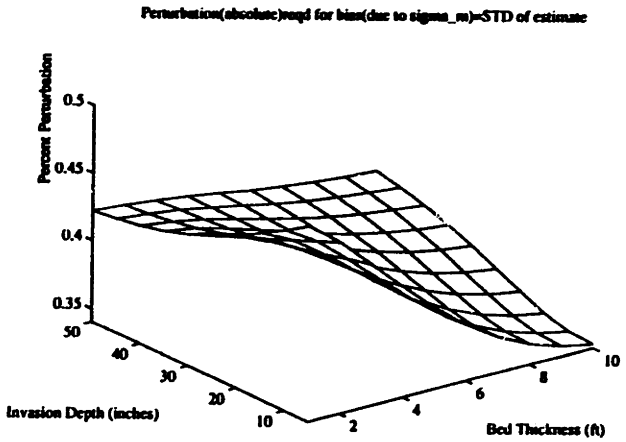

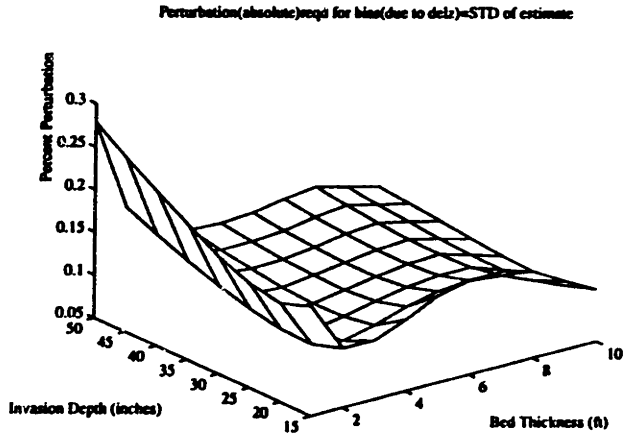

Figure 3-5: Perturbations required in the various parameters to produce bias terms as large as the standard deviation of the estimate of σ_t obtained when measurement noise is the only corrupting factor

2) The perturbation necessary to produce an error in the estimate equal to the error produced by the noise alone is determined.

This is done by solving the above Equation (3.28) for $\delta\theta_i$, i.e.,

$$\delta\theta_i = \frac{\sqrt{F_1^{-1}}\theta_i}{G_{\theta_i}} \tag{3.29}$$

If, for example, the required perturbations turn out to be very large, then the amount of bias introduced in practice will be small, and the estimate will be noise driven.

The results for case E are shown in Figures 3.5 (a) - (f). The required perturbation is expressed as a percentage of the true value of the parameter, $\left(\left(\frac{\delta\theta_i}{\theta_i}\right) \times 100\right)$. Also, the required perturbation surfaces are displayed as the absolute values of the actual perturbations required.

The percent perturbations are examined in Figures 3.6 (a) and 3.6 (b) for two different h's corresponding to shallow and deep invasion. The following observations are readily appparent:

1. The estimate is relatively more robust to perturbations in $delz$ and σ_m. The perturbations required in their magnitude to produce a bias error equal to that due to noise, while still small, is much larger than that required for the other parameters. Further, at least for the case of σ_m, the required perturbation varies little with h, the invasion depth.

2. As before, with an increase in invasion depth, the parameters of invasion, h and σ_{xo} play a more important role. The reason for that is the same as was discussed earlier in part 1.

3. Relative variations aside, it is apparent that on the whole the perturbations required in any parameter to alone produce a bias equal to the error due to noise is very small. Since the overall bias is the sum of these individual bias terms, the corresponding perturbations required to produce an overall bias equal to the error due to noise alone will be even smaller.

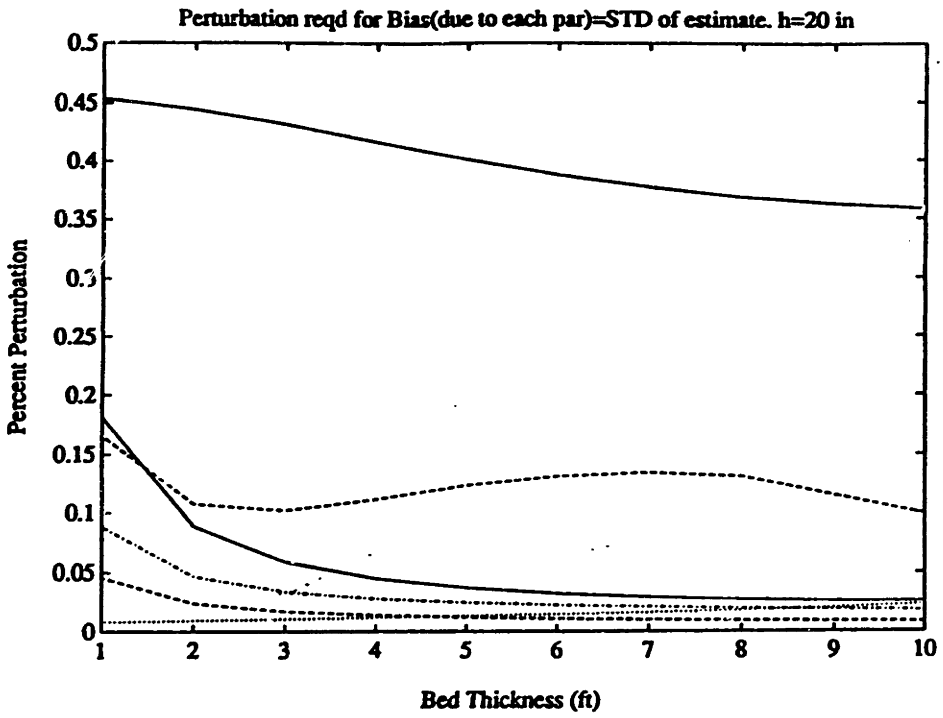
Perturbation reqd for Bias(due to each par)=STD of estimate. h=20 in
Percent Perturbation
0.5
0.45
0.4
0.35
0.3
0.25
0.2
0.15
0.1
0.05
0
1
2
3
4
5
6
7
8
9
10
Bed Thickness (ft)

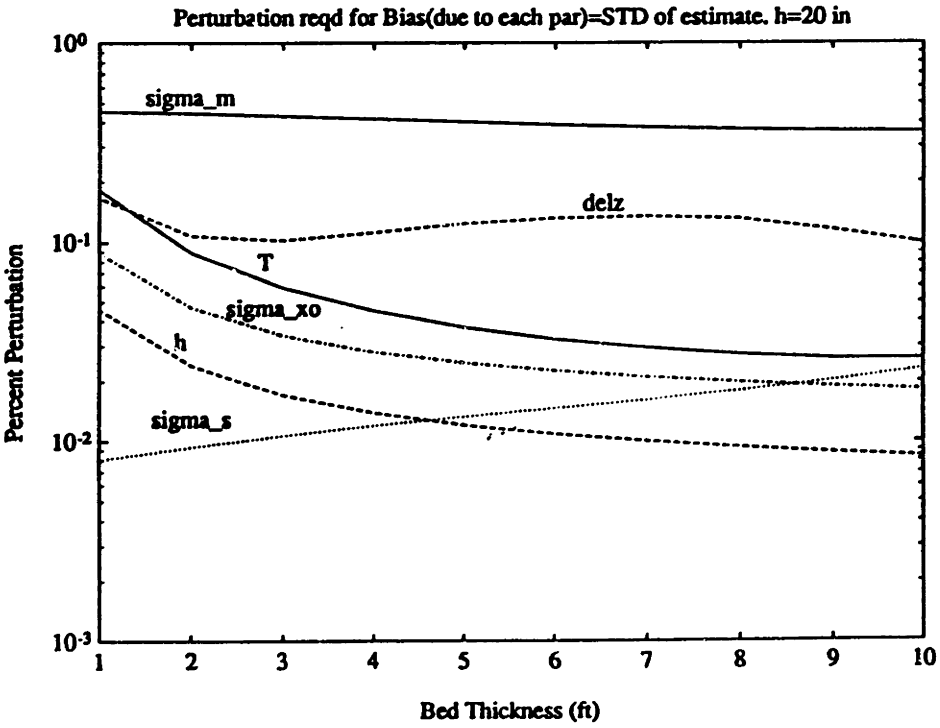
Perturbation reqd for Bias(due to each par)=STD of estimate. h=20 in
Percent Perturbation
10⁰
10⁻¹
10⁻²
10⁻³
sigma_m
delz
T
sigma_xo
h
sigma_s
1
2
3
4
5
6
7
8
9
10
Bed Thickness (ft)

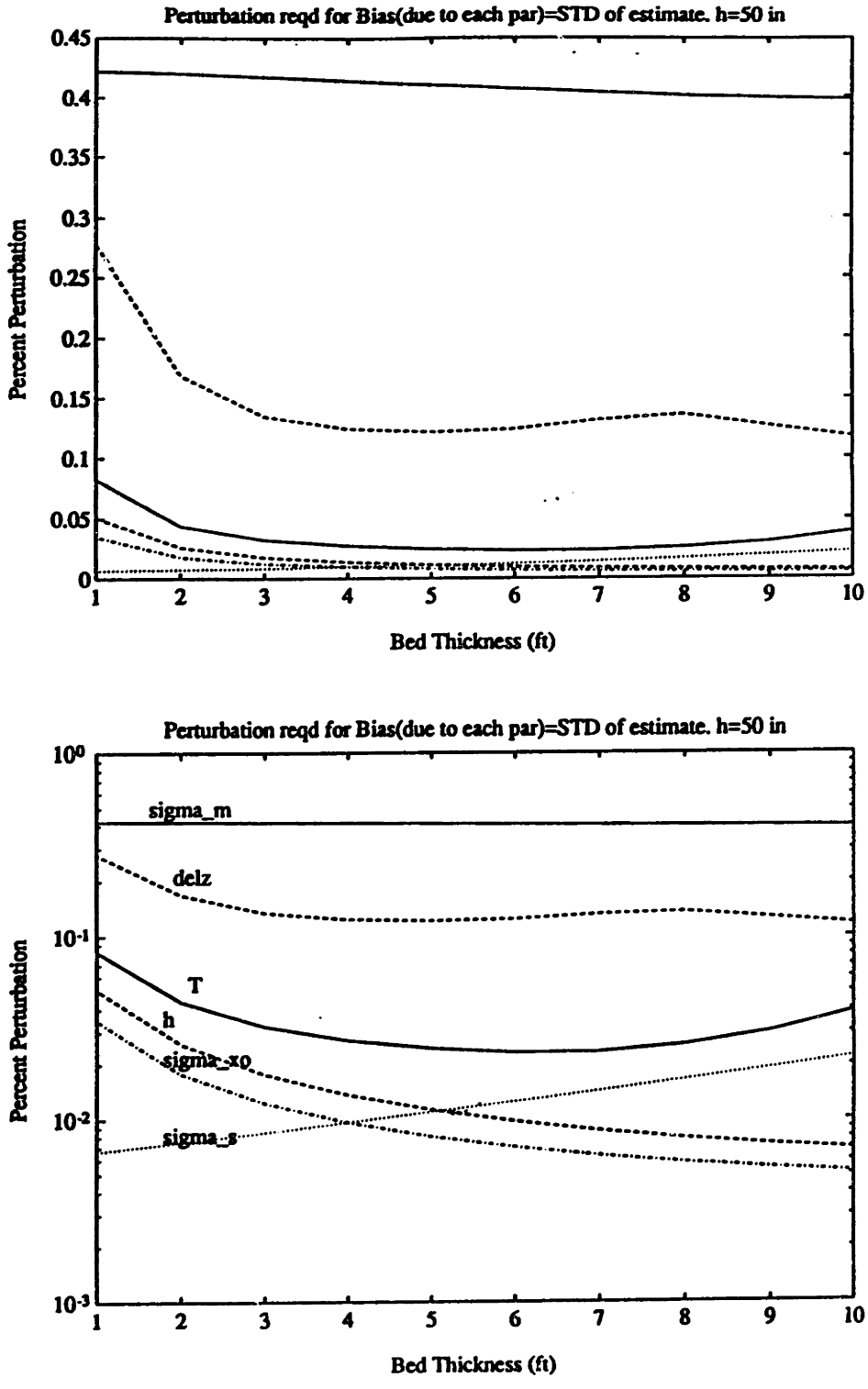

Figure 3-6: Required perturbations examined for shallow and deep invasion depths

In a realistic context one could never imagine obtaining values of the nuisance parameters to within such a high degree of required precision. The imprecision that one will likely encounter will be considerably larger and the resulting bias introduced, that much more. Therefore, it seems reasonable to conclude that *the error due to bias is the dominant contributor to the overall error produced in the estimation.*

Random Perturbations

It is assumed here that $\boldsymbol{\theta}$ has a known probabilistic description. This would be the case, for instance, when $\boldsymbol{\theta}_o$ is arrived at through a sequential estimation such as that refered to in Chapter 2. In that case, since the choice of operating point, $\boldsymbol{\theta}_o$, is an estimate, i.e., a function of random observations, $\boldsymbol{\theta}$ will be random.

As before,

$$\boldsymbol{\theta} = \boldsymbol{\theta}_o + \delta\boldsymbol{\theta} \tag{3.30}$$

where the $\delta\theta_i s$ are now random variables. It shall be assumed that the $\delta\theta_i s$ are zero mean, uncorrelated Gaussian random variables with variance p_i

Substituting the above description of $\delta\boldsymbol{\theta}$ into Equation (3.19), it can be seen that there is now no constant bias term. The term, $\mathbf{b} = {F_1}^{-1} M_2 \delta\boldsymbol{\theta}$, contributes an additional variance term to the overall estimate of $\mathbf{x}$.

The estimate of $\delta\mathbf{x}$ therefore consists of the true value $\delta\mathbf{x}$ plus two zero mean Gaussian random vectors. The resulting estimate has mean $\delta\mathbf{x}$, (i.e., it is unbiased), and covariance ${F_1}^{-1} + \sum_{i=1}^{n} (\mathrm{G}_{\theta_i})^2 p_i$

It can be seen from a comparison with the estimate obtained in (3.9), that the effect of the $\delta\boldsymbol{\theta}$ term is to produce an additional variance term in addition to ${F_1}^{-1}$, the variance term due to the noise alone.

Figures 3.7 (a)-(f) show the additional variance terms contributed by the various parameters in $\boldsymbol{\theta}$ when the standard deviation of $\delta\theta_i$ is assumed to be 1 percent of the operating point value of the parameter, i.e.,

Additional Variance produced in estimate due to zero mean perturbation in T with S.T.D(dT)=1% of T

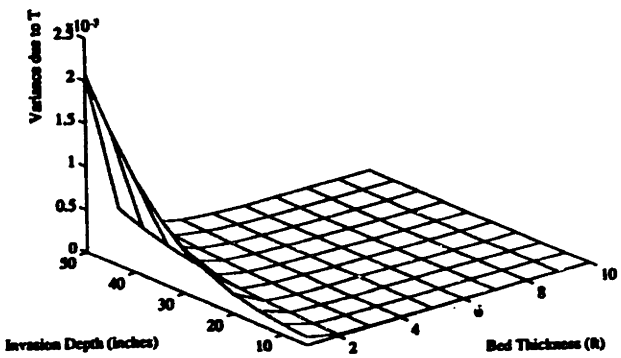

Additional Variance produced in estimate due to zero mean perturbation in h with S.T.D(h)=1% of h.

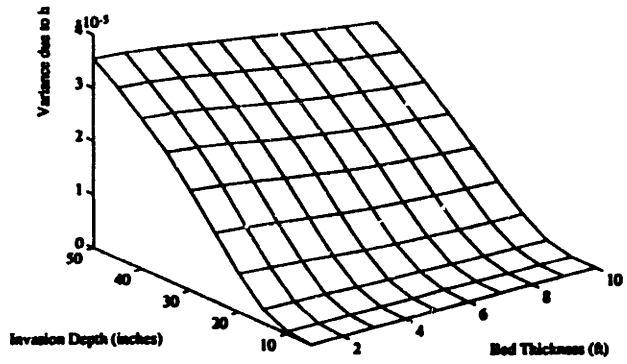

Additional Variance produced in estimate due to zero mean perturbation in sigma_xo with S.T.D(dsigma_xo)=1% of sigma_xo

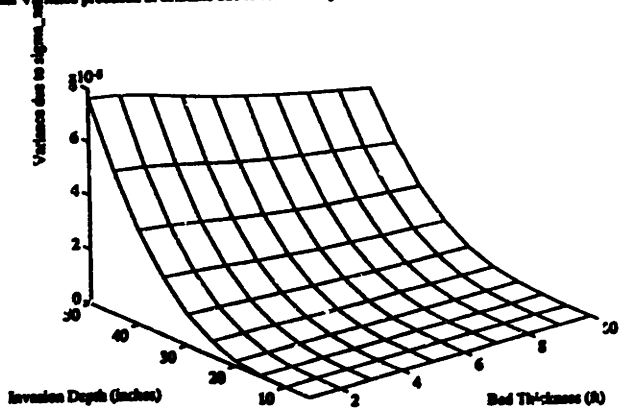

Additional Variance produced in estimate due to zero mean perturbation in sigma_s with S.T.D(dsigma_s)=1% of sigma_s

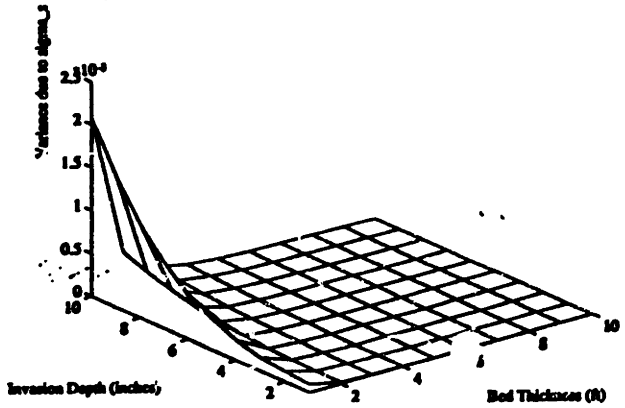

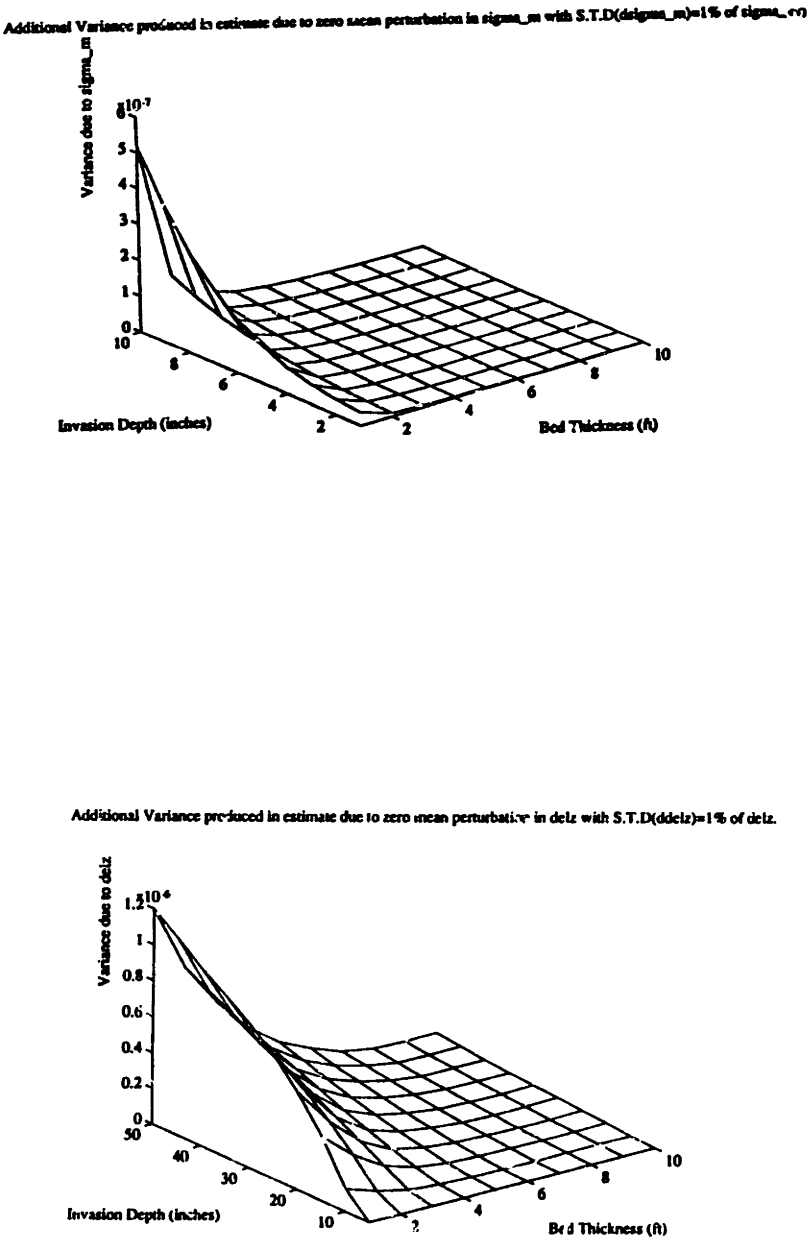

Figure 3-7: Additional variance terms introduced into the σ_t estimate due to random perturbations in the parameters

$$\text{STD}(\delta\theta_i) = \sqrt{p_i} = \frac{\theta_i}{100} \tag{3.31}$$

Further, if we assume $h = 20$ inches and 50 inches representing moderate and deep invasion, we can obtain a ranking of the parameters by their sensitivities as before. This is shown in Figures 3.8 (a) and (b). We obtain similar sensitivity results as for the $\delta\boldsymbol{\theta}$ non-random case because of the choice of the standard deviation of $\theta_i s$. It can be seen therefore that incorporating the case of $\delta\boldsymbol{\theta}$ random into the previously existing framework poses no problem.

We have a way, therefore, of arriving at a ranking of the parameters by their sensitivity, and a means for actually computing the additional variance terms contributed due to uncertainty in their knowledge for the $\delta\boldsymbol{\theta}$ random case as well.

The perturbations necessary to produce a variance term as large as that due to noise alone were seen to be very small[3]. The results for that investigation are not shown in the interest of brevity. The conclusions, however, are very forthcoming from the extremely large amount of variance produced by the 1 percent perturbations in the parameters, as also from the following section which provides an intuitive visualization of the interrelationship between the different approaches undertaken thus far.

3.4 Theoretical Interlude

The relationship between the cases in which (1) $\boldsymbol{\theta}$ is known perfectly, (2) $\boldsymbol{\theta}$ is imprecisely known and is deterministic, and (3) $\boldsymbol{\theta}$ is imprecisely known and is stochastic, can be visualized as in Figure 3-9. In the absence of $\delta\boldsymbol{\theta}$, i.e., for the case where $\boldsymbol{\theta}$ is known perfectly, the presence of noise produces a cloud of variance that surrounds the true value of the estimate as can be seen in Figure 3-9 (a).

When there is imprecision in $\boldsymbol{\theta}$, and more specifically, when $\boldsymbol{\theta}$ is non-random, the resulting bias term skews the vector in another direction, as shown in Figure 3-9 (b).

[3]This corresponds to part 2 of the $\delta\boldsymbol{\theta}$ non-random case

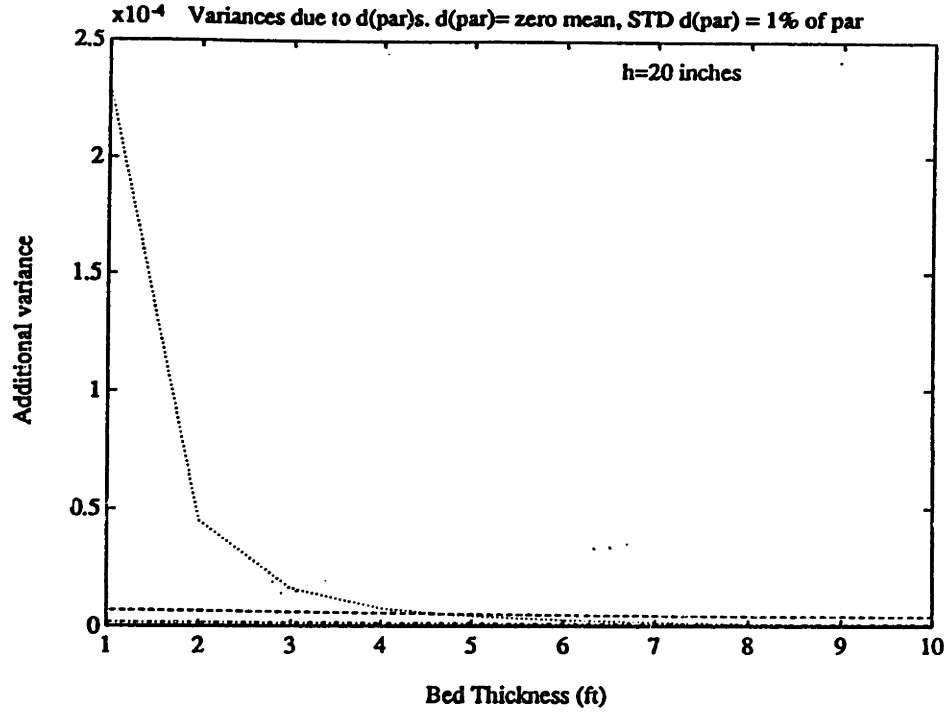
x10-4 Variances due to d(par)s. d(par)= zero mean, STD d(par) = 1% of par
h=20 inches
Additional variance
Bed Thickness (ft)

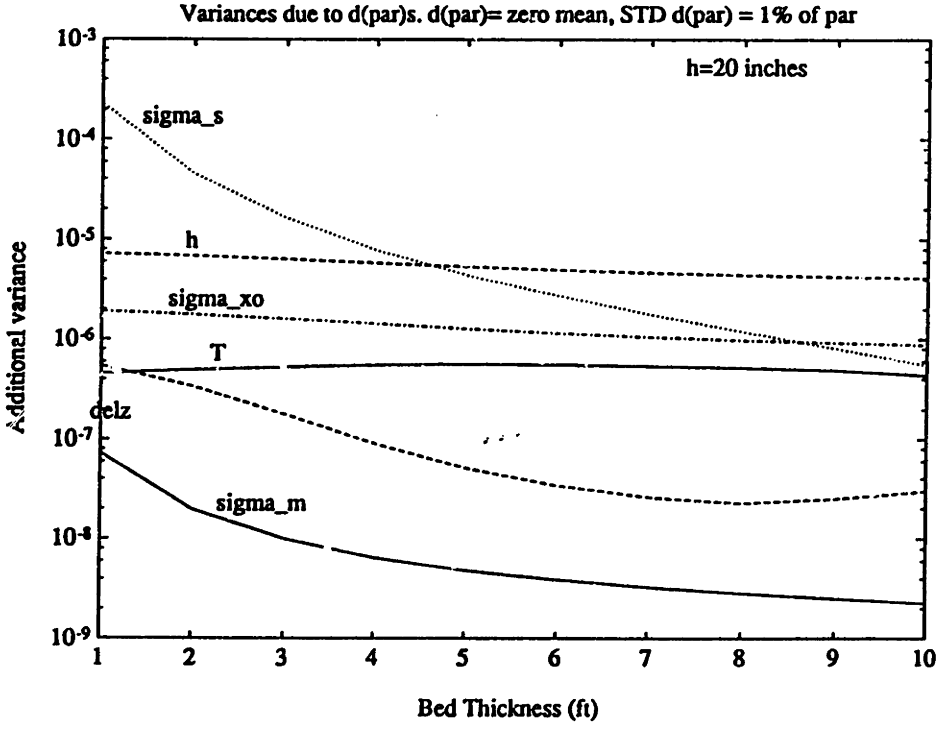
Variances due to d(par)s. d(par)= zero mean, STD d(par) = 1% of par
h=20 inches
sigma_s
h
sigma_xo
T
delz
sigma_m
Additional variance
Bed Thickness (ft)

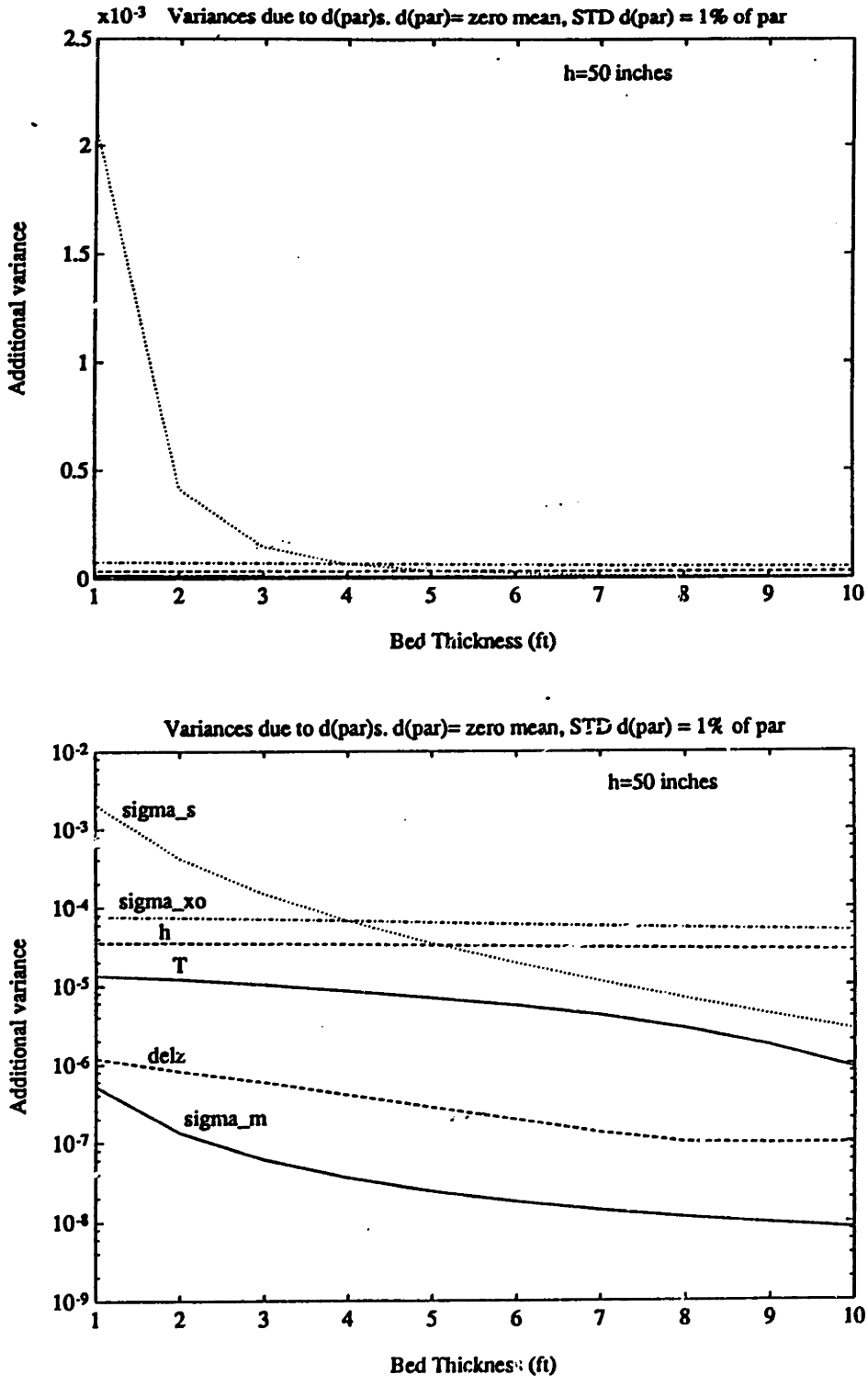

Figure 3-8: Additional variance terms examined for shallow and deep invasion depths

This corresponds to a constant offset, or bias, from the true value, and one of the results of the above analysis was to show that the bias vector throws the estimate off from the true value much more than the cloud due to the noise possibly could.

When $\boldsymbol{\theta}$ is probabilistic (i.e., when the parameters in $\boldsymbol{\theta}$ take on one of many values with a certain probability), then there is uncertainty as to the amount of offset from one realization of $\delta\boldsymbol{\theta}$ to the next. Hence there is no constant offset or bias term as was observed for the deterministic case. In the limiting case as the variance of $\delta\boldsymbol{\theta}$ goes to zero, one obtains a bias term[4], however; in general, the amount of offset from the true value is intimately tied to the probabilistic description of $\boldsymbol{\theta}$ itself. When the $\delta\theta_i$s were assumed to be zero mean, Gaussian variables one obtains an additional variance term in the estimate of $\mathbf{x}$. This corresponds to another cloud of variance, shown in Figure 3-9 (c). The analysis of this chapter showed that this cloud is much bigger than that produced due to the noise alone.

The mean square estimation error is the sum of the bias term and the standard deviation of the error. In going from $\delta\boldsymbol{\theta}$ deterministic to $\delta\boldsymbol{\theta}$ probabilistic what one effectively does is to push all the error into the two variance terms.

3.5 Conclusion

The performance of the estimator was considered under the assumption of perfect knowledge of the nuisance parameters. This enabled the characterization of estimator performance under noise alone, and provided an upper bound on performance to be used in comparison with the cases where noise is not the sole degrading factor. It was found that the error variance of the estimate, as given by the Cramer-Rao lower bound, was very small. This was found to be the case quite independent of the operating point being considered, indicating that irrespective of the conductivity contrast, and geometric variation of the model, an exceptional performance can be expected if noise is the sole corrupting factor.

That, of course, it is not. Therefore, it was then assumed that $\boldsymbol{\theta}$ was imprecisely known. Two cases were considered. In the first case $\boldsymbol{\theta}$ was assumed to be deterministic.

[4]thus the $\delta\boldsymbol{\theta}$ non-random case can be thought of as a special case of the $\delta\boldsymbol{\theta}$ random case

SOURCE OF ERROR		ERROR INTRODUCED (in mhos)	% OF TOTAL ERROR	% OF σ_t
Measurement noise		3.275×10^{-5}	0.4290	0.0655
Imprecision in knowledge of parameters		0.0076	99.5710	15.2
Parameter	*% perturbation*			
σ_s	1	2.85×10^{-3}	37.339	5.7
σ_{xo}	1	1.2×10^{-3}	15.7217	2.4
σ_m	1	8×10^{-5}	1.0481	0.16
h	1	2.41×10^{-3}	31.5745	4.82
T	1	7.1×10^{-4}	9.302	1.42
$delz$	1	3×10^{-4}	3.9304	0.6

Table 3.1: The relative contributions of the different sources of error in the estimation of σ_t.

The bias due to imprecision in the knowledge of the parameters in $\boldsymbol{\theta}$ could be simply expressed as the sum of the biases introduced by each parameter separately.

The bias introduced by a 1 percent perturbation in the parameter values was computed and used as the basis for a ranking of parameters by their sensitivities. Table 3.1 displays the result of the sensitivity analysis for a bed thickness, T, of 4 feet, and shows how such a ranking may be obtained.

It was emphasized that any such ranking depended on the operating point being considered as also on the relative size of perturbations in the various parameters. Once these are known, the procedure outlined can be used to obtain the sensitivity ranking specific to that particular case. It was then established that the estimate of x was bias driven. This was done by setting the bias produced by the parameters equal to error produced by the noise alone and calculating the perturbations in the parameters necessary for such a bias to be produced. These were found to be very small; a realistic estimate of $\boldsymbol{\theta}$ would undoubtedly have imprecisions greater than that, and hence the conclusion that the dominant source of error is imprecision in the knowledge of the nuisance parameters.

In the second case, $\boldsymbol{\theta}$ was assumed to be random. The $\delta\theta_i s$ were assumed to be zero mean uncorrelated Gaussian random variables with variances p_i. Instead of the bias term one now obtained an additional variance term due to imprecisions in each parameter. The rest of the treatment was similar to the $\boldsymbol{\theta}$ non-random case, with the

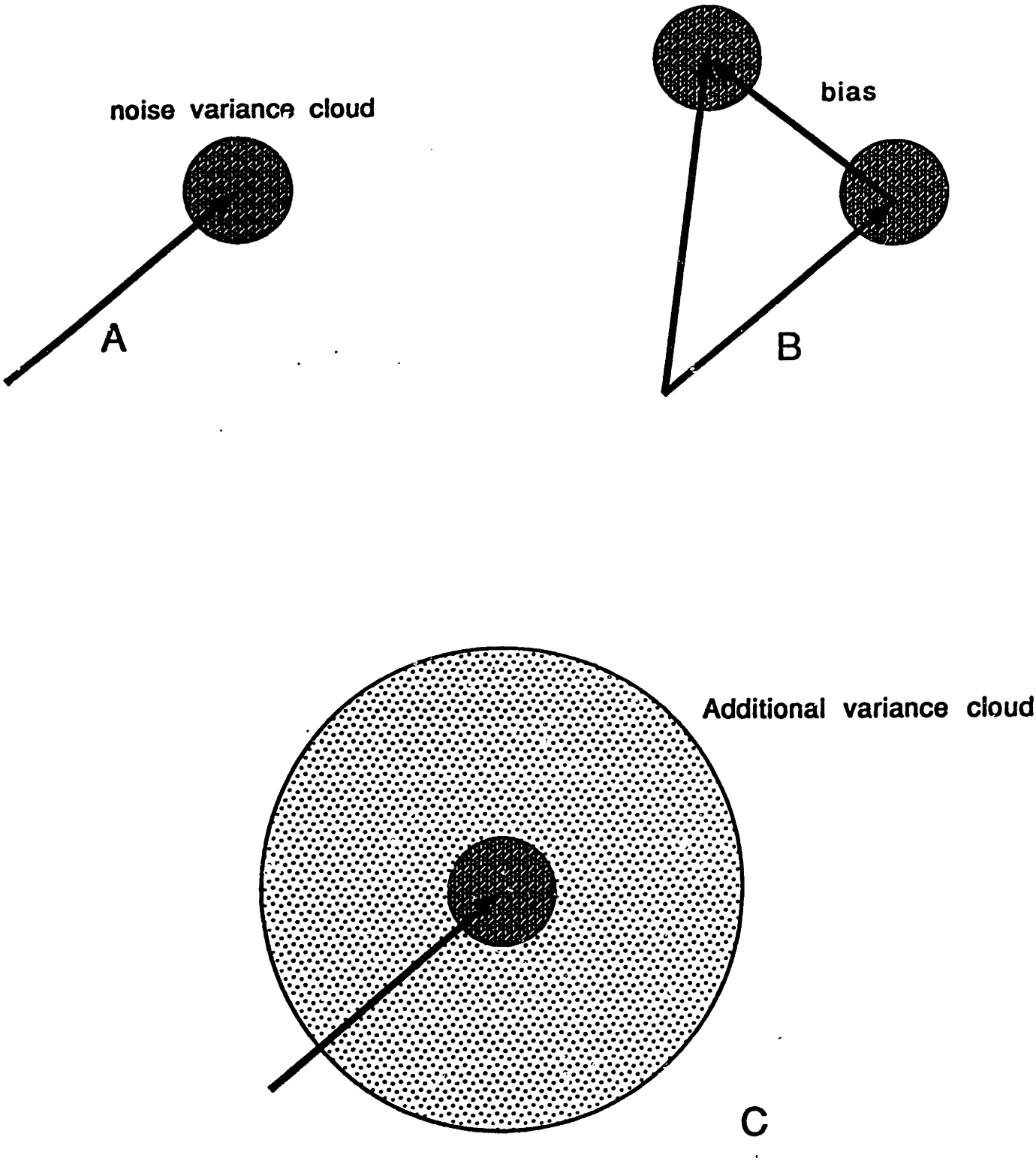

Figure 3-9: A pictorial view of the cases studied thus far

only semantic difference being that one cannot now talk of the estimate as being bias driven. It is more correct to say that the error due to imprecision in $\boldsymbol{\theta}$ (which has not a constant, bias value in this case) is much more dominant than that due to the presence of noise.

Lastly, a visual model was developed to aid the understanding of the estimation procedure so far, and to place it in a more physically intuitive context.

Chapter 4

Multiparameter Estimation and the Incorporation of Auxiliary Measurements

4.1 Introduction

The previous chapter underscored the fact that imprecision in the knowledge of the nuisance parameters was the major detrimental factor in the performance of the estimator for σ_t. Knowledge of the parameters in $\boldsymbol{\theta}$ is bound to be at a level of precision that cannot guarantee that there will be no bias in the estimate.

In the first part of this chapter we explore the possibilities of estimating all or a subset of the parameters in $\boldsymbol{\theta}$. The additional precision in $\boldsymbol{\theta}$ and the subsequent increase in accuracy of the estimate of σ_t will likely come at a cost in the precision of the estimate of σ_t. This degradation in precision in the estimation of σ_t due to a multiparameter estimation from the same observation set will be examined under various choices of $\mathbf{x}$.

The second part of the chapter is concerned with the incorporation of auxiliary measurements on some of the nuisance parameters into the framework for estimation that has already been built. Such measurements may come from additional shallow measurements of σ_{xo} and σ_m or from other logging tools that may provide information

on bed boundaries (i.e., T in the thesis model). One contribution of this investigation would obviously be to see how the performance of the estimates of σ_t and the other nuisance parameters being estimated will improve with this auxiliary information. In addition, it will enable us to set a threshold on how good the additional information must be for it to enable a significant improvement on the estimate of σ_t.

4.2 Multiparameter Estimation

The treatment that follows is different from the preceding one in that $\boldsymbol{\theta}$ is recognized to be imprecisely known and needs to be estimated either in whole or in part along with σ_t. In the first case that was considered in the previous chapter, the knowledge of the nuisance parameters was assumed to be perfect and the linearized approximation that was employed for the forward model took into account only the first order perturbation in $\mathbf{x}$. Subsequently it was suggested that the knowledge of $\boldsymbol{\theta}$ was in fact not perfect. The linearized model of the first case was used anyway and, for the $\boldsymbol{\theta}$ non-random case, a bias term was obtained. (This corresponded to the cost of unmodelled $\delta\boldsymbol{\theta}$.)

Now $\boldsymbol{\theta}$ is treated as imprecise. The prediction function is approximated by a multi-dimensional Taylor series expansion about $\mathbf{x}$ *and* $\boldsymbol{\theta}$.

4.2.1 Mathematical Development

Performance Analysis: Error variances of the estimates of $\mathbf{x}$ and $\boldsymbol{\theta}$ assuming $\boldsymbol{\theta}$ is unknown.

Equation (3.17) may be rewritten as

$$\delta\mathbf{y} \doteq \begin{pmatrix} H_x & H_\theta \end{pmatrix} \begin{pmatrix} \delta\mathbf{x} \\ \delta\boldsymbol{\theta} \end{pmatrix} + \mathbf{v} \tag{4.1}$$

In this case the weighted least squares estimates of $\delta\mathbf{x}$ and $\delta\boldsymbol{\theta}$ with respect to the weight matrix R (also the maximum likelihood estimates under the assumption of Gaussian noise with zero mean and autocorrelation R) are

$$\begin{pmatrix} \delta\hat{\mathbf{x}} \\ \delta\hat{\boldsymbol{\theta}} \end{pmatrix}_{WLS} = F_2^{-1} \begin{pmatrix} H_x^T \\ H_\theta^T \end{pmatrix} R^{-1} \partial \mathbf{y} \tag{4.2}$$

where the Fisher's Information matrix is:

$$F_2 = \left(\begin{pmatrix} H_x^T \\ H_\theta^T \end{pmatrix} R^{-1} \begin{pmatrix} H_x & H_\theta \end{pmatrix} \right) \tag{4.3}$$

Substituting (4.1) into (4.2) yields:

$$\begin{pmatrix} \delta\hat{\mathbf{x}} \\ \delta\hat{\boldsymbol{\theta}} \end{pmatrix}_{WLS} = \begin{pmatrix} \delta\mathbf{x} \\ \delta\boldsymbol{\theta} \end{pmatrix} + F_2^{-1} \begin{pmatrix} H_x^T \\ H_\theta^T \end{pmatrix} R^{-1} \mathbf{v} \tag{4.4}$$

So the estimated quantities equal the true values plus a zero mean Gaussian vector whose covariance matrix is given by the Cramer-Rao lower bound

$$CRB_2 = F_2^{-1} \tag{4.5}$$

The diagonal entries of CRB_2 correspond to the variances of the individual scalar parameters in $\mathbf{x}$ and $\boldsymbol{\theta}$.

Introducing a new variable

$$M_3 = H_\theta^T R^{-1} H_\theta \tag{4.6}$$

F_2 can be expressed as

$$F_2 = \begin{pmatrix} F_1 & M_2 \\ M_2^T & M_3 \end{pmatrix} \tag{4.7}$$

The formulation in (4.1)-(4.7) was used to examine the degrading effect on the estimate of true conductivity, σ_t, due to the estimating of a larger set of parameters. Further, it was possible to evaluate the tradeoff in performance as more and more parameters are estimated simultaneously.

4.2.2 Results and Analysis

A few points deserve some attention at this stage. From the results of the previous chapter, the bias factor multiplied by the perturbation provides a measure of the need of a given parameter to be estimated. The bias factors were computed for the family of operating points in Case E, and in theory could readily be computed for any choice of operating point. If, in addition, the order of magnitude of the perturbation in each parameter is known a priori, then, as was shown earlier, a ranking of the parameters by sensitivities [1]could easily be obtained. This would also costitute a ranking of the parameters by their *need* to be estimated.

In this chapter, the process of estimating some or all of the nuisance parameters is studied. The Cramer-Rao lower bound is used to obtain a measure of the performance of the estimate of σ_t and of the other parameters being estimated. Estimating more parameters is bound to result in a loss of estimator performance. This is a consequence of the fact that any increase in measurement precision for one of the measured system parameters must be accompanied by a compensating decrease in measurement precision for the remaining parameters if they are measured simultaneously from the same set of information data[4]. The estimating of certain parameters instead of certain others may result in a greater loss in performance. Therefore, the increase in variance of the estimates of σ_t and the other parameters also being estimated, if any, due to the inclusion of a certain parameter, θ_i, as an additional parameter to be estimated provides a measure of the *cost* of estimating that particular parameter.

The two notions of 'need' and 'cost' are intimately tied together and one aspect of this chapter is to explore their relationship with a view to determining an optimum set of parameters to estimate in addition to σ_t. It will be seen that the cost of estimating a certain parameter is inversely related to the sensitivity of the measurement to perturbations in that parameter. In simpler terms, it is easier to estimate a parameter to which the estimate is more sensitive. This is a comforting result because the parameters to which the estimate is more sensitive are the ones that would be estimated first of all.[2]

[1]more correctly, a ranking of the parameters by the sensitivity of the estimate to perturbations in the parameters

[2]There is a little more here than may immediately meet the eye. The fact that it costs less to

In this chapter any reference to need and cost will assume that these two terms are measured by the criteria indicated above. The fact that one obtains an unbiased estimate of a certain nuisance parameter θ_i in addition to σ_t implies that, on average, the size of the perturbation in θ_i will be zero, and hence the expected value of the bias in the estimate of σ_t (averaged over θ_i) is zero. On a single realization we will get a non-zero perturbation in the estimate of θ_i causing the estimate of σ_t to be biased. The size of the perturbation in θ_i that can be expected is proportional to the standard deviation of the estimate of θ_i, and for this reason it is crucial to pay close attention to the Cramer-Rao lower bound on the auxiliary parameters that we choose to estimate. If the error variances were too large it would mean that we will obtain big enough perturbations in our estimates of $\boldsymbol{\theta}$, on average, to produce an undesirable bias.

The issues mentioned above will be made clearer in the light of the following cases, all of which assume the operating point family given by Case E:

Case 1

Defining,

- Case 1a where $\mathbf{x} = \{\sigma_t, T\}, \boldsymbol{\theta} = \{\sigma_s, \sigma_{xo}, \sigma_m, h, r, \mathbf{z}\}$
- Case 1b where $\mathbf{x} = \{\sigma_t, h\}, \boldsymbol{\theta} = \{\sigma_s, \sigma_{xo}, \sigma_m, T, r, \mathbf{z}\}$
- Case 1c where $\mathbf{x} = \{\sigma_t, \sigma_s\}, \boldsymbol{\theta} = \{\sigma_{xo}, \sigma_m, T, h, r, \mathbf{z}\}$
- Case 1d where $\mathbf{x} = \{\sigma_t, \sigma_{xo}\}, \boldsymbol{\theta} = \{\sigma_s, \sigma_m, T, h, r, \mathbf{z}\}$

The above provide four illustrative examples of possible 2 parameter estimation cases.

Figures 4-1 (a) - (d) show the Cramer-Rao lower bounds on the estimate of σ_t and the additional parameter being estimated for each of these cases.

---

estimate parameters to which the estimate is more sensitive would most likely imply that the operating point knowledge of these parameters (obtained by a Gauss-Newton type iterative estimation) would be superior in the first place. This implies smaller perturbations and hence a lower need to be estimated. Note that this will be true when the values of these parameters are obtained from the same measurements that are used to obtain the estimate of σ_t

1a. z=f(sigma_r,T)

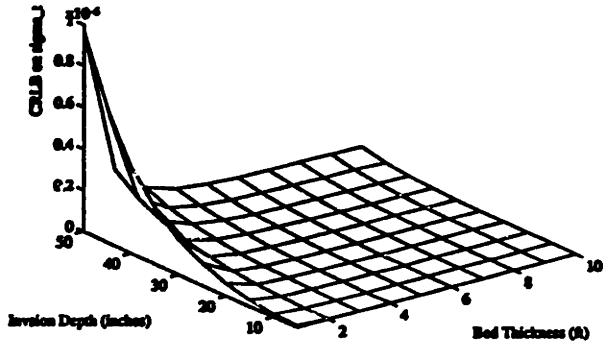

1a. z=f(sigma_r,T)

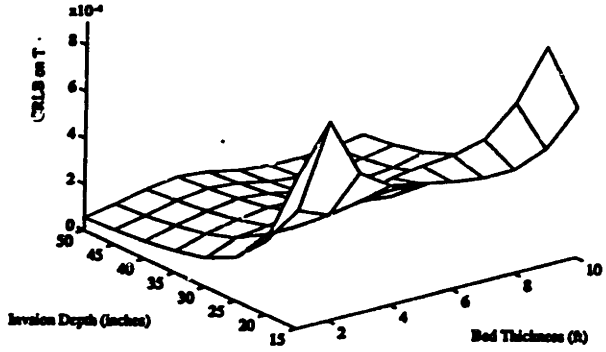

1b. z=f(sigma_r,h)

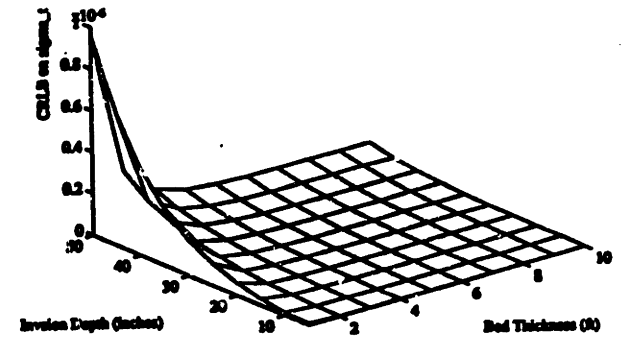

1b. z=f(sigma_r,h)

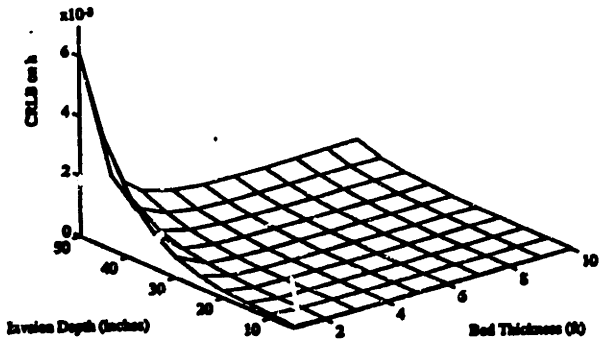

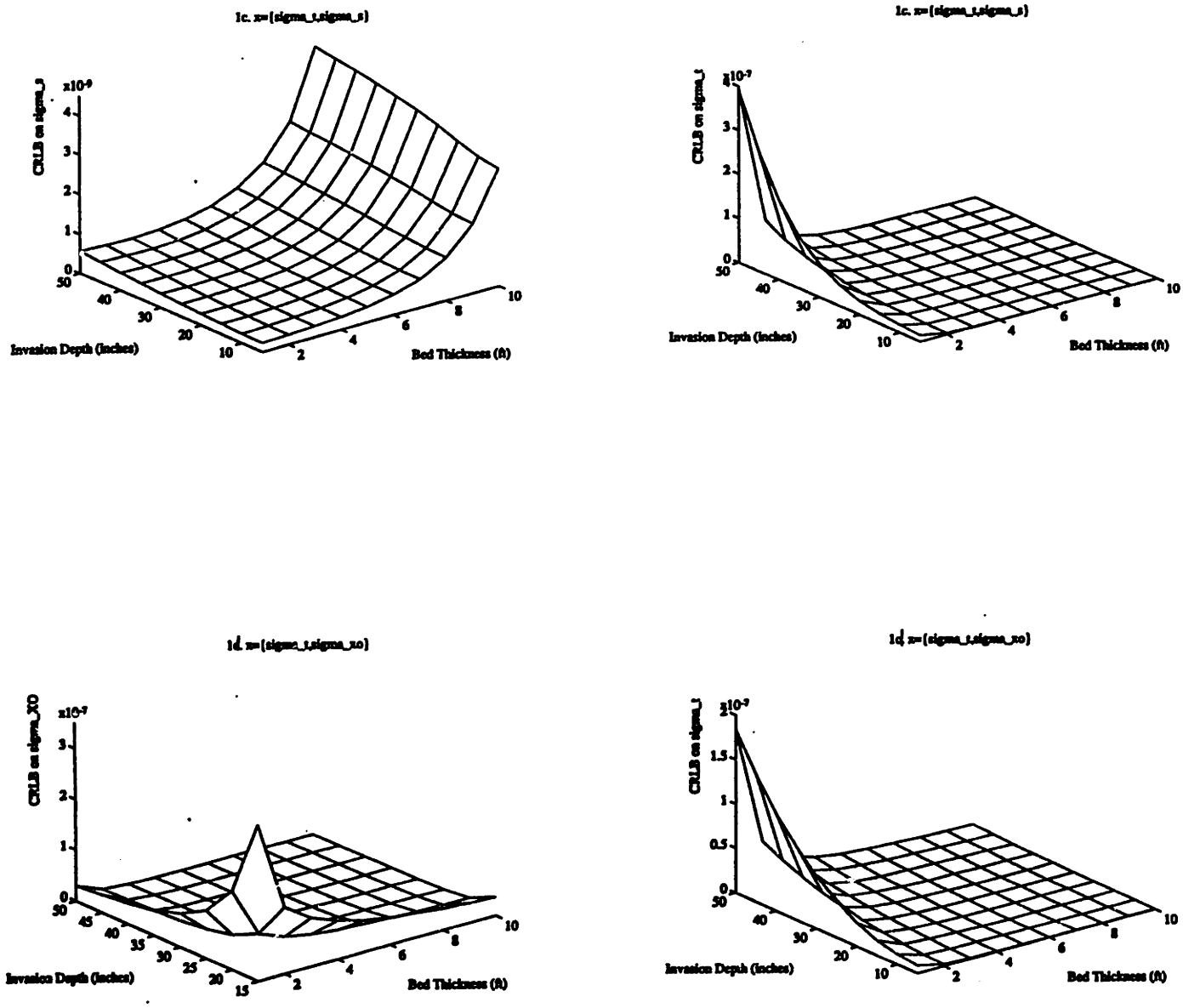

Figure 4-1: Cramer-Rao lower bounds on the estimate of σ_t and the aditional parameter to be estimated. Case 1.

For example, Figure 4-1 (a(i)) shows the CRLB on the estimate of T. It can be seen that the estimate of T has very small error variance, and that the estimate of σ_t has not suffered a very large increase in error variance in going from the case where T is assumed known to the one in which it is estimated. Therefore, it can be concluded that Case 1a effectively provides a situation in which the bias due to imprecision in T is reduced to zero, on average. On a particular realization of T, the standard deviation of the estimate of T provides a measure of the size of the perturbation in T that can be expected, and this too is observed to be very small. Furthermore, this good news comes at a cost, as measured by the decrease in precision in the estimate of σ_t that is not too severe at all. Statements such as this can be made about each of the above cases individually. In all of them it is seen that the two parameter estimation case results in the situation that the errors due to bias due to a given parameter (i.e., inaccuracy in the estimate of σ_t) can be reduced, on average, without an appreciable decline in estimator precision of σ_t.

There is something to be learned from comparing these cases as well. Figure 4-2 shows the Cramer-Rao lower bound as a function of bed thickness in the four different cases for a particular choice of $h = 20$ inches, corresponding to moderate invasion. It can be seen that the error variance on the estimate of σ_t is larger for the cases in which h and T are estimated, indicating that these two parameters are more costly to measure (i.e., more precision in σ_t has to be sacrificed to estimate h and T than for the other parameters considered). Referring back to Figure 3-4 (b), computed for the same h, we see that these were parameters that would feature lower in a ranking of the 4 parameters in terms of the sensitivity of the estimate to perturbations in them. This provides an example of the inverse relationship that exists between the need of a parameter to be estimated and the cost of actually estimating it.

Case 2

If instead of estimating one additional parameter one chooses to estimate two, then, as before, several choices exist. Suppose the choice, Case 2a, were made:

- Case 2a: $\mathbf{x} = \{\sigma_t, \sigma_s, T\}, \boldsymbol{\theta} = \{\sigma_{xo}, \sigma_m, h, r, \mathbf{z}\}$

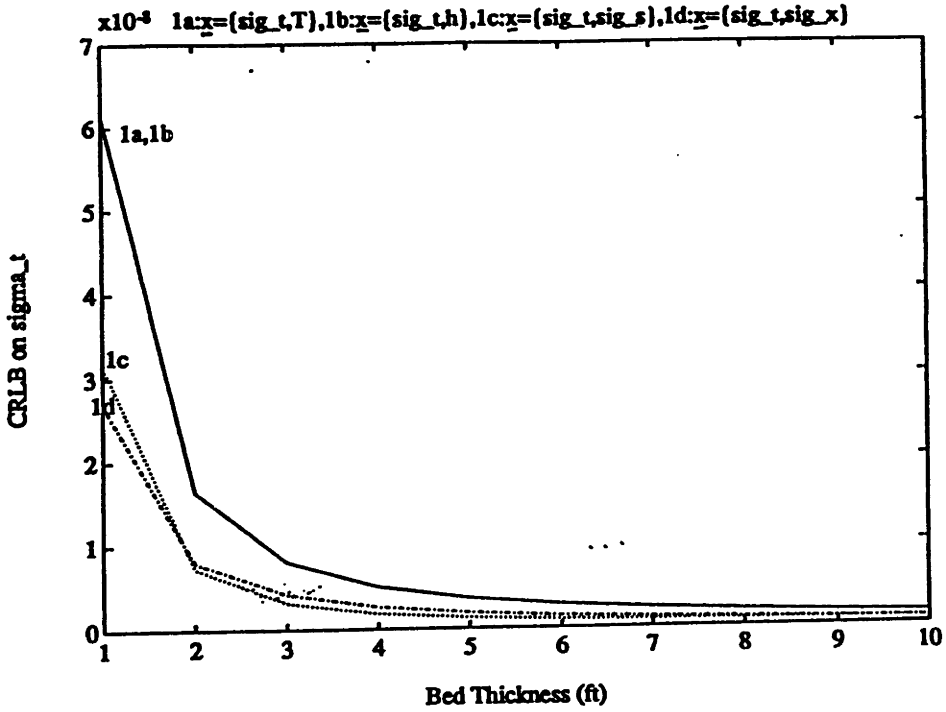

Figure 4-2: Cramer-Rao lower bound on the σ_t estimate for different choices of the additional parameter to be estimated. h=20 inches. Case 1

The Cramer-Rao lower bounds on the estimates of σ_t, σ_s and T are shown in Figures 4-3 (a) - (c). Comparison with Figure 4-1 shows that the loss in precision of the estimate of σ_t is not too significant. Further, comparison with Figures 4-1 (c) and (a) shows that in going from $\mathbf{x} = \{\sigma_t, \sigma_s\}$ to $\mathbf{x} = \{\sigma_t, \sigma_s, T\}$ and going from $\mathbf{x} = \{\sigma_t, T\}$ to $\mathbf{x} = \{\sigma_t, T, \sigma_s\}$ does not result in a large increase in the error variances of σ_s and T respectively. The standard deviations of these estimates are still quite small and the expected value of the perturbations in them is thus reasonably within limits.

It can therefore be concluded that for this operating point family, an increase in the precision of the estimates of T and σ_s and the consequent increase in accuracy of the estimate of σ_t can be obtained without appreciable loss of precision in the estimate of σ_t.

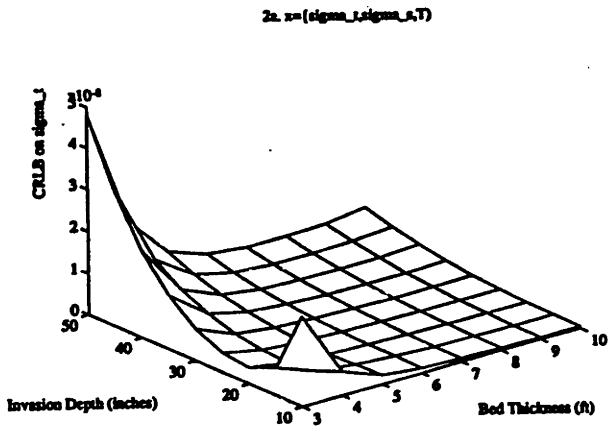

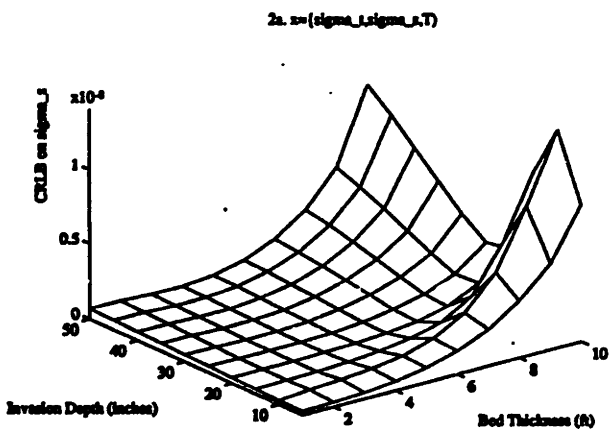

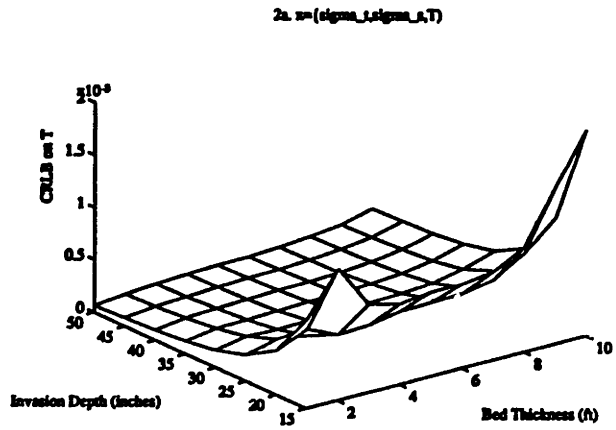

Figure 4-3: Cramer-Rao lower bounds for the σ_t, σ_s and T estimates of Case 2.

Case 3

We consider now the limiting case where every nuisance parameter is estimated. Figures 4-4 (a)-(f) show the Cramer-Rao lower bounds on each of the estimated parameters. Figure 4-5 shows the error variance of σ_t alongside each other for the two extreme cases where all parameters are assumed known and where all are assumed unknown and have to be estimated. The loss of estimator performance is visible, but it is still not very severe. At worst, the estimate of σ_t is 15% off from its true value. More so, in the regime of h and T values that one will usually encounter in practice, the performance is quite remarkable. For moderately invaded beds, the multiparameter estimation can be carried out without resulting in an estimate of σ_t that has a percent standard deviation of error greater than 5 percent. This is certainly acceptable performance.

Figure 4-6 (computed for $h = 20$ inches) shows that in going from the case of estimating σ_s as the only additional parameter in $\mathbf{x}$ to the case where it is estimated along with all the rest, we see that the percent standard deviation of the estimate of σ_s stays within a half percent. An intermediate case, case 3b, (in which $\mathbf{x} = \{\sigma_t, \sigma_s, T, h\}$ and $\boldsymbol{\theta} = \{\sigma_{xo}, \sigma_m, r, \mathbf{z}\}$) is also shown to indicate the behavior of a case intermediary to the two extreme ones. Therefore, the decrease in estimator performance of the nuisance parameters also seems to be within acceptable bounds. Similar comparisons were made for the other parameters and the conclusions are basically the same. It is possible to obtain an estimate with reasonably small variance, i.e., one that is reasonably accurate and precise.

Case 4

The above three cases provide examples of situations in which the number of parameters being estimated was fixed and an analysis done of the performance of the parameters within in each case and then between the cases themselves. In practice, however, one is more likely to follow a procedure that would be a natural extension of the results of the earlier chapter. The earlier results indicated a ranking of the parameters by the sensitivity of the estimates to them as follows:

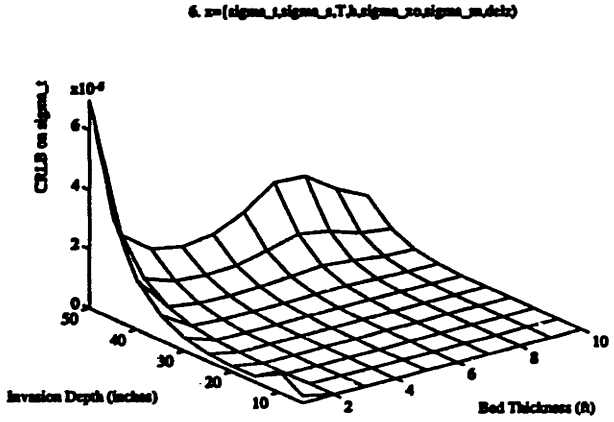
x10-6
CRLB on sigma_t
Invasion Depth (inches)
Bed Thickness (ft)

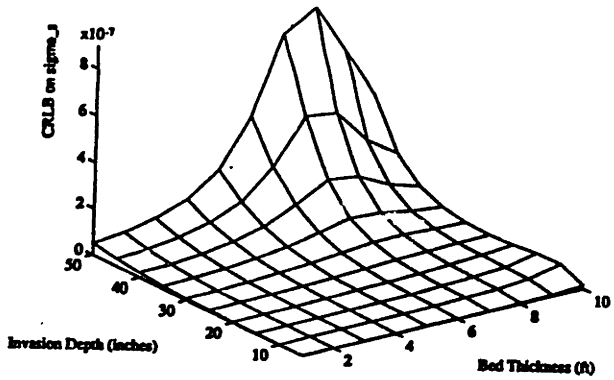
x10-7
CRLB on sigma_s
Invasion Depth (inches)
Bed Thickness (ft)

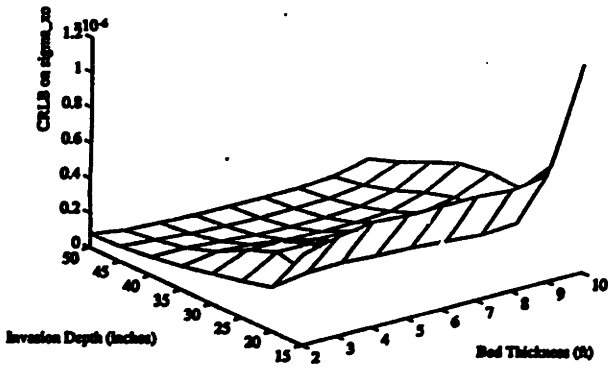
x10-4
CRLB on sigma_xo
Invasion Depth (inches)
Bed Thickness (ft)

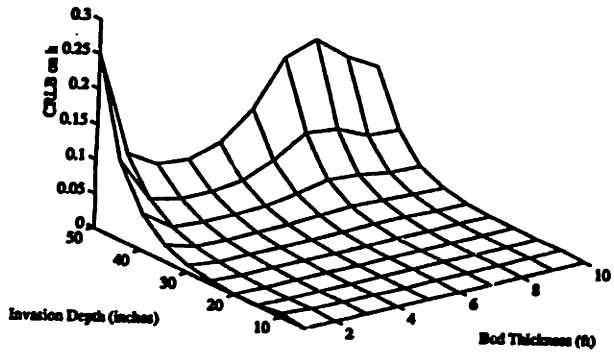
CRLB on m
Invasion Depth (inches)
Bed Thickness (ft)

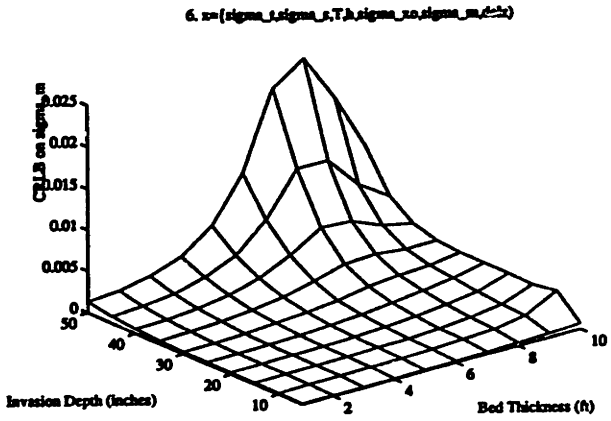

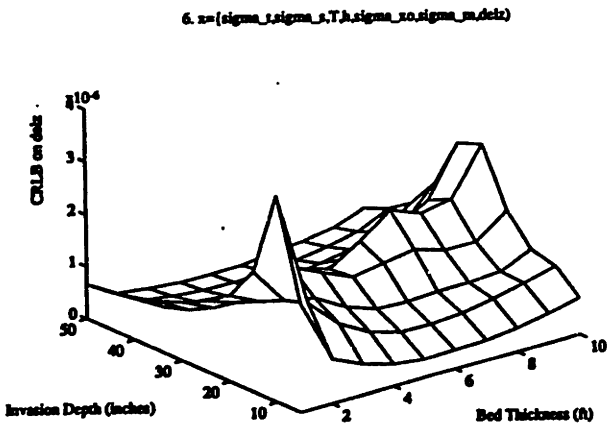

Figure 4-4: Cramer-Rao lower bounds on the estimate of σ_t and all the other parameters. Case 3.

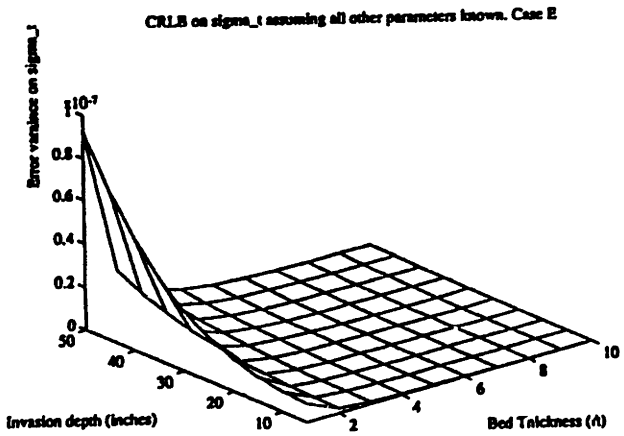

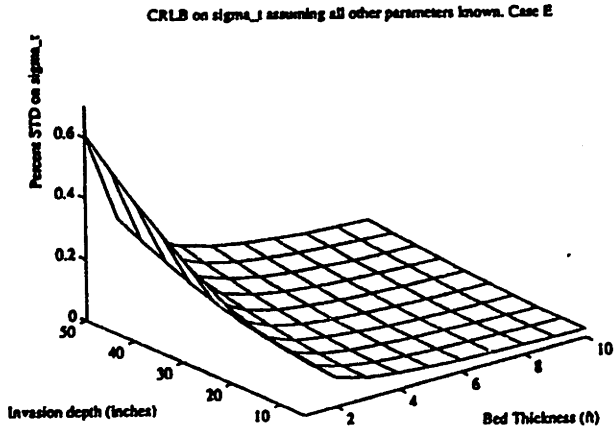

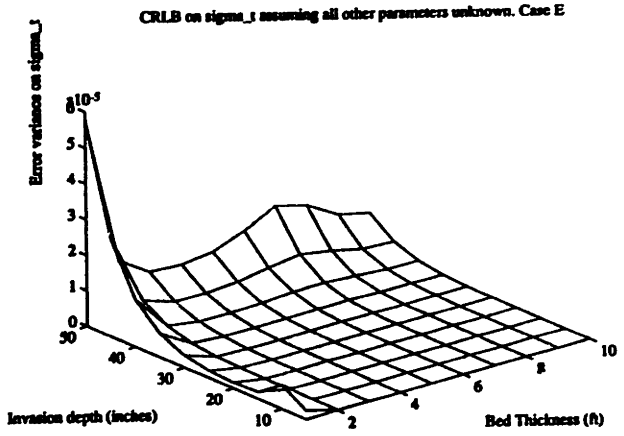

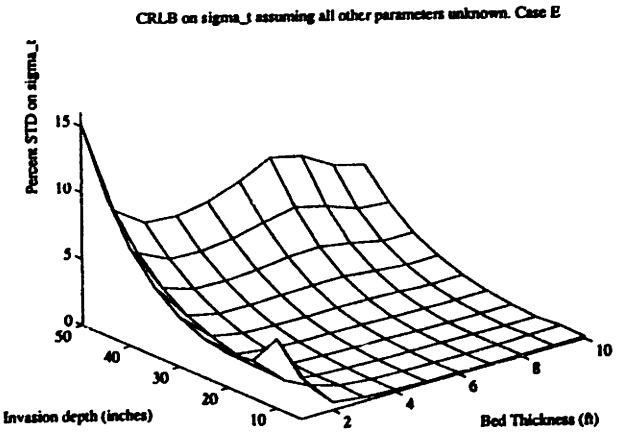

Figure 4-5: Comparison of the Cramer-Rao lower bound on the estimate of σ_t for the case where all the parameters are perfectly known and for the case where all the parameters are imprecisely known and have to be estimated

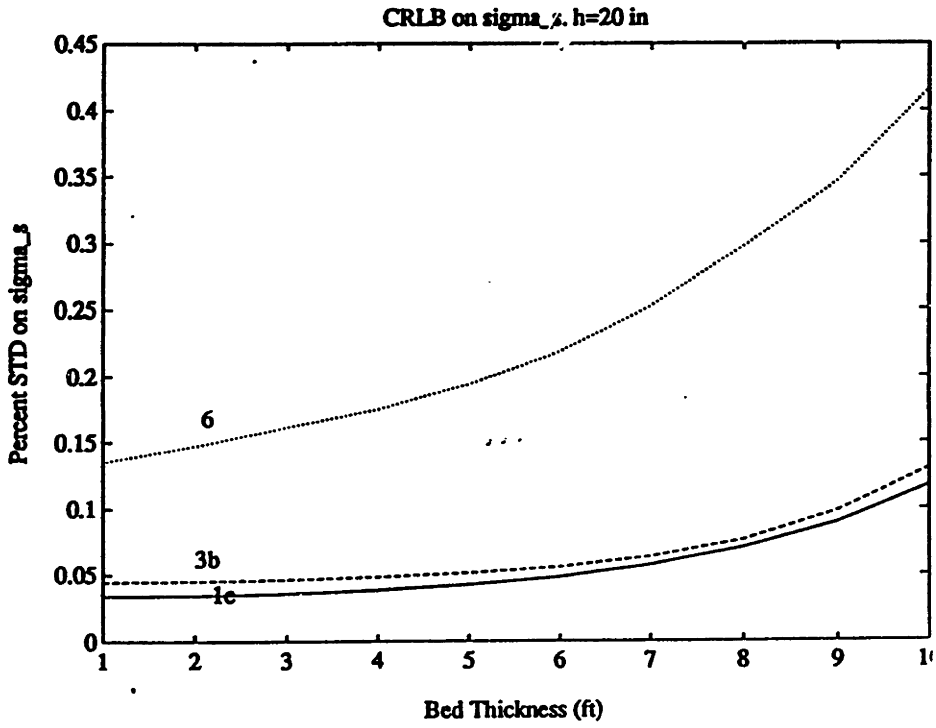

Figure 4-6: Increase in the Cramer-Rao lower bound on the estimate of σ_s as more parameters are estimated. Case 3.

1) σ_s

2) σ_{xo}, h

3) T

4) σ_m, *delz* where, in 2) and 4) the separation between the parameter sensitivities was not appreciable or depended on the interval of h and T being considered.

One would then carry out an estimation scheme that would estimate the additional parameters in this order. Therefore, if we define:

- Case 2b where $\mathbf{x} = \{\sigma_t, \sigma_s, h\}, \boldsymbol{\theta} = \{\sigma_{xo}, \sigma_m, T, r, \mathbf{z}\}$
- Case 2c where $\mathbf{x} = \{\sigma_t, \sigma_s, \sigma_{xo}\}, \boldsymbol{\theta} = \{\sigma_m, T, h, r, \mathbf{z}\}$
- Case 4 where $\mathbf{x} = \{\sigma_t, \sigma_s, \sigma_{xo}, h, T\}, \boldsymbol{\theta} = \{\sigma_m, r, \mathbf{z}\}$

a logical choice of successive cases would be going from

1. Case 1c, where σ_t and σ_s are estimated
2. to Cases 2b and 2c, where σ_t, σ_s, h or σ_t, σ_s, σ_{xo} are estimated, to

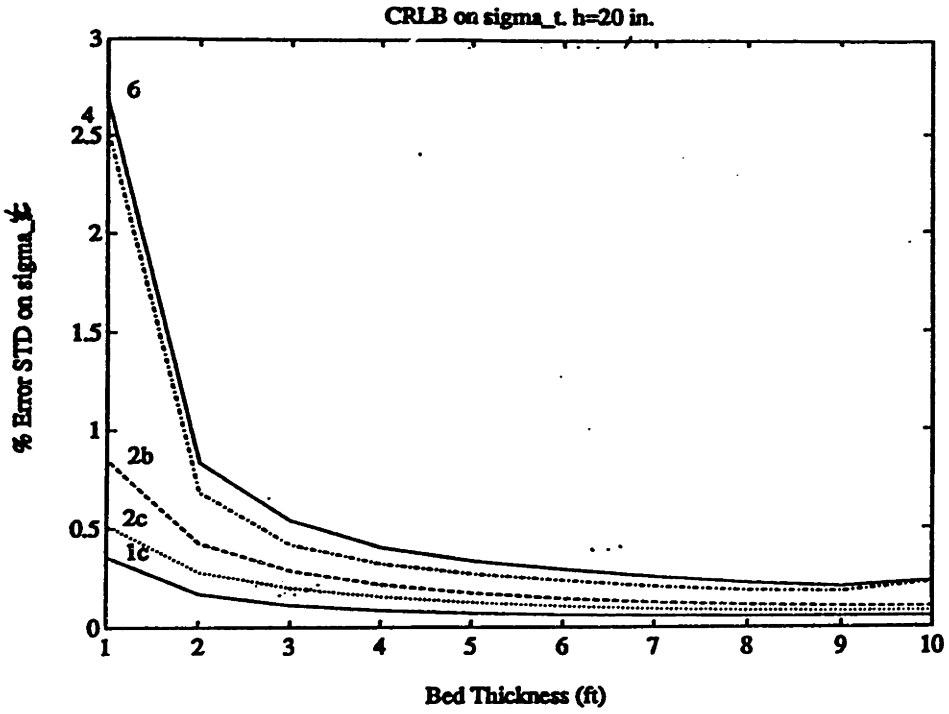

Figure 4-7: Cramer-Rao lower bound on the estimate of σ_t when the estimation scheme of Case 4 is employed. h = 20 inches

3. to Case 4, where σ_t, σ_s, h, σ_{xo}, T are estimated, to

4. Case 6 where all the parameters are estimated.

If at any point along this process the estimate of σ_t degraded beyond an acceptable level, we would know what subset of $\boldsymbol{\theta}$ it would be optimal to estimate in that case. Optimality, here is defined by some desired compromise between the accuracy and precision of the estimate of the parameters in $\mathbf{x}$.

Figure 4-7 shows the Cramer-Rao lower bound on the estimate of σ_t for the various choices of $\mathbf{x}$ just described assuming $h = 20$ inches. As was mentioned before, we see that at least for this value of h, estimating all the parameters (Case 6) rather than estimating just one (Case 1c), does not result in too large of an increase in the variance of σ_t. The estimate of σ_t is still within 3% of its true value even for Case 6. Further, the difference is even smaller for beds thicker than two feet which is what one usually encounters in practice.

It must be remembered that estimating for *delz* involves the estimation of a single parameter, which corresponds to the constant offset, ϵ, in each component of the vector of tool depth positions.

Another point deserves mention at this stage. It was seen that for the three bed model estimating all the parameters in $\boldsymbol{\theta}$ in addition to σ_t results in a loss of estimator precision that is not unreasonable. As such there is no need in this model to select a subset of $\boldsymbol{\theta}$ to estimate. This, however, need not be the case for more complex multi-bed models with many more model parameters. For such models the choice of what subset of $\boldsymbol{\theta}$ to estimate in addition to σ_t is made by following the procedure adopted in case 4: keep on increasing the number of parameters to be estimated, $(\mathbf{x})$, in accordance with the ordering of the parameters (obtained by the methods of Chapter 3) until the loss in estimator precision becomes unacceptable.

4.3 Auxiliary Measurements

Additional information may be available to us from many sources: auxiliary knowledge of $\boldsymbol{\theta}$ could come from additional wellbore measurements, for example, of the Formation Micro-Scanner, FMS, which provides information about the layer boundaries or bed thickness. As another example, auxiliary measurements of the invaded zone conductivity, σ_{xo}, may be known from additional shallow reading instruments. The purpose of this part of the chapter is to develop a mathematical framework for the incorporation of additional measurements of $\boldsymbol{\theta}$ into the estimation rule. Then, a performance analysis is carried out for a sample case, and certain inferences drawn from it which yield valuable information on the requisite quality of the additional measurements that is needed for the estimator to show a marked decrease in variance

4.3.1 Mathematical Development

Error variance of the estimate of $\mathbf{x}$ assuming auxiliary measurements of $\boldsymbol{\theta}$ are available.

Suppose, in addition to the measurements $\mathbf{y}$ already introduced, auxiliary mea-

surements $\mathbf{q}$ are available, for a total set:

$$\mathbf{y} = \mathbf{h}(\mathbf{x},\boldsymbol{\theta}) + \mathbf{v} \tag{4.8}$$

$$\mathbf{q} = \mathbf{f}(\boldsymbol{\theta}) + \mathbf{w} \tag{4.9}$$

where $\mathbf{q}$ is the vector of additional measurements and $\mathbf{w}$ is white, Gaussian noise of variance Q.

Let $\mathbf{q_0}$ correspond to the noise-free response to $\boldsymbol{\theta_0}$, i.e.,

$$\mathbf{q_0} = \mathbf{f}(\boldsymbol{\theta_0}) \tag{4.10}$$

and let $\mathbf{q}$ be a perturbation about $\mathbf{q_0}$,

$$\mathbf{q} = \mathbf{q_0} + \delta\mathbf{q} \tag{4.11}$$

Assuming, as before, that the second and higher order terms are negligible,

$$\delta\mathbf{q} \approx F_\theta \delta\boldsymbol{\theta} + \mathbf{w} \tag{4.12}$$

where

$$F_\theta = \frac{\partial \mathbf{f}}{\partial \boldsymbol{\theta}} \tag{4.13}$$

The linearized measurement model is now given by:

$$\begin{pmatrix} \delta\mathbf{y} \\ \delta\mathbf{q} \end{pmatrix} \approx \begin{pmatrix} H_x & H_\theta \\ 0 & F_\theta \end{pmatrix} \begin{pmatrix} \delta\mathbf{x} \\ \delta\boldsymbol{\theta} \end{pmatrix} + \begin{pmatrix} \mathbf{v} \\ \mathbf{w} \end{pmatrix} \tag{4.14}$$

As before, it is understood that the perturbations are small enough so that the linearized model stays valid.

The weighted least squares estimates in this case are:

$$\begin{pmatrix} \delta\hat{\mathbf{x}} \\ \delta\hat{\boldsymbol{\theta}} \end{pmatrix}_{WLS} = {F_3}^{-1} \begin{pmatrix} {H_x}^T & {H_\theta}^T \\ 0 & {F_\theta}^T \end{pmatrix} \begin{pmatrix} R^{-1} & 0 \\ 0 & Q^{-1} \end{pmatrix} \begin{pmatrix} \delta\mathbf{y} \\ \delta\mathbf{z} \end{pmatrix} \tag{4.15}$$

where Fisher's Information matrix, F_3, is:

$$F_3 = \left(\begin{pmatrix} {H_x}^T & 0 \\ {H_\theta}^T & {F_\theta}^T \end{pmatrix} \begin{pmatrix} R^{-1} & 0 \\ 0 & Q^{-1} \end{pmatrix} \begin{pmatrix} H_x & H_\theta \\ 0 & F_\theta \end{pmatrix} \right) \tag{4.16}$$

Following a procedure similar to that used in Case 1 and Case 3 it can be shown that the Cramer-Rao lower bound, CRB_3, is:

$$CRB_3 = F_3^{-1} \tag{4.17}$$

Defining

$$M_4 = {F_\theta}^T Q^{-1} F_\theta \tag{4.18}$$

we get

$$CRB_3 = \left(\begin{pmatrix} F_1 & M_2 \\ {M_2}^T & M_3 + M_4 \end{pmatrix} \right)^{-1} \tag{4.19}$$

so that

$${CRB_3}^{-1} = {CRB_2}^{-1} + \begin{pmatrix} 0 & 0 \\ 0 & M_4 \end{pmatrix} \tag{4.20}$$

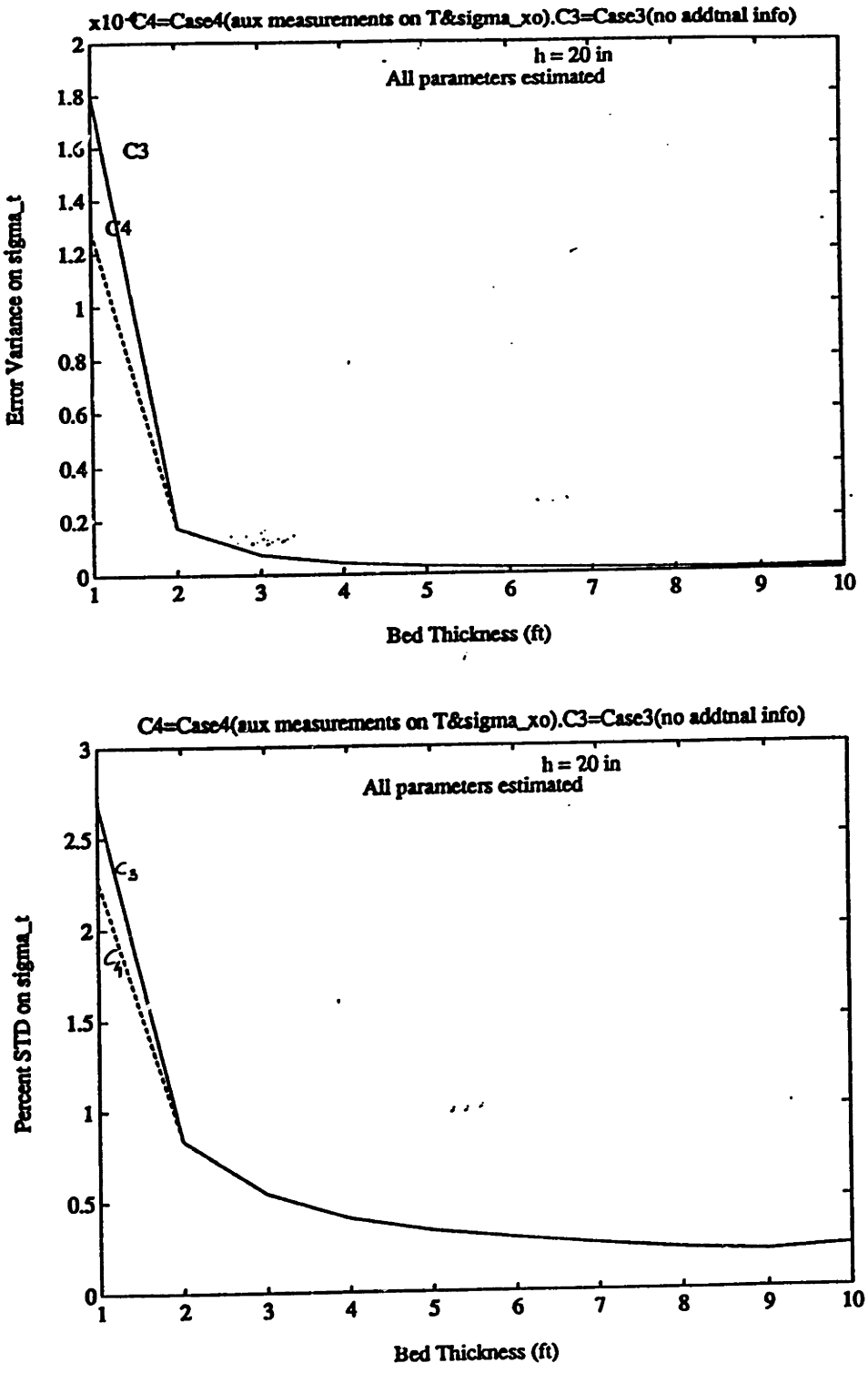

Figure 4-8: Cramer-Rao lower bounds on the estimate of σ_t illustrating the effect of having additional information on T and σ_{xo} available. h = 20 inches.

4.3.2 Results and Analysis

It is assumed that auxiliary measurements of T and σ_{xo} are available in the following form:

$$T = T_o + q_T \tag{4.21}$$

$$\sigma_{xo} = \sigma_{xoo} + q_{\sigma_{xo}} \tag{4.22}$$

where $q_{\theta_i} = N(0, Q_i)$, and the standard deviation of Q_i is chosen for the purposes of illustration to be one percent of the true value of the parameter θ_i. i.e.,

$$\sqrt{Q_i} = 1\% \text{ of } \theta_i \tag{4.23}$$

Figure 4-8 shows the error variance and the percent standard deviation of the error in the estimate of σ_t. It can be seen that for additional information of this quality performance is improved only for thin beds. Had the $Q_i's$ been smaller, the error variance would have been even smaller. However, as was mentioned in the introduction, for the auxiliary information to be of value after the multiparameter estimation procedure has been completed, the information has to be at least of a certain quality, and what we have here is a way of determining what that necessary quality (as measured by the $Q_i's$) ought to be for any given case.

Similar decreases in variances are seen in Figures 4-9 (a) and (b) for the estimates of T and σ_{xo}. In all of this it must be reemphasized that more precise auxiliary measurements will lead to smaller variances in the estimates of all our parameters. Decrease in the error variances of T and σ_{xo} will translate to lower imprecisions in T and σ_{xo} in general and hence less bias introduced into the estimates of the parameters in $\mathbf{x}$.

It should be remembered at this stage that additional information which is of little use in reducing error variance at this stage is likely to have already been folded into the estimation process at an earlier stage; i.e., at the stage where $\mathbf{x}_o$ and $\boldsymbol{\theta}_o$, the operating points we assumed to be known at the outset, were being estimated.

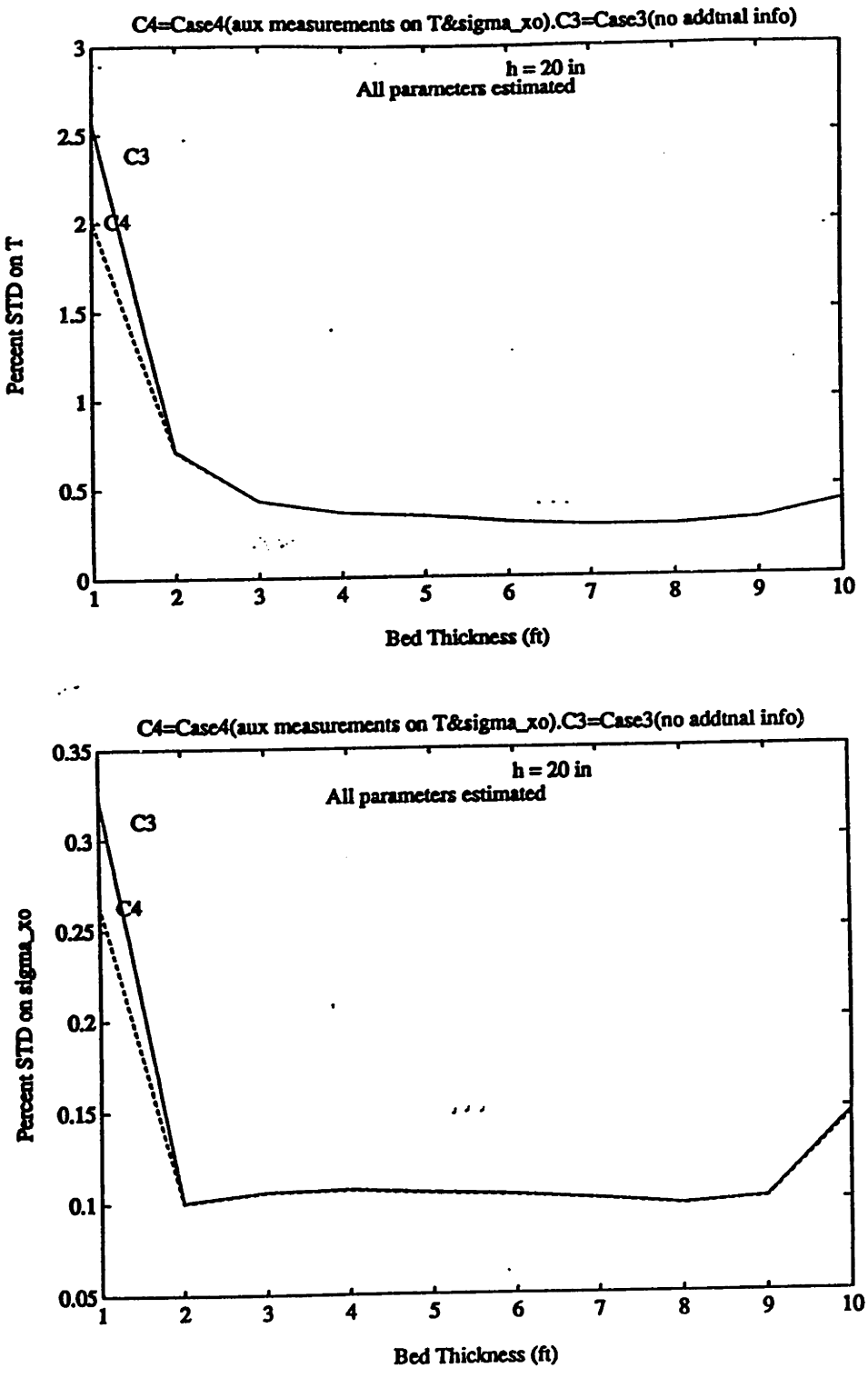

Figure 4-9: Cramer-Rao lower bounds on the estimates of T and σ_{xo} illustrating the effect of having additional information on these parameters available. h = 20 inches.

Further, auxiliary information that is of little use in reducing error variance in this model will probably be of more value in more complex formation models in which the estimator performance (in the absence of auxiliary measurements) can be expected to be worse than in the three bed model.

4.4 Conclusion

The performance of the estimator was considered under the assumption of imperfect knowledge of the nuisance parameters. The results of the previous chapter indicated that imprecision in the knowledge of the nuisance parameters was the major source of error in the inversion. By using an estimator constructed on the assumption of perfect knowledge of the parameters in $\boldsymbol{\theta}$ one obtained an estimate that was precise but, potentially[3], highly inaccurate. In this chapter the transition from such an estimate to one that is more accurate but less precise is made.

Chapter 3 provided the means for obtaining a ranking of the parameters by their need to be estimated (as measured by the amount of bias introduced into the estimate by a given perturbation in their magnitude). This chapter provides the means for determining the cost and feasibility of estimating the respective parameters (as measured by the incremental loss of precision in the estimate induced by the additional estimation of each parameter).

Various estimation scenarios were considered. The number of parameters to be estimated was successively increased in keeping with the ordering of the parameters by their need to be estimated. It was seen that for this model estimating all of the nuisance parameters resulted in an increase in the error variance of the estimate of σ_t that was not unreasonable on the whole and much less so in regimes of common interest. For example, for an invasion depth of 20 inches it was seen that for the case when all the parameters are estimated along with σ_t, the estimate of σ_t was within 3 percent of the true value. Thus the increased accuracy of the estimate of σ_t does not result in a substantial loss in estimator precision. This can be seen in Table 4.1 which shows the incremental standard deviation added to the σ_t estimate for the successive

[3]depending upon the size of the perturbation in $\boldsymbol{\theta}$

CASES	ERROR St.Dev ON ESTIMATE (in % of σ_t)	INCREMENTAL St.Dev ADDED TO ESTIMATE (in % of σ_t)
ϕ perfectly known	0.0655	-
Case 1c	0.089	0.0235
Case 2b	0.1547	0.0657
Case 2c	0.2113	0.1223
Case 4	0.3125	0.1012
Case 6	0.4018	0.0893

Table 4.1: Degradation in the σ_t estimate caused by the successive multiparameter estimation cases

estimation scenarios.

The error variances on the estimates of the other parameters being estimated are also of importance because they provide indicators of the size of perturbations to be expected on average. These were seen to be within reasonable limits - for instance, in the case when all the parameters are estimated along with σ_t, the estimate of σ_s for an invasion depth of 20 inches, stays within 0.5 percent of its true value..

In the second part of this chapter it was assumed that auxiliary information on some of the parameters was available through other sources. The incorporation of these additional measurements into the pre-existing mathematical framework for error analysis was formalized. The performance of the estimator was considered in the light of this additional knowledge. It was seen that for the chosen quality of auxiliary information the estimator performance did not improve remarkably, though a marginal improvement was seen for thinner beds. For a 1 foot thick bed, with an invasion depth of 20 inches for instance, an improvement of about 0.5 percent of the true value of σ_t results from the incorporation of auxiliary measurements of the quality described in Section 4.3.2. Such results, however, are entirely a function of the quality of the additional measurements chosen and need not reflect estimator performance given superior auxiliary information.

The methodology developed in the previous chapter enabled the ordering of the parameters by the sensitivity of the estimate of σ_t to them. By using the methodolgy developed in this chapter, the percentage increase in the variance of the σ_t estimate that results from estimating some or all of the nuisance parameters can be computed.

Further, the quality of auxiliary measurements needed to be of use in reducing the variance of the estimate of σ_t can also be determined using the framework developed in this chapter.

Chapter 5

Further Issues

5.1 Introduction

In the preceding chapters we considered a performance and robustness analysis of the inversion of induction log data for the 3 bed model. The logs are noisy nonlinear functions of the formation parameters for which the inversion is carried out. Such an analysis was possible for a 3 bed model because the fewer number of parameters involved made a mathematical error analysis possible[1]. The results of the performance and robustness analysis for the 3 bed model are of value for more complex models, (with more possible sources of error), because they provide an upper bound on achievable estimator performance and, more importantly, because the primary complicating effects faced in the inversion for the true conductivity of the formation using the simpler model are encountered in inversion from more complex models as well. These are:

- the presence of shoulder beds, (T is not infinite and $\sigma_s \neq \sigma_t$)
- the presence of the borehole, ($r \neq 0$ and $\sigma_m \neq \sigma_t$)
- the presence of an invaded zone, ($h \neq 0$ and $\sigma_{xo} \neq \sigma_t$)
- tool depth position uncertainty, ($delz$ is not constant)

[1] Another outcome of such a choice of model is that the fast, approximate tool response modelling codes are more accurate for such a simple model

These four complicating effects were considered in the preceding analysis under the following simplifying assumptions:

1. The shoulder beds are assumed to be semi-infinite in length and equal in conductivity.

2. The borehole wall is not rugose; i.e., the wellbore is a cylinder of constant radius.

3. There is no transition zone; i.e., the conductivity profile has a step-like profile in the center bed.

4. The tool positions, if they are in error, are assumed to be skewed by a constant offset in one direction only.

In the first section of this chapter we expand our study of the above mentioned complicating effects by examining more closely the assumptions made in their modelling. In the second section we extend the analysis of the previous chapters to different choices of operating points and parameter imprecision values.

5.2 Tool Depth Position Uncertainty

In the analysis of Chapter 3 it was assumed that imprecisions in the tool position were as shown in Figure 5-1 (a). The tool position was off from its expected value by a constant amount given by ϵ, ($\epsilon > 0$). We now extend the treatment of imprecisions in the logging tool's position to the case where the error in the tool position alternates between constant positive and negative values of $+\epsilon$ and $-\epsilon$ as shown in Figure 5-1 (b).

Both of these cases are examples of systematic errors. These are errors due to one or a few definite causes acting according to a definite rule. The error in Figure 5-1 (a) is one-sided. It may arise in a situation in which the cable length is measured incorrectly or if the cable has suffered stretching by a constant amount. The error shown in Figure 5-1 (b) is skew symmetric. The tool goes from being in positive error at one depth position to being in negative error at the next. This may arise in a situation in which the tool alternately experiences an acceleration and deceleration

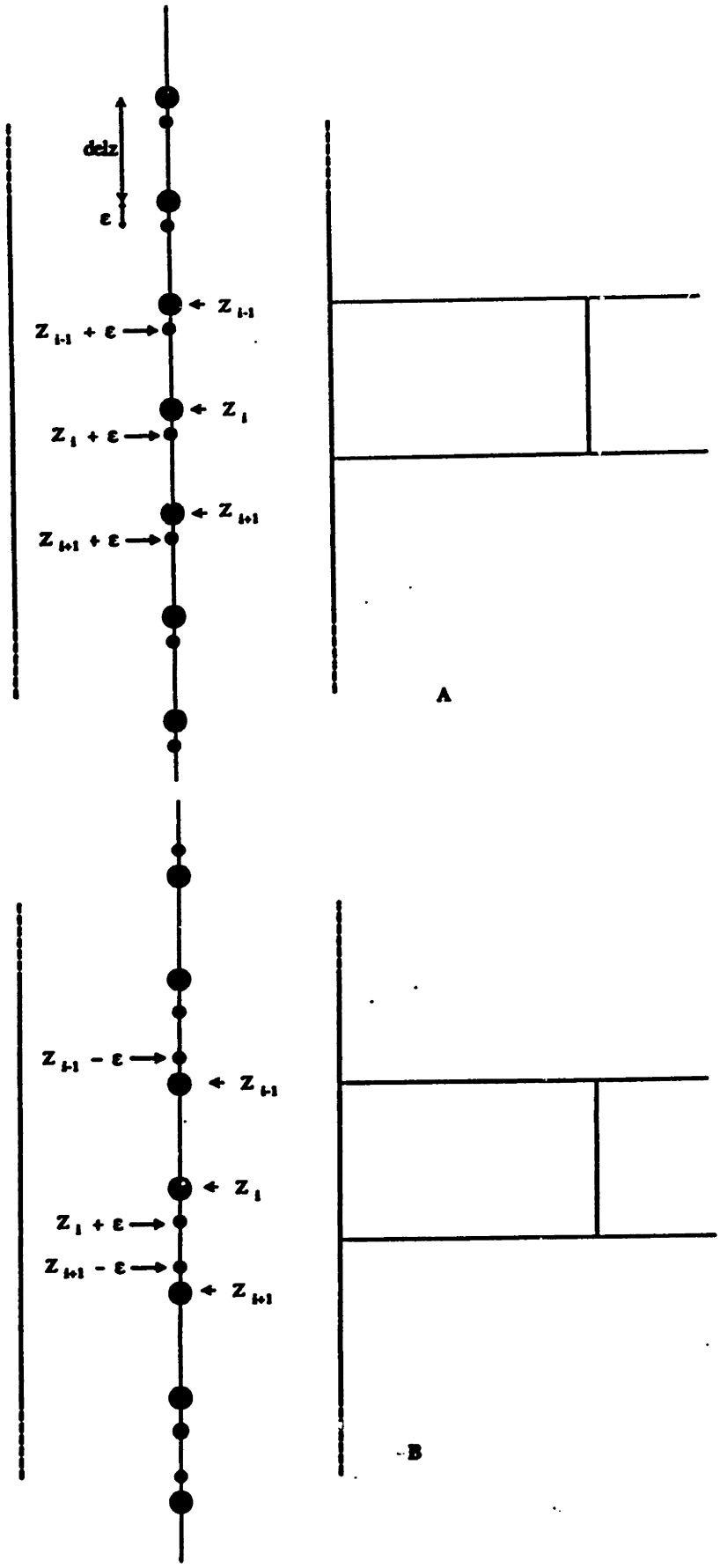

Figure 5-1: Expected and actual tool positions. (a) one-sided perturbation, (b) skew-symmetric perturbation. (Borehole diameter exaggerated)

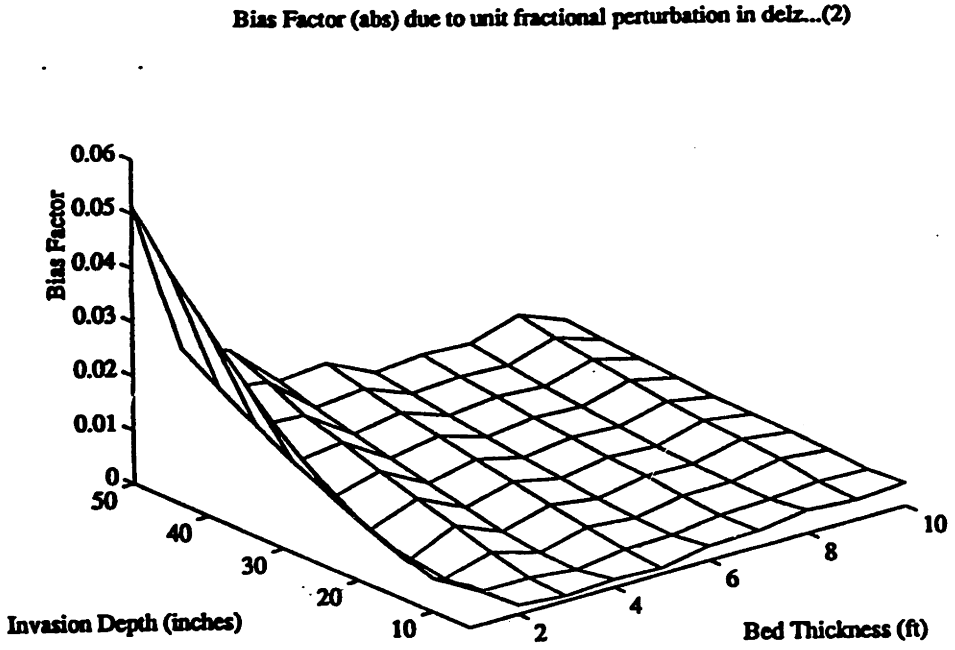

Figure 5-2: Bias Factor for skew-symmetric perturbation

while being raised out of the borehole. If it is assumed, for simplicity, that this speeding up and slowing down occurs successively and by equal amounts then the tool position will oscillate between the expected tool position plus and minus a certain ϵ. This is a rudimentary model of 'tool yoyo', which is a source of tool position uncertainty. In reality, the yoyo-like behaviour induced by tool speed fluctuations creates random perturbations in the tool depth position that do not have to obey a systematic model such as the one being employed (which can be thought of as a limiting case of the more general tool speed fluctuation problem).

Figures 5-1 (a) and (b) show the expected and actual (perturbed) tool positions. An equivalent representation can be obtained by assuming that the tool's sampling step size, *delz*, is perturbed by $+\epsilon$ in Figure 5-1 (a) and by $+\epsilon$ and $-\epsilon$ successively in Figure 5-1 (b).

In Section 3.32 the bias introduced into the estimate of σ_t due to a non-random perturbation in the parameters was considered. Figures 3-4 (a) - (h) showed the Bias Factors obtained for the various parameters assuming that Case E was the

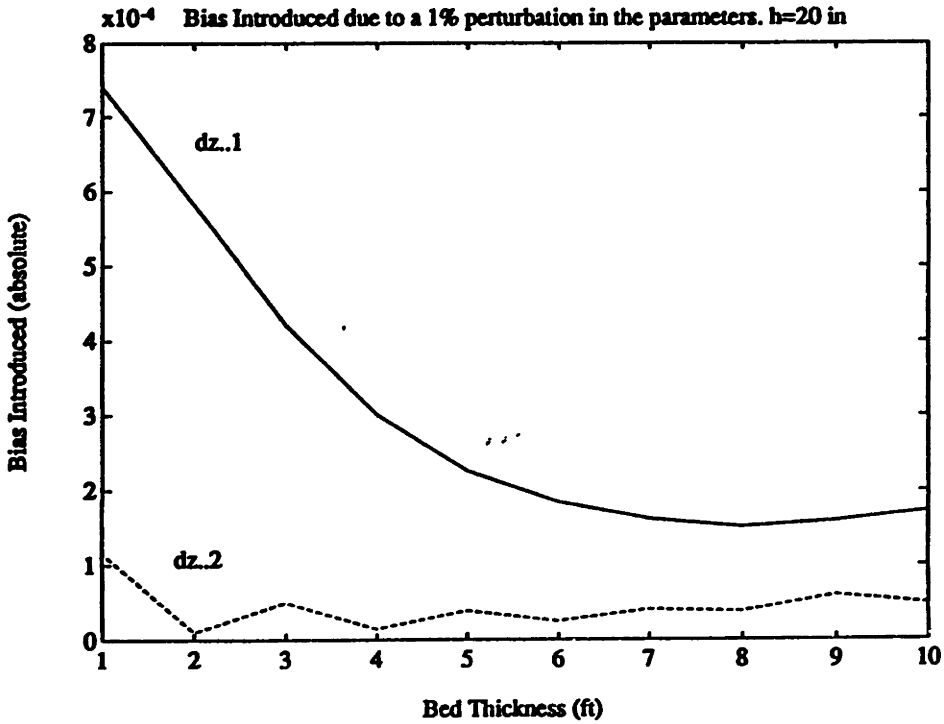

Figure 5-3: Comparison of the absolute bias (in mhos) introduced for the two types of perturbations

chosen operating point family. The Bias Factor obtained assuming a non-random perturbation of *delz* of the type depicted in Figure 5-1 (b) is shown in Figure 5-2. We shall refer to this kind of perturbation in *delz* (and, consequently, depth position) by dz_2. This result should be compared with those obtained in Figure 3-4 (h) where the perturbations, dz_1, obey the pattern indicated in Figure 5-1 (a). It can be seen that the Bias Factor obtained for the one-sided error case of dz_1 is larger than the corresponding Bias Factor for dz_2 over the entire space of h and T considered.

Figure 5-3 shows a comparison of the bias introduced into the estimate of σ_t due to a 1% perturbation in each of the parameters for the two cases when the invasion depth is assumed to be 20 inches. The difference between the two cases is most pronounced for thinner beds. Further, for the skew symmetric case the bias introduced is relatively independent of bed thickness while for the one-sided depth position error case the bias introduced decreases as the bed thickness increases.

Now, dz_1 was the case that was used in the preceding analyses for imprecision in *delz*. We saw earlier that the estimate of σ_t was most robust to σ_m and *delz*, i.e., dz_1.

We see here that if an ordering were to be made between dz_1 and dz_2 based on the sensitivity of the estimate of σ_t to perturbations in these parameters values we would find that dz_1 would feature above dz_2, i.e., the estimate is more robust to dz_2 than dz_1. Therefore, any conclusions drawn earlier about the relative robustness of the estimate to perturbations in dz_1 as compared to the rest of the parameters (except σ_m) will also be valid for dz_2.

5.3 A Different Choice of Operating Point

So far in this thesis all the results presented have been restricted to the range of operating points associated with the conductivity contrast given by Case E (each case was termed an operating point family). As was mentioned in Chapter 1, the investigation was performed for 5 different conductivity contrasts that reflected commonly encountered formations in well logging. In all of these, the conductivities were given by Cases A-E and the parameters governing the geometry of the formation, viz, h and T, varied over the ranges 0 to 50 inches and 1 to 10 feet respectively.

In this section we address the questions: how would the results obtained in Chapters 3 and 4 for the operating point family, Case E, be any different for the other cases and how would the different choice of operating points influence the conclusions made in those chapters? We further extend the results of the robustness analysis to a more realistic choice of the resolution with which the tool/formation parameters are known. In this section it is assumed that *delz* corresponds to a constant offset of ϵ in the tool depth position, i.e., the dz_1 model of the previous section.

The five cases are:

- Case A: $\sigma_s = 0.5$ mho, $\sigma_{xo} = 0.2$ mho, $\sigma_t = 0.1$ mho, $\sigma_m = 1$ mho.
- Case B: $\sigma_s = 0.5$ mho, $\sigma_{xo} = 0.05$ mho, $\sigma_t = 0.1$ mho, $\sigma_m = 1$ mho
- Case C: $\sigma_s = 0.5$ mho, $\sigma_{xo} = 0.02$ mho, $\sigma_t = 0.01$ mho, $\sigma_m = 1$ mho
- Case D: $\sigma_s = 1$ mho, $\sigma_{xo} = 0.2$ mho, $\sigma_t = 0.04$ mho, $\sigma_m = 1$ mho
- Case E: $\sigma_s = 0.2$ mho, $\sigma_{xo} = 0.5$ mho, $\sigma_t = 0.05$mho, $\sigma_m = 1$ mho

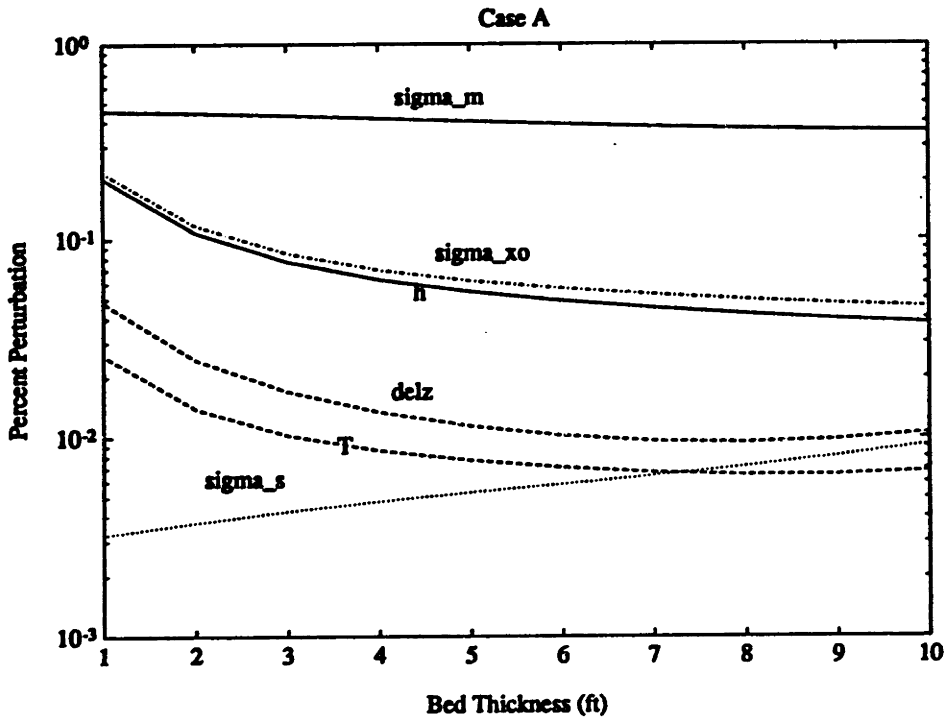
Case A
sigma_m
sigma_xo
h
delz
T
sigma_s
Percent Perturbation
Bed Thickness (ft)

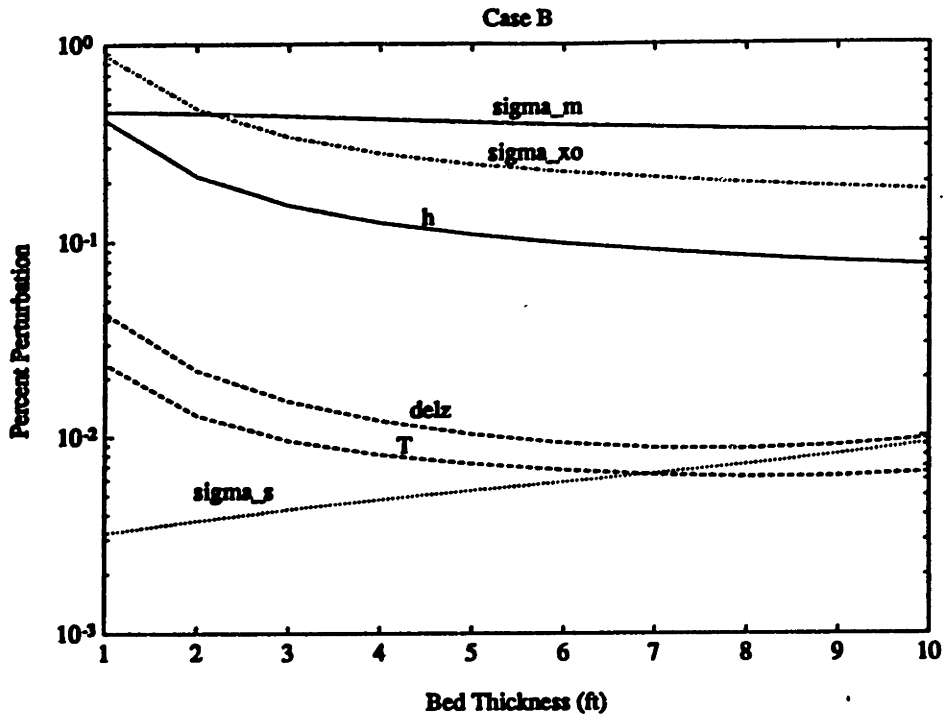
Case B
sigma_m
sigma_xo
h
delz
T
sigma_s
Percent Perturbation
Bed Thickness (ft)

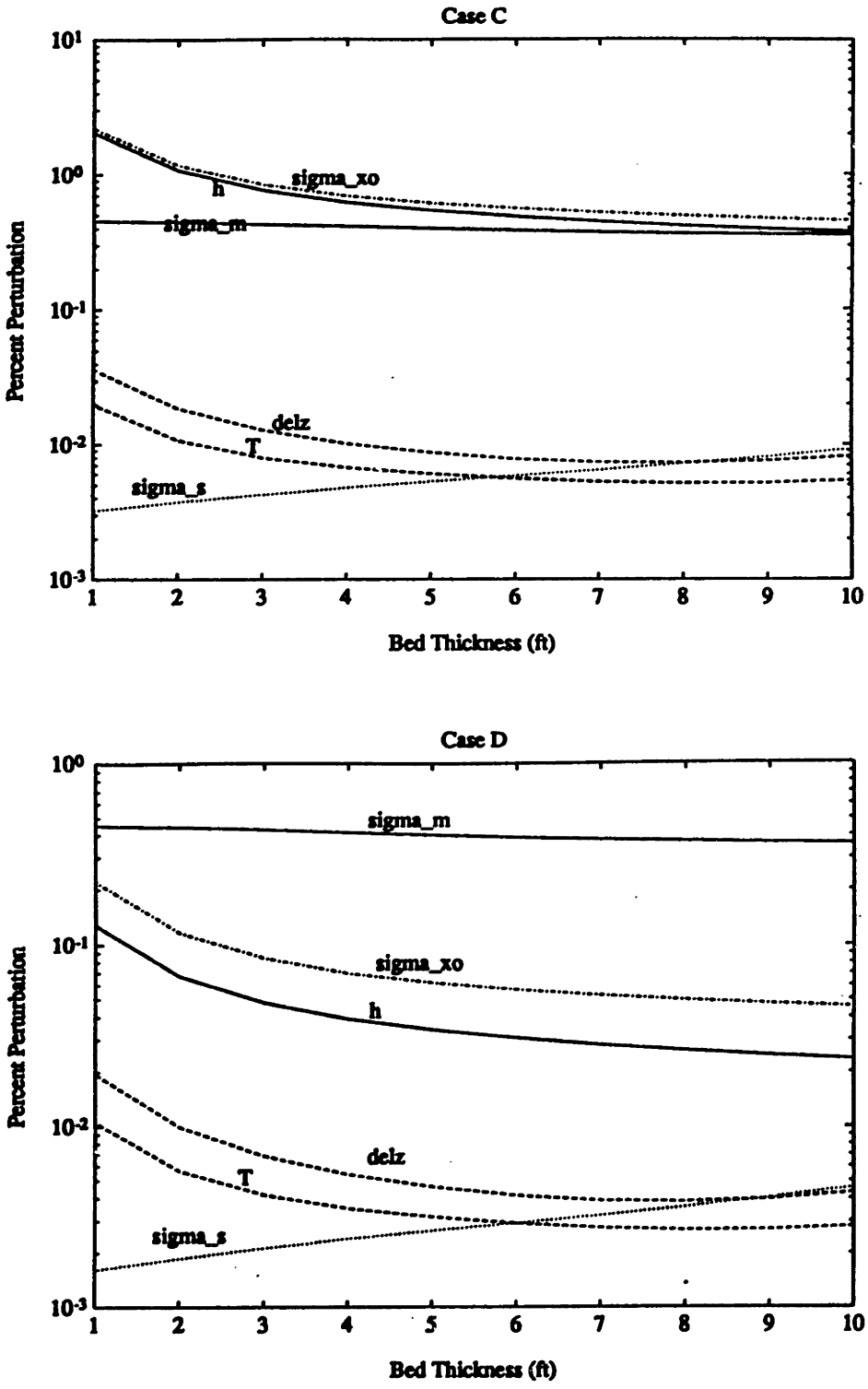

Figure 5-4: Percent perturbations required in the various parameters to produce bias terms as large as the standard deviation of the estimate of σ_t obtained when measurement noise is the only corrupting factor. Cases A-D, h=20 inches

In all of the above h varies from 0 to 50 inches, T from 1 to 10 feet, and the wellbore radius, r, is 5 inches.

In Cases A-C, the shoulders (of conductivity $\sigma_s = 0.5$ mhos) are more conductive than the central bed. These cases represent three situations in which:

1. the invaded zone is twice as conductive as the virgin formation,
2. the deep conductivity is 20 times more than that of the uninvaded zone, and
3. the invaded zone is twice as conductive as the uninvaded zone.

In Case D, the shoulders are still more conductive than the central bed ($\sigma_s = 1$ mho), but the invaded zone is 50 times more conductive than the uninvaded zone.

As was mentioned in Chapter 2, when the measurement sensor noise is the only source of uncertainty in the deep conductivity estimate, i.e., when all the assumed known parameters are precisely known, the Cramer-Rao lower bound on the error variance of the estimate of σ_t is seen to be virtually identical for all the cases. The conclusion that the measurement noise is not the dominant contributor to the error in the estimation appears to hold irrespective of the choice of operating point.

Figure 5-4 (a)-(d) shows the percent perturbations in the different parameters required to produce in the estimate of σ_t a bias as large as the error introduced by the measurement noise alone. It can be seen that for cases A, B and D, the percent perturbations required are less than 1% for all the parameters. In case C, the perturbations are no larger than 2% (for beds of 1 foot thickness and more) for any of the parameters. These results are similar in spirit to those obtained in Chapter 2 for Case E, where the required perturbations did not exceed 0.5% for any of the parameters. Such levels of imprecision are inevitable in practice, and so it can be concluded that the bias contributed by the various parameters will be the dominant source of error for the operating points spanned by these 5 cases.

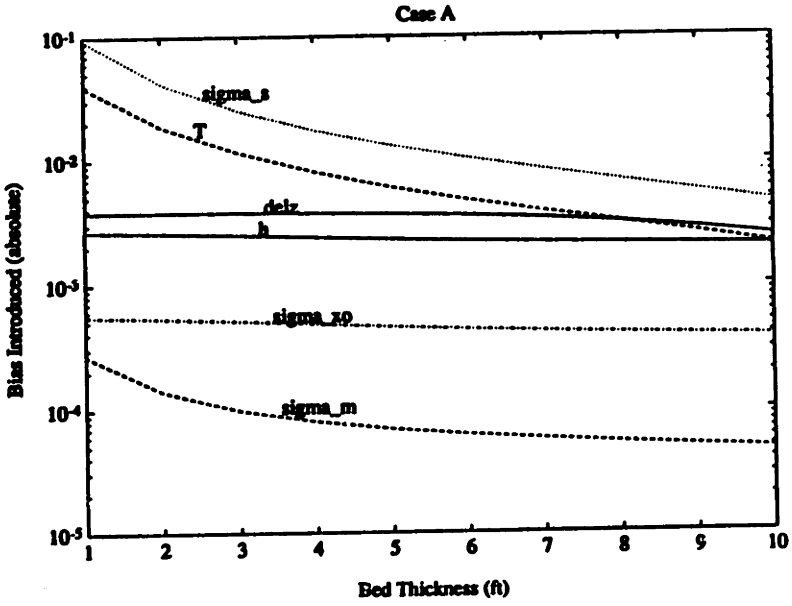
Case A
sigma_s
T
delz
h
sigma_xo
sigma_m
Bias Introduced (absolute)
Bed Thickness (ft)

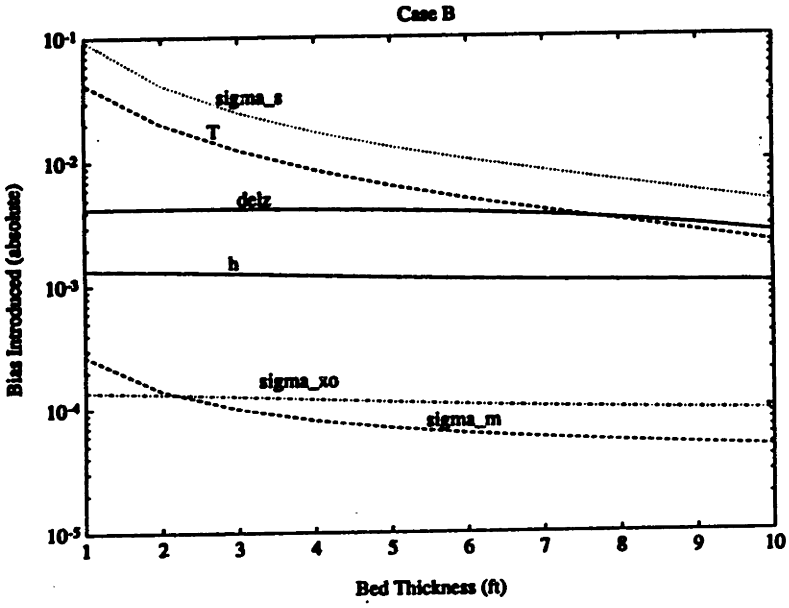
Case B
sigma_s
T
delz
h
sigma_xo
sigma_m
Bias Introduced (absolute)
Bed Thickness (ft)

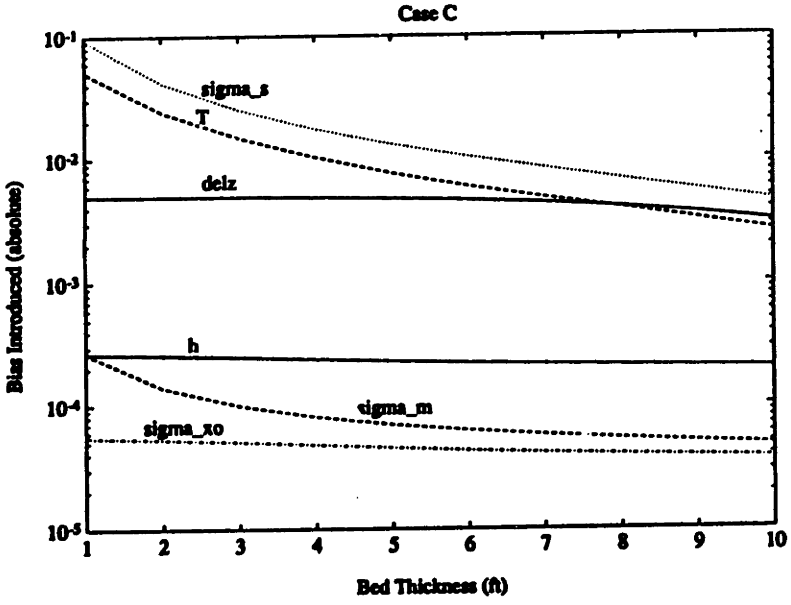
Case C
sigma_s
T
delz
h
sigma_m
sigma_xo
Bias Introduced (absolute)
Bed Thickness (ft)

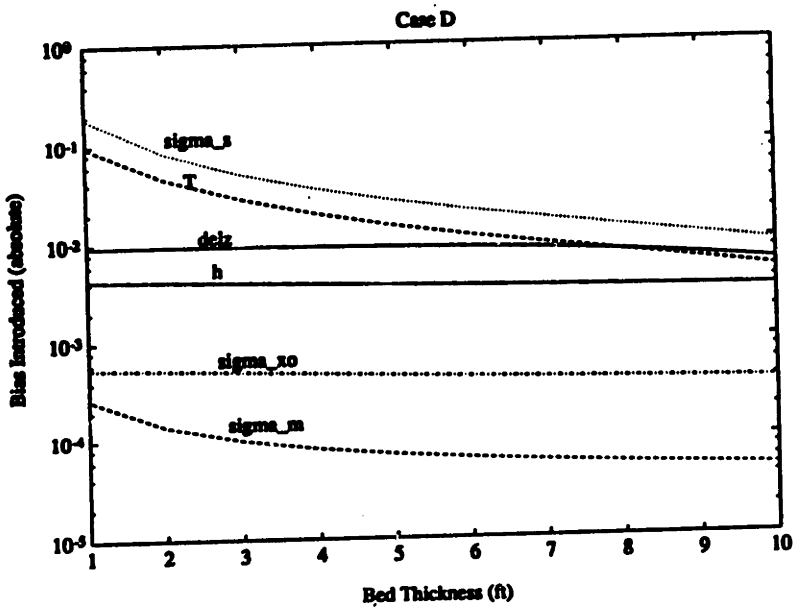

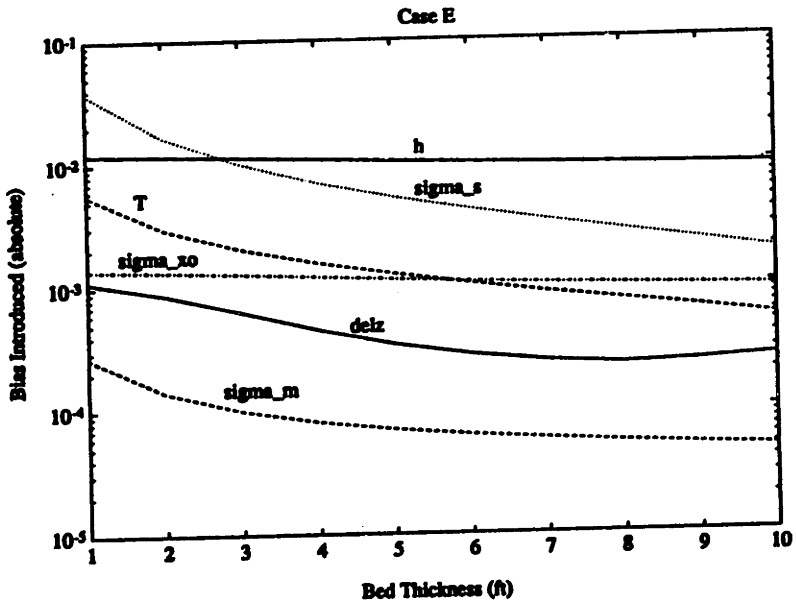

Figure 5-5: Bias introduced into the σ_t estimate for cases A-E. h = 20 inches

The relative bias terms introduced by imprecisions in the various parameters is a function of the choice of operating point. In Section 3.3.2 the bias introduced into the deep conductivity estimate was examined for the case in which all the parameters are known to within 1 percent of their true value (the perturbations were further assumed to be non-random). This is an unrealistic assumption. It does not take into account the fact that in reality the different parameters will be known with different degrees of certainty to the log analyst; for instance, the mud conductivity, σ_t is bound to be more precisely known than the invasion depth, h.

Figures 5-5 (a)-(e) show the absolute bias introduced (in mhos) into the estimate of σ_t for the 5 cases assuming an invasion depth of 20 inches and the following set of a priori known perturbations:

- $\sigma_s = 2.5\%$ of its true value
- $\sigma_{xo} = 1\%$ of its true value
- $\sigma_m = 1\%$ of its true value
- $h = 4.5\%$ of its true value
- $delz = 1.5\%$ of its true value, and
- T is known to within an inch[2]

In cases A -D, σ_s, T, $delz$ and h, in that order, are the parameters to which the estimate of σ_t is most sensitive. In case C, the low conductivity value of σ_{xo} makes the deep conductivity estimate least sensitive to it; in all other cases σ_m is the parameter to which the estimate of σ_t is most robust. The relative sensitivity of the estimate to h and σ_{xo}, the parameters characterizing invasion, is seen to vary in cases A-D, though the variation is not enough to induce a change in the ranking of the parameters by the sensitvity of the estimate to them. Sensitivity to h, for instance, is more in Case D than in cases A-C because σ_{xo} contributes more to the overall signal energy, and a

[2]This is because the estimate of T is obtained by a detection scheme for a point of inflection in the induction log response [7]. This detection can be performed to within a known resolution of about an inch irrespective of the bed thickness

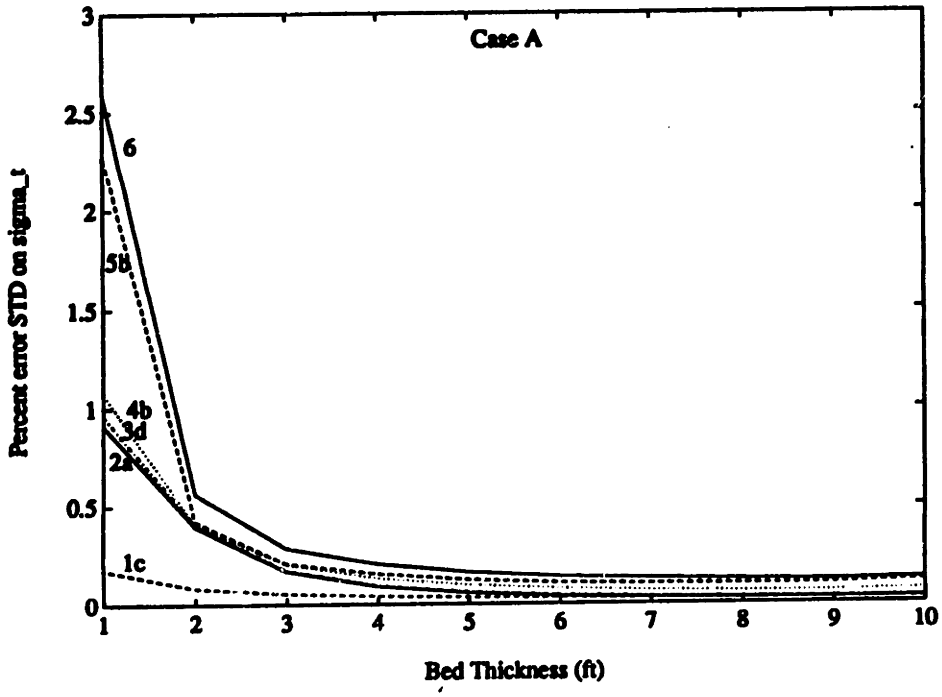

Figure 5-6: Cramer-Rao lower bound on the estimate of σ_t for different choices of the parameter set to be estimated

change in h directly influences the contribution of the invaded zone to the measured signal energy.

In Case E, the changes are most dramatic. For bed thicknesses in excess of 3 feet it is seen that the estimate of σ_t is most sensitive to h. The parameters σ_s and T continue to remain parameters to which the estimate is highly sensitive but the choice of operating point in Case E (with σ_{xo} ten times more than the true conductivity and 2.5 times greater than the shoulder bed conductivities) results in an enhanced sensitivity of the estimate to the parameters that govern the description of invasion in the formation model. (The estimate is seen to be more sensitive to h than σ_{xo} for all the conductivity contrasts chosen in this study). Thus, for bed thicknesses greater than 6 feet it can be seen that σ_{xo} assumes a higher place in the sensitivity ranking than even the bed thickness, something that is not seen in any of the other cases.

A systematic appraisal of the results of the sensitivity analysis for Case A assuming an h of 20 inches and a T of 4 feet is shown in Table 5.1. The error due to parameter imprecision is seen to be more than 99.9% of the total error and 43.8% of the true

SOURCE OF ERROR		ERROR INTRODUCED (in mhos)	% OF TOTAL ERROR	% OF σ_t
Measurement noise		4.303×10^{-5}	0.0981	0.043
Imprecision in knowledge of parameters		0.0438	99.9019	43.8
Parameter	*% perturbation*			
σ_s	2.5	0.0252	57.5173	25.2174
σ_{xo}	1	5.07×10^{-4}	1.1569	0.5072
σ_m	1	9.973×10^{-1}	0.2275	0.0998
h	4.5	0.0025	5.734	2.514
T	within an inch	0.0117	26.6039	11.664
delz	1.5	0.0038	8.6763	3.804

Table 5.1: The relative contributions of the different sources of error in the estimation of σ_t.

value of σ_t. This clearly illustrates the dwarfing of the error due to noise by that due to imprecision in the assumed known parameter values. For the choice of percent perturbations assumed in this section it is seen that σ_s and T contribute the most error - 57.5% and 26.6% respectively - with the rest of the parameters introducing errors less than 10% of the total error. It is easy to appreciate, from the results in this table, that refining the parameter values via a joint estimation with σ_t is an option worth considering.

Figure 5-6 shows the error standard deviation of the estimate of σ_t when the parameter set to be estimated is expanded in accordance with the results of the sensitivity analysis for Case A. Therefore the estimation scheme goes from:

- 1c: in which σ_t and σ_s are estimated, to
- 2a: in which σ_t, σ_s and T are estimated, to
- 3d: in which σ_t, σ_s, T and *delz* are estimated, to
- 4b: in which σ_t, σ_s, T, *delz* and h are estimated, to
- 5b: in which σ_t, σ_s, T, *delz*, h and σ_{xo} are estimated, to
- 6: in which σ_t, σ_s, T, *delz*, h and σ_{xo} and σ_m, i.e., all the parameters, are estimated.

CASES	ERROR St.Dev ON ESTIMATE (in % of σ_t)	INCREMENTAL St.Dev ADDED TO ESTIMATE (in % of σ_t)
θ perfectly known	0.043	-
Case 1c	0.0561	0.0131
Case 2a	0.17	0.1139
Case 3d	0.1734	0.0034
Case 4b	0.2055	0.0321
Case 5b	0.21	0.0045
Case 6	0.2878	0.0778

Table 5.2: Degradation in the σ_t estimate caused by the successive multiparameter estimation cases

It can be seen that even for the case in which all the parameters are estimated along with σ_t, the error standard deviation on σ_t is within 2.7% of the true value of σ_t. Thus, as was seen earlier for Case E, the loss in estimator precision due to the additional estimation of the assumed known parameters is within acceptable limits.

Table 5.2 shows the results for Case A in table form for a bed thickness, T, of 4 feet. For this choice of operating point it is seen that for the case in which all the parameters are estimated for in the multi-parameter estimation, the error standard deviation of the estimate is within 0.3% of the estimate. The last column of the table shows the incremental standard deviation added to the estimate by the succesive addition of one more parameter to the set of parameters to be estimated. It provides, therefore, a way to assess the cost of estimating a certain parameter as measured by the loss in precision of the σ_t estimate that accrues from estimating it. It can be seen that the largest increase comes from estimating T. Note, however, that even in this case, the incremental standard deviation added to the σ_t estimate is 0.1139% of the true value of σ_t (from Table 5.2), an amount which is far less[3] than the uncertainty introduced into the σ_t estimate due to imprecisions in some of the parameters as is seen in the last column of Table 5.1 where a 1.5% perturbation in *delz* and a 2.5% perturbation in σ_s produce, respectively, errors of magnitude 3.804 % and 25.2174 % of the true value of σ_t.

[3]except for perturbations in σ_m and σ_{so}, to which the estimate of σ_t is reasonably robust (see Chapter 3).

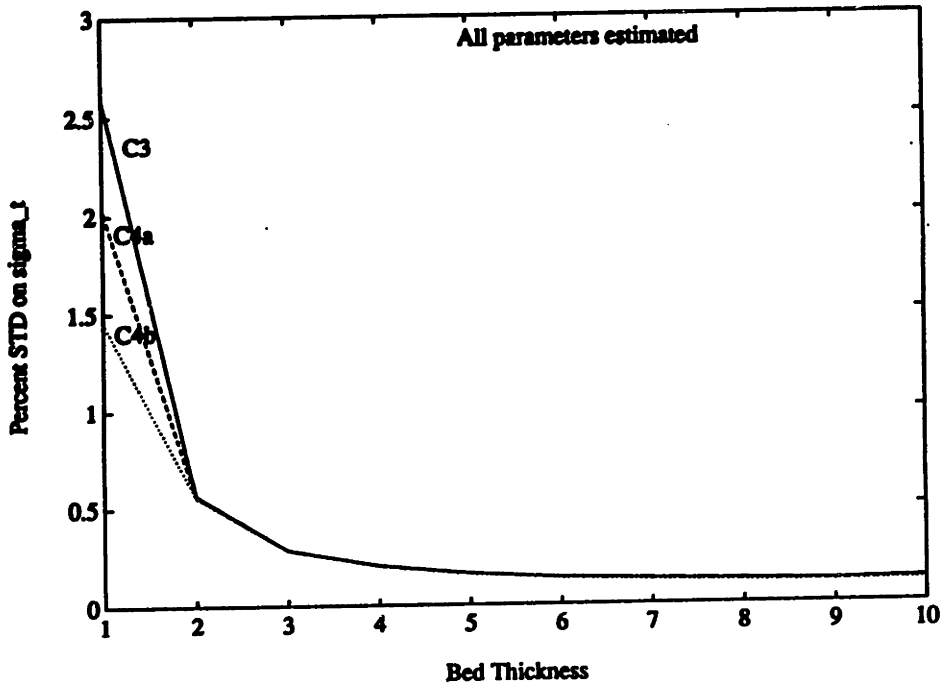

Figure 5-7: Cramer-Rao lower bounds on the estimate of σ_t illustrating the effect of improving quality of additional information on T and σ_{xo}. h = 20 inches

Finally, Figure 5-7 illustrates the Cramer-Rao lower bound on the σ_t estimate in Case A, expressed as a percent standard deviation of σ_t, when auxiliary information on T and σ_{xo} are available. In this illustrative example we go from:

- C3: no auxiliary information, to
- C4a: $\sqrt{Q_i} = 1\%$ of θ_i, to
- C4b: $\sqrt{Q_i} = 0.5\%$ of θ_i

where the Q_i's are as in (4.23), h is 20 inches and all parameters are being estimated along with σ_t. Notice that in going from C4a to C4b the quality of the additional information is being improved. As was seen in Case E, an improvement in estimator precision is seen only for thinly bedded formations. For bed thicknesses less than 2 feet, the quality of the additional information greatly determines the improvement in the precision of the deep conductivity estimate.

5.4 Conclusion

In this chapter some issues complementary to the investigation conducted in the preceding two chapters were addressed. The issue of tool depth imprecision was considered in detail in the first section. It was seen that the bias introduced into the deep conductivity estimate due to a one-sided, or systematic, tool position error was more severe than that caused by tool position errors that oscillated from positive to negative values.

In the second section, the consequences of a different choice of operating point on the conclusions of the earlier two chapters were addressed. It was seen that while the conclusion that parameter imprecision is the dominant source of error in the estimation held true for all cases, the sensitivity rankings obtained as in Chapter 3 are very much a function of the chosen operating point. A more realistic robustness analysis was performed in which the parameter imprecisions were assigned values in keeping with the resolution with which they may be known in practice. The performance analysis for the multiparameter estimation revealed that the loss in estimator precision incurred when all the tool/formation parameters are refined via a joint estimation with σ_t is within reasonable bounds. Finally, it was seen that additional information was of value in improving the quality of the estimation in thinly bedded formations.

Chapter 6

Conclusion

This thesis was motivated by the need to develop a methodology to characterize quantitatively the uncertainty associated with the estimates obtained using a model-based inversion of log data. In this thesis we have focussed on the problem of the induction log response in a three layer, invaded medium model. The methodology of error characterization, however, is applicable to more complex formations and more sophisticated tool responses as well. This chapter summarizes the main contributions of this thesis and suggests some directions for future work.

6.1 Thesis Contributions

- The parametric inversion problem was defined for the thesis model. The motivation for choosing this particular model was discussed. The stochastic nature of the logs required that techniques of statistical estimation be applied; the inherently nonlinear nature of the forward models implied that the error characterization required methods, such as the Cramer-Rao lower bound, that are new to petrophysical interpretation. Four separate performance/robustness cases were identified.

- It was seen that when all the nuisance parameters are perfectly known, i.e., when the only source of uncertainty is the measurement sensor noise (which for induction tools is very small), the estimate was extremely accurate. This

was seen to be the case irrespective of the choice of operating point. This case served as a useful upper bound on estimator performance in the sense that it represented the best performance that one could expect to achieve.

- When the nuisance parameters are assumed to be known to only within a certain degree of precision, as is the case in practice, this imprecision in the parameters is another source of error in the estimation. The bias produced by this imprecision in the assumed known parameters which is inevitable in practice, was seen to dominate the error due to the measurement noise alone. This result was seen to be independent of the choice of operating point as well. A methodology was then developed to assess the individual contribution of the imprecision in each of the assumed known parameters to the overall bias term. If one assumed a priori known values for the imprecisions in the various parameters[1] then this enabled a ranking of the parameters by the sensitivity of the deep conductivity estimate to imprecision in these parameters. It was observed that this ranking of the parameters was highly operating point specific. A model for the formation in which the conductivity of the invaded zone, σ_{xo}, greatly exceeded those in the other zones implied that the parameters h and σ_{xo} assumed greater importance and the slightest of perturbations in their values was sufficient to make imprecisions in them the dominant source of the error in the estimation. The important contribution of this component of the study was that a methodology was developed that could be used to obtain the sensitivity ranking for any choice of operating point.

- A performance analysis was then conducted for a multiparameter estimation scheme in which some or all of the tool/formation parameters were estimated along with the deep conductivity. In choosing what subset of the tool/formation parameters to estimate, the ranking obtained from the sensitivity analysis was adhered to. In other words, the quantity most likely to introduce the most bias in the estimate was the one to be refined first of all via this joint estimation

[1]This is possible because knowledge of the assumed known parameters, i.e., the tool/formation descriptors, comes from different measurement sources, the quality of whose estimates may be established from test pit experiments

scheme. Since this additional refinement derives from the same log data that is used to determine the deep conductivity, a corresponding degradation in the quality of the deep conductivity estimate is to be expected. It was seen that even for the case in which all the parameters are estimated along with the deep conductivity, the loss in the precision of the deep conductivity estimate is within acceptable bounds.

- Finally, a performance analysis was conducted for the case in which additional information on some of the tool/formation descriptors becomes available through some auxiliary measurement source, such as the FMS[7]. The error characterization methodology was expanded to determine the extent to which additional measurements of formation descriptors translate to a reduction in the uncertainty of the final estimate of the deep conductivity. It was seen that additional information about the bed thickness, T, in thinnly bedded formations was of particular importance in reducing the uncertainty of the deep conductivity estimate. Another important contribution of this component of the study was that it led to a means of defining the minimum quality of the auxiliary information needed for any improvement in the quality of the deep conductivity estimate to be achievable.

6.2 Directions for Future Work

There are several issues that arise in the wake of this investigation. In Chapter 5 the results of the performance/robustness analysis were presented for different choices of operating points to illustrate how a different conductivity contrast could influence the ranking of the parameters obtained from the sensitivity analysis. The methodology of the preceding chapters was also extended to embrace the case of tool depth imprecision and tool yoyo. In a similar vein, future work could be directed at addressing the effects of some of the other complicating factors that have not been modelled in this thesis. These include the assumption of the shoulders being equal in conductivity and semi-infinite in extent, the absence of dip, the piston-like nature of the invasion front and the absence of caves and any rugosity in the wall of the well. The bias introduced

into the estimate due to each of these complicating factors can be computed and a sensitivity analysis similar to the one performed in Chapter 3 can be conducted to see whether any of these factors is a dominant source of error in the estimation.

Another possible avenue for future work is the design and implementation of actual estimation algorithms for the parameters of interest. Subsequent simulations of these algorithms can be carried out to see how close the estimation errors approach the bounds arrived at in this investigation.

The methodology of error characterization illustrated in this thesis can be extended to other tools with different forward responses. For instance, a similar error characterization may be performed for the neutron tool[8] which is used to yield a formation density estimate. In this case the measurement noise will be Poissonian but the performance/robustness analysis conducted in this thesis can readily be performed assuming the availability of the necessary forward model. Furthermore, this error characterization methodology may be extended to more sophisticated formation models in the future; these models may explicitly account for dipped beds, rugose walls and may have several beds with more than one invaded zone. Eventually, this methodology may be extended to an error characterization of the estimates of the parameters of eventual petrophysical interest, viz, porosity, ϕ, and water saturation, S_w. These estimates are themselves derived from estimates of formation measurables such as the deep conductivity, and an error characterization of the estimation of these two quantities will be of extreme interest and value to petrophysical interpretation.

Bibliography

[1] George Asquith and Charles Gibson. *Basic Well Log Analysis for Geologists.* American Association of Petroleum Geologists, 1981.

[2] D. T Barber and A. R Rosthal. Using a multiarray induction tool to achieve high-resolution logs with minimum environmental effects. *Society of Petroleum Engineers Conference*, October 1991.

[3] W. C Chew, Z Nie, Q. H Liu, and B Anderson. An efficient solution for the response of electrical well logging tools in a complex environment. *IEEE Transactions, Geosci. Remote Sensing*, March 1991.

[4] Ralph Deutsch. *Estimation Theory.* Prentice Hall Inc, 1965.

[5] T. John Dewan. *Essentials of Open-hole Log Interpretation.* Penwell Publishing Company, 1983.

[6] Alvin Drake. *Fundamentals of Applied Probability Theory.* McGraw-Hill, 1986.

[7] M. P Ekstrom, C. A Dahan, M. Y Chen, P. M Lloyd, and D. J Rossi. Formation imaging with microelectrical scanning arrays. *Log Analyst*, May 1987.

[8] Darwin Ellis. *Well-Logging for Earth Scientists.* Elsevier Science Publishing Company, 1987.

[9] Gelb. *Applied Optimal Estimation.* MIT Press, 1974.

[10] Alexander Kaufman and George Keller. *Induction Logging.* Elsevier Science Publishing Company, 1989.

[11] H. J Moran and S. K Kunz. Basic theory of induction logging and application to study of two-coil sondes. *Geophysics*, December 1962.

[12] O Serra. *Fundamentals of Well Log Interpretation. 1. The Acquisition of Logging Data.* Elsevier Science Publishing Company, 1984.

[13] Schlumberger Educational Services. *Log Interpretation Principles/Applications*, 1989.

[14] Jay Tittman. *Geophysical Well Logging.* Academic Press Inc, 1986.

[15] Harry Van Trees. *Detection, Estimation and Modulation Theory. Part 1.* John Wiley and Sons, 1968.

[16] A. S Willsky and Jeffery Shapiro. *Stochastic Processes, Detection and Estimation.* Class Notes for MIT Course 6.432, 1991.